



MILANO BICOCCA UNIVERSITY

DOCTORATE SCHOOL

School of Medicine and Surgery

**PhD PROGRAM IN MOLECULAR AND
TRANSLATIONAL MEDICINE - DIMET**

XXXI CYCLE

**Characterization of disease genes and mechanisms
causing neurodegenerative phenotypes**

Alessia Catania, MD

Matr. no. 745475

Tutor: Valeria Tiranti, PhD

Co-tutor: Daniele Ghezzi, PhD

Coordinator: Prof. Andrea Biondi

Academic year 2017/2018

*To my parents,
for giving me life and wings to my dreams every day.*

*To Pierrot,
for testifying to the extraordinary power of combining science with
unselfishness.*

Table of contents

Chapter 1	7
General introduction	7
Next Generation Sequencing (NGS) for rare diseases diagnosis.....	7
• Hereditary Spastic Paraplegias (HSPs)	11
- Genetics of HSP.....	11
- Role of NGS in HSP and related disorders.....	19
• Mitochondrial diseases	22
- Genetics of mitochondrial diseases.....	22
- Role of NGS in mitochondrial diseases.....	31
Aim of the thesis	35
References	36
Chapter 2	42
R106C <i>TFG</i> variant causes infantile neuroaxonal dystrophy “plus” syndrome.	
Chapter 3	71
Compound heterozygous and deep intronic variants in <i>NDUFA6</i> unravelling by exome sequencing and mRNA analysis.	
Chapter 4	96
Homozygous variant in <i>OTX2</i> and possible genetic modifiers identified in a patient with combined pituitary hormone deficiency, ocular involvement, myopathy, ataxia and mitochondrial impairment.	
Chapter 5	118
A novel dominant mutation in <i>DNMT1</i> underlying a case of cerebellar ataxia, deafness and narcolepsy syndrome (ADCA-DN).	
Chapter 6	125

Xenotopic transfection with alternative dehydrogenases as a potential therapy for mitochondrial CI deficiency: preliminary results and perspectives.

Chapter 7	159
• Summary.....	159
• Conclusion and future perspectives.....	161
- Opportunities and drawbacks of NGS technologies.	161
• References.....	163
Publications	164
Acknowledgments	165

Chapter 1

GENERAL INTRODUCTION

Next Generation Sequencing (NGS) for rare diseases diagnosis

The development of Next Generation Sequencing (NGS) Technologies has definitely improved the efficiency of mutation discovery, replacing the traditional Sanger sequencing and facilitating the diagnosis of rare diseases, with remarkable advantages not only in terms of diagnostic scores, but also in terms of time consumed and saving of money^{1,2}. Depending on the target regions of the genome sequenced, we can easily classify NGS techniques into three main groups³⁻⁵:

- Whole Genome Sequencing: the most extensive approach which allows sequencing of the whole (coding and non-coding) human genome.
- Whole Exome Sequencing: the broadest targeted sequencing method which allows a comprehensive sequencing of the exome (coding region of the genome). It represents only 2% of the entire genome but include almost the 85% of the recognized pathogenic variants.
- Targeted Sequencing: more focused panels which allow a high-resolution sequencing of targeted (and customized) genes of interest across many samples within the same assay. Usually, targeted panels are designed in order to spotlight genes with a known or suspected association with a specific disease or phenotype (e.g: mitochondrial diseases, hereditary spastic paraplegias, spinocerebellar ataxia...), thus simplifying and speeding up the data analysis step (Figure 1).

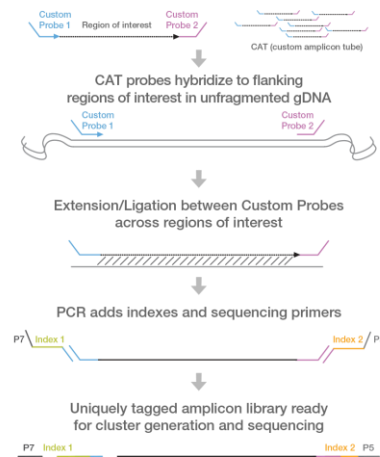


Figure 1. Simplified workflow of NGS custom amplicon technique (www.illumina.com)

Even if protocols and procedures are distinct for each technique⁶, they share common conceptual workflows: a typical NGS assay starts with preparation of libraries from individual DNA samples that allow the parallel amplification and sequencing of single strand DNA fragments obtained from mechanical or enzymatic digestion resulting in simultaneous collection of millions of reads. Targeted sequence requires an additional step: regions of interest are enriched by hybridization with biotinylated probes and isolation of the fragments by magnetic pulldown. Then, specific adaptors are linked to both ends of the fragments so they can be easily captured by a surface equipped with complementary adaptors or amplified using specific couples of primers. The sequencing cycle requires detection of fluorescent signals derived from single base nucleotides as they're incorporated into the template strands. Sequencing is followed by an accurate bioinformatic analysis which starts with the alignment of the sequences with the reference

genome. Sequence divergences are thus identified (a process known as variant calling), and annotated (extraction of biological information on the variants). The initial pool of variants is further filtered by bioinformatic tools which allow to prioritize the potentially pathogenic variants distinguishing them from other polymorphisms or frequent variants.

More in detail, candidate variants are classified depending on their population frequency (usually only variants with Minor Frequency Allele – MAF- <1% are selected), available data on public population and disease-specific databases (ExAC, gnomAD, 1000Genomes...), biological effect on the transcript or protein (e.g. missense non-synonymous, frame-shift, splicing, stop-loss and stop-gain variants), conservation throughout evolution of the aminoacidic region affected by the nucleotide change, and quality of the coverage of targeted region. Besides SNVs (single nucleotide variations) and INDELS (small insertions and deletions), specific bioinformatic software allow to identify CNVs (copy number variations) as well as larger insertions and deletions (Figure 2).

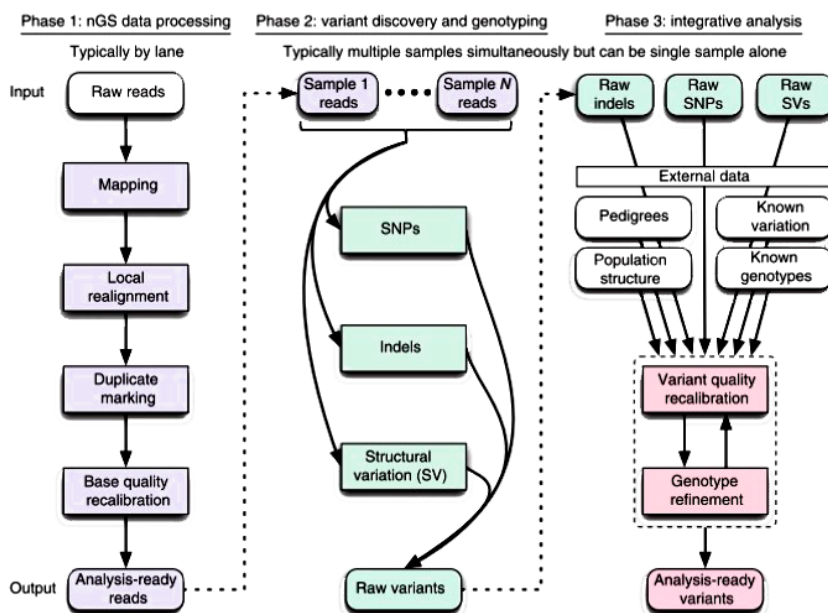


Figure 2. General workflow of NGS data processing (<https://software.broadinstitute.org/gatk>)

If the candidate variant doesn't turn out as a known pathogenic mutation after an accurate review of literature, or doesn't affect known disease-causing genes, further experimental validations will be required in order to establish its pathogenicity. Such validation can be achieved more easily if unrelated subjects or families with the same phenotype are found to carry the same genetic mutation, while in vitro and/or in vivo functional studies will be required to demonstrate a damaging biological effect of the mutation when just a single case or family is available. In such cases an accurate analysis of family history and segregation of the variant is mandatory in order to draw definite conclusions and to establish mode of inheritance (recessive or dominant) of candidate variants^{7,8}.

Hereditary spastic paraplegias (HSPs)

Genetics of HSP

The hereditary spastic paraplegias (HSPs) are a group of extremely clinically and genetically heterogeneous disorders with an estimated prevalence ranging from 0.1 to 9.6 per 10.000⁹.

They are characterized by progressive spasticity and weakness of lower extremities, which is mostly attributable to a selective degeneration of upper motor neurons.

HSP syndromes are mainly classified as pure HSP, when spinal involvement is isolated, and complicated when they are associated with other neurologic signs, such as ataxia, cognitive impairment, extrapyramidal signs, neuropathy, epilepsy, visual or hearing involvement.

Main pathologic finding consists in degeneration of distal portion of cortico-spinal tracts sometimes extended proximally to cervical spine, brain stem and brain. Degeneration of long axons of *fasciculus gracilis* is often reported in association. These observations may suggest that the specific vulnerability of long axons of the central nervous system underlies the pathogenesis of HSP axonopathy. Nevertheless, many HSP subtypes have been associated with structural abnormalities extending to other brain structures, white matter and frequently to lower motor neurons¹⁰.

While pure HSPs show just a slight variability in the clinical picture (mainly represented by slowly progressive and symmetrical spasticity rarely extending to upper limbs, with an age of onset ranging from childhood to late adulthood and a variable severity), complex HSPs encompass a wide range of different syndromes.

From a genetic point of view, the number of loci associated to HSPs is steadily growing and over 80 genes with all modes of inheritance have been already described.

Even though specific genetic types usually exhibit rather complicated than uncomplicated phenotypes, this statement is not always true, as many genetic subtypes of HSP may be associated with both clinical entities¹⁰.

The common presence of composite phenotypes (such as ataxic-spastic or dystonic spastic conditions), the heterogeneity in age of onset and progression rate amongst and within clinical subtypes and the extremely variable genetic background, make the diagnostic workflow a genuine challenge both for clinicians and geneticists.

Also, especially early onset inherited spasticity is often characterized by nonspecific symptoms which further contribute to hamper phenotypization and diagnostic codification/assignment¹¹.

A comprehensive review of all the genes responsible for pure and complicated HSP phenotypes and their molecular and clinical characterization goes beyond the aim of my thesis.

Nevertheless, an updated overview of disease-causing genes identified in association with pure and complicated phenotypes, with their main clinical features is provided below in Table 1.

HSP subtype (<i>gene; locus</i>)	Clinical and neuroimaging findings
SPG1 (<i>LICAM</i> ; Xq28)	XLR; Gareis–Mason syndrome; MASA syndrome, CRASH syndrome; hydrocephalus, agenesis of the corpus callosum
SPG2 (<i>PLP1</i> ; Xq22.2)	XLR; nystagmus, optic atrophy, severe hypomyelination
SPG3A (<i>ATL1</i> ; 14q22.1)	AD; rarely optic atrophy, seizures and thin corpus callosum
SPG4 (<i>SPAST</i> ; 2p22.3)	AD; classical Strümpell–Lorrain disease
SPG5A (<i>CYP7B1</i> ; 8q12.3)	AR; cerebellar ataxia, spastic ataxia, optic atrophy
SPG6 (<i>NIPA1</i> ; 15q11.2)	AD; postural tremor, seizures
SPG7 (<i>SPG7</i> ; 16q24.3)	AR; cerebellar ataxia, chronic progressive external ophthalmoplegia, cerebellar atrophy
SPG8 (<i>KIAA0196</i> ; 8q24.13)	AD; lower limb distal amyotrophy
SPG9A (<i>ALDH18A1</i> ; 10q24.1)	AD; CMNSS, SPACGR, cerebellar ataxia, ALS-like
SPG9B (<i>ALDH18A1</i> ; 10q24.1)	AR; facial dysmorphism, tremor, mental retardation, microcephaly, atrophy of the corpus callosum
SPG10 (<i>KIF5A</i> ; 12q13.3)	AD; rarely with Parkinsonism, cerebellar ataxia, neuropathy, distal amyotrophy, cognitive decline
SPG11 (<i>SPG11</i> ; 15q21.1)	AR; cerebellar ataxia, mental retardation, parkinsonism, distal amyotrophy, maculopathy, thin corpus callosum, “ears-of-the-lynx” sign, mild white matter changes
SPG12 (<i>RTN2</i> ; 19q13.32)	AD; classical pure HSP
SPG13 (<i>HSPD1</i> ; 2q33.1)	AD; classical pure HSP, marked spasticity
SPG14 (3q27-q28)	AR; distal motor neuropathy, mental retardation
SPG15 (<i>ZFYVE26</i> ; 14q24.1)	AR; Kjellin syndrome, distal amyotrophy, hearing loss, retinal degeneration, neuropathy, psychosis, cerebellar ataxia, levodopa-responsive Parkinsonism, epilepsy; thin corpus callosum, mild white matter changes
SPG16 (Xq11.2-q23)	XLR; motor aphasia, mental retardation, maxillary hypoplasia, short and thick distal phalanges
SPG17 (<i>BSCL2</i> ; 11q12.3)	AD; Silver syndrome, ALS-like phenotype, prominent thenar and interossei musculature wasting
SPG18 (<i>ERLIN2</i> ; 8p11.23)	AR; severe spasticity, seizures, mental retardation, multiple joint contractures
SPG19 (9q)	AD; mild neuropathy
SPG20 (<i>SPG20</i> ; 13q13.3)	AR; Troyer syndrome, multiple dysmorphisms, distal amyotrophy; rarely cerebellar ataxia, tongue

HSP subtype (<i>gene</i> ; locus)	Clinical and neuroimaging findings
	dyspraxia, cerebellar atrophy, mild white matter changes
SPG21 (<i>ACP33</i> ; 15q22.31)	AR; MAST syndrome, cognitive decline, extrapyramidal and cerebellar signs, neuropathy, thin corpus callosum, frontotemporal atrophy
SPG22 (<i>SLC16A2</i> ; Xq13.2)	XLSD; cerebellar ataxia, mental retardation, dystonia, typical dysmorphisms, hypomyelinating leukodystrophy
SPG23 (2q24-q32)	AR; Lison syndrome, patchy vitiligo, hyperpigmentation of exposed areas, lentigenes, facial features, mental retardation, mild neuropathy
SPG24 (13q14)	AR; pure HSP
SPG25 (6q23.3-q24.1)	AR; “familial intervertebral disk disease”
SPG26 (<i>B4GALNT1</i> ; 12p11.1-q14)	AR; mental retardation, neuropathy, distal amyotrophy, cerebellar ataxia, nystagmus, dystonia, dyskinesias
SPG27 (10q22.1-q24.1)	AR; typical pure HSP
SPG28 (<i>DDHD1</i> ; 14q22.1)	AR; typical pure HSP
SPG29 (1p31.1-p21.1)	AD; hearing loss, genetic anticipation, hiatal hernia
SPG30 (<i>KIF1A</i> ; 2q37.3)	AR; mild neuropathy, mild cerebellar ataxia, mild cerebellar atrophy
SPG31 (<i>REEPI</i> ; 2p11.2)	AD; distal amyotrophy
SPG32 (14q12-q21)	AR; mild mental retardation
SPG33 (<i>ZFYVE27</i> ; 10q24.2)	AD; pure HSP
SPG34 (Xq24-q25)	XLR; Brazilian family, pure HSP
SPG35 (<i>FA2H</i> ; 16q23.1)	AR; FAHN syndrome, cognitive decline, cerebellar ataxia, dystonia, optic atrophy, leukodystrophy, brain iron accumulation; rarely strabismus and seizures
SPG36 (12q23-q24)	AD; neuropathy
SPG37 (8p21.1-q13.3)	AD; pure HSP
SPG38 (4p16-p15)	AD; ALS-like phenotype, Silver syndrome-like
SPG39 (<i>PNPLA6</i> ; 19p13.2)	AR; Troyer syndrome-like, marked distal amyotrophy, cerebellar and thoracic spinal cord atrophy
SPG40 (unknown)	AD; pure HSP, genetic anticipation
SPG41 (11p14.1-p11.2)	AD; pure HSP
SPG42 (<i>SLC33A1</i> ; 3q25.31)	AD; pure HSP
SPG43 (<i>C19ORF12</i> ; 19q12)	AR; Malian and Brazilian families, severe amyotrophy, multiple contractures
SPG44 (<i>GJC2</i> ; 1q42.13)	AR; cerebellar ataxia, mental retardation, hearing loss, seizures, painful spasms, thin corpus callosum, hypomyelinating leukodystrophy

HSP subtype (<i>gene; locus</i>)	Clinical and neuroimaging findings
SPG45/SPG65 (<i>NT5C2</i> ; 10q24.32-q24.33)	AR; mental retardation, optic atrophy, joint contractures, strabismus, nystagmus, dysplastic corpus callosum, white matter changes
SPG46 (<i>GBA2</i> ; 9p13.3)	AR; cerebellar ataxia, mental retardation, head tremor, congenital cataracts, hearing loss, small testicles, cerebellar atrophy, thin corpus callosum
SPG47 (<i>AP4BI</i> ; 1p13.2)	AR; neonatal hypotonia, mental retardation, dysmorphisms, stereotypic laughter, shy character, spastic tongue protrusion, dystonia, late-onset febrile seizures, thin corpus callosum, white matter changes
SPG48 (<i>AP5ZI</i> ; 7p22.1)	AR; pure HSP, mild cervical spine hyperintensities
SPG49 (<i>TECPR2</i> ; 14q32.31)	AR; mental retardation, cerebellar ataxia, complicated gastroesophageal reflux, recurrent respiratory infections, dysmorphisms, recurrent central apnea, seizures, thin corpus callosum, cerebellar atrophy
SPG50 (<i>AP4MI</i> ; 7q22.1)	AR; neonatal hypotonia, mental retardation, strabismus, dysmorphisms, infantile-onset seizures, ventriculomegaly, thin corpus callosum, white matter changes
SPG51 (<i>AP4EI</i> ; 15q21.2)	AR; neonatal hypotonia, mental retardation, short stature, dysmorphisms, shy character, stereotypic laughter, seizures, nystagmus, joint contractures, marked leukodystrophy, ventriculomegaly, cerebellar atrophy
SPG52 (<i>AP4SI</i> ; 14q12)	AR; neonatal hypotonia, mental retardation, joint contractures, smiling attitude, shy character, dysmorphisms
SPG53 (<i>VPS37A</i> ; 8p22)	AR; mental retardation, dystonia, pectus carinatum, hypertrichosis
SPG54 (<i>DDHD2</i> ; 8p11.23)	AR; mental retardation, joint contractures, dysmorphisms, strabismus, optic nerve hypoplasia, thin corpus callosum, white matter changes, abnormal lipid peaks
SPG55 (<i>C12ORF65</i> ; 12q24.31)	AR; progressive visual loss, optic atrophy, strabismus, distal neuropathy, mental retardation, mild facial dysmorphisms, hypoplastic corpus callosum
SPG56 (<i>CYP2U1</i> ; 4q25)	AR; neuropathy, dystonia, mental retardation, white matter changes, thin corpus callosum, basal ganglia calcification
SPG57 (<i>TFG</i> ; 3q12.2)	AR; optic atrophy, neuropathy, contractures
SPG58 (<i>KIF1C</i> ; 17p13.2)	AR; cerebellar ataxia, hypodontia, mental retardation, microcephaly, short stature, fragmentary clonus, chorea, white matter changes
SPG59 (<i>USP8</i> ; 15q21.2)	AR; pure HSP
SPG60 (<i>WDR48</i> ; 3p22.2)	AR; nystagmus, neuropathy
SPG61 (<i>ARL6IP1</i> ; 16p12.3)	AR; severe neuropathy, severe mutilating acropathy
SPG62 (<i>ERLIN1</i> ; 10q24.31)	AR; cerebellar ataxia, distal amyotrophy

HSP subtype (<i>gene</i> ; locus)	Clinical and neuroimaging findings
SPG63 (<i>AMPD2</i> ; 1p13.3)	AR; short stature, white matter changes, thin corpus callosum
SPG64 (<i>ENTPDI</i> ; 10q24.1)	AR; mental retardation, microcephaly, delayed puberty, mild white matter changes
SPG66 (<i>ARSI</i> ; 5q32)	AR; severe neuropathy, thin corpus callosum, colpocephaly, cerebellar hypoplasia
SPG67 (<i>PGAPI</i> ; 2q33.1)	AR; global developmental delay, hand tremor, agenesis of the corpus callosum, cerebellar vermis hypoplasia, hypomyelination
SPG68 (<i>FLRT1</i> ; 11q13.1)	AR; mild amyotrophy, nystagmus, optic atrophy; without marked spasticity
SPG69 (<i>RAB3GAP2</i> ; 1q41)	AR; mental retardation, deafness, cataracts
SPG70 (<i>MARS</i> ; 12q13.3)	AD; mild mental retardation, nephrotic syndrome
SPG71 (<i>ZFR</i> ; 5p13.3)	AR; pure HSP, thin corpus callosum
SPG72 (<i>REEP2</i> ; 5q31.2)	AR/AD; postural tremor
SPG73 (<i>CPTIC</i> ; 19q13.33)	AD; mild amyotrophy
SPG74 (<i>IBA57</i> ; 1q42.13)	AR; neuropathy, optic atrophy
IAHSP (<i>ALS2</i> ; 2q33.1)	AR; ascending phenotype, marked pyramidal hypersignal
SPOAN (<i>KLC2</i> ; 11q13.2)	AR; Brazil, Egypt; nystagmus, optic atrophy, hyperhidrosis, marked acoustic startle reflex, distal amyotrophy, neuropathy; Parkinsonism; mild spine atrophy
CPSQ-I (<i>GADI</i> ; 2q31.1)	AR; mental retardation, occasional seizures, microcephaly, multiple contractures
Spastic paraplegia with deafness	XL; tremor, cataracts, deafness, short stature, hypogonadism
<i>BICD2</i> -associated HSP (9q22.31)	AR; amyotrophy
<i>CCT5</i> -associated HSP (5p15.2)	AR; Cavanagh variant, severe neuropathy, mutilating acropathy, vagal hyperactivity, mild spine atrophy
<i>FAM134B</i> -associated HSP (5p15.1)	AR; painless neuropathy, mutilating acropathy, hyperhidrosis
<i>EXOSC3</i> -associated HSP (9p13.2)	AR; short stature, mental retardation, cerebellar ataxia, strabismus, distal amyotrophy, tongue atrophy, adducted thumbs, cerebellar atrophy, enlarged cisterna magna
<i>LYST</i> -associated HSP (1q42.3)	AR; cerebellar ataxia, neuropathy, thoracic spine and cerebellar atrophy
<i>GRID2</i> -associated HSP (4q22.1-q22.2)	AR; cerebellar ataxia, frontotemporal dementia, lower motor neuron syndrome, ALS-like phenotype, cerebellar atrophy
<i>IFIH1</i> -related HSP (2q24.2)	AD; British families, multisystem inflammatory disorders
<i>ADARI</i> -related HSP (1q21.3)	AD; pure HSP, high interferon-1 levels

HSP subtype (<i>gene</i> ; locus)	Clinical and neuroimaging findings
<i>RNASEH2B</i> -related HSP (13q14.3)	AD; pure HSP, unspecific white matter changes
<i>KLC4</i> -associated HSP (6p21.1)	AR; joint contractures, marked pyramidal tract hypersignal, thin corpus callosum, white matter changes, cerebellar atrophy, dentate nucleus hypersignal
<i>PMCA4</i> -associated HSP (1q32.1)	AD; Chinese families, pure HSP
<i>MAG</i> -associated HSP (19q13.12)	AR; mental retardation, cerebellar ataxia, amyotrophy
<i>TUBB4A</i> -related HSP (19p13.3)	AR; cerebellar ataxia, hypomyelinating leukodystrophy
<i>FARS2</i> -associated HSP (6p25.1)	AR; pure HSP
<i>DNM2</i> -associated HSP (19p13.2)	AD; pure HSP
<i>MT-CO3</i> gene mutations	Mitochondrial; mental retardation, ophthalmoplegia, severe lactic acidosis, Leigh-like features, COX deficiency
<i>MT-TI</i> gene mutations	Mitochondrial; cerebellar ataxia, mental retardation, chronic progressive external ophthalmoplegia; normal muscle biopsy; cardiomyopathy, hearing loss, diabetes
<i>MT-ND4</i> gene mutations	Mitochondrial; visual loss (Leber-like)
<i>MT-ATP6</i> gene mutations	Mitochondrial; neuropathy, normal lactate, normal muscle biopsy

Table 1: Current classification of HSP (from *de Souza et al.* ¹²)

AD autosomal dominant; AR autosomal recessive; *XLR* X-linked recessive; *XLSD* X-linked semi-dominant; *ALS* amyotrophic lateral sclerosis; *MASA* mental retardation, aphasia, shuffling gait, and adducted thumbs; *CRASH* corpus callosum hypoplasia, retardation, adducted thumbs, spastic paraplegia, and hydrocephalus; *CMNSS* cataracts with motor neuropathy, short stature, and skeletal abnormalities; *SPACGR* spastic paraparesis with amyopathy, cataracts, and gastroesophageal reflux; *FAHN* fatty acid hydroxylase-associated neurodegeneration.

Despite this large genetic heterogeneity, it is possible to recognize specific groups of biological modules underlying pathogenesis of most HSP subtypes (Table 2). These encompass: dysfunction of lipid metabolism; axonal transport disturbances; disorder of myelination; neural development abnormalities; mitochondrial dysfunction; impairment of vesicular trafficking; structural disturbances of Endoplasmic Reticulum (ER) and ER-stress related to abnormal protein

morphogenesis; DNA repair and oxidative stress. Many genes associated to HSP encode for protein involved in similar biological functions, and equally a single protein can participate to several of the above-mentioned functions¹³.

HSP classification based on intracellular pathophysiological mechanisms	
Membrane trafficking and organelle shaping	SPG3A, SPG4, SPG6, SPG11, SPG15, SPG18, SPG20, SPG31, SPG59, SPG60, SPG61, SPG62, SPG69, SPG72
Axonal transport	SPG4, SPG10, SPG30, SPG58
Mitochondrial dysfunction	SPG7, SPG20, SPG31
Lipid metabolism disturbances	SPG5, SPG26, SPG28, SPG35, SPG39, SPG46, SPG54, SPG56
Myelination abnormalities	SPG1, SPG2, SPG39, SPG42, SPG67

Table 2. HSP classification based on intracellular pathophysiological mechanisms (from *de Souza et al.*¹²)

Amongst the others, the importance of many HSP related genes for ER network maintenance and modelling is well known. Autosomal dominant mutation in atlastin-1 (*SPG3A*), receptor expression enhancing protein 1 (*REEP1*; *SPG31*), and spastin (*SPG4*) underly more than a half of HSP cases and all of them have been associated to an evident dysfunction of the ER network¹⁴.

To date, no effective or preventing treatment exists for HSP. Symptomatic therapies such as drugs or physical therapy to reduce spasticity can be helpful to delay motor deterioration. Anticholinergic drugs and pregabalin or gabapentin are often used for urinary urgency and neuropathic pain, respectively¹⁰.

Identification of responsible genes, pattern of inheritance and deeper understanding of common pathways underlying pathophysiology of diseases, represents a pre-requisite for the development of adequate models to test possible therapies and eventually to select of patient for personalized treatment options.

Role of NGS in HSP and related disorders

The evolution of NGS technologies had a major impact on diagnosis and screening of HSP patients. The availability of Next-generation sequencing, and disease-specific gene panels for HSPs, has improved the ability to reach a molecular diagnosis with an advantage in terms of cost-effectiveness.

The most accurate diagnostic approach to patient with a diagnosis of possible inherited HSP, relies on a preliminary detailed clinical investigation in parallel with collection of family history and, if necessary, phenotyping of family members.

The possibility to perform a genetic screening at early stages of diagnostic workup, often allows to avoid other unnecessary expensive or invasive investigations.

In a cross-sectional study on 519 HSP families of German origin, NGS technologies were crucial for the molecular diagnosis of 240 patients, with higher diagnostic yields in familial cases, and much lower (28%) in sporadic patients¹⁵.

In another paediatric cohort studied with a systematic approach including targeted sequencing of HSP related genes, the diagnosis was reached in 62% of patients¹⁶.

Overall, recent reports estimated genetic diagnosis in heterogeneous cohorts of HSP patients can be reached in >50% of individuals with the application of new high throughput technologies^{17,18}.

Additionally, patients affected by complicated HSP and overlapping phenotypes represent an ideal candidate for NGS, and the application of WES in cases with unusual combination of signs and symptoms has already revealed its advantages.

Benefits of NGS introduction are detectable in the diagnostic area of rare neurometabolic disorders, another category of highly heterogeneous diseases in which spasticity often represents a leading sign. A recent systematic review estimated a diagnostic yield of WES ranging from 16% to 68% in this category of rare inherited conditions when unsolved after biochemical and clinical analysis¹⁹.

An increasingly recognized extremely heterogeneous category of patients is represented by subjects affected by hereditary “spastic ataxia” (SPAX), where symptoms of spasticity and spinocerebellar ataxia (SCA) co-occur in the same individual, and can also be combined

with other neurological or extra-neurological signs. In a cohort of HSP and SCA patients, the application of a broader targeted sequencing panel, suggested that one of the leading causes of spastic ataxia phenotype is the *SPG7* gene, which could be alone responsible of about 50% of cases. *SPG7* is normally classified as a HSP gene, being found in about 8-9% of autosomal recessive patients, but has also been associated to mixed phenotypes and pure ataxia²⁰.

Vice versa, overlapping phenotypes with spasticity as a major sign, have been also associated to more typical SCA-related genes, such as *SYNE1*, and also to *SACS* gene. Recent evidence supports the use of Exome Sequencing in these group of patients to grant greater diagnostic outputs²¹.

This phenomenon, also known as pleiotropy, is applicable to most categories of complex neurodegenerative disorders with locus and allelic heterogeneity, indicating that similar phenotypes can be caused by mutations in several different genes, and parallelly, mutations in the same gene or even the same mutation can be associated to different phenotypes. Explanations for pleiotropy are likely multiple: different mutations in the same gene could have diverse downstream effects on the encoded protein, or their phenotypic expression could be changed by other modifier genes; meanwhile, it is undisputed that different genes involved in the same biological pathways can give raise to the same phenotypes²².

The evidence of common genes and molecular pathways involved in both categories of patients, and the high frequency of overlapping

phenotypes, suggest that classification of HSP and SCA entities should adopt a more systematic approach based on pathophysiological mechanism and gene function rather than phenotype, which could also help selection of patients for possible future therapeutic approaches²³.

Overall, the introduction of NGS has undoubtedly given a boost to gene/variant discovery in the field of HSP, contributing to the elucidation of pathways involved in disease aetiology. Nevertheless, also pitfalls and new challenges for researchers emerge: establishing pathogenicity or contribution to the disease of variants of “unknown significance” and distinguishing them from benign polymorphisms, often reveals arduous; most importantly, much work has to be devoted to achieve translation of novel genetic information to a better understanding of pathomechanisms of neurodegenerative disorders, and finally to the development of targeted therapeutic strategies.

Mitochondrial diseases

Genetics of mitochondrial diseases

Mitochondria, also known as the powerhouse of cells, are highly dynamic organelles of endosymbiotic origin, which conserve their own genome and gene expression machinery. Mitochondria fulfil various important roles in cellular metabolism. They are the crossroad of main catabolic pathways, namely citric acid cycle, β -oxidation, electron transfer and oxidative phosphorylation (OXPHOS), which are responsible for the production of the majority of cellular ATP

(adenosine 5'-triphosphate). Additionally, mitochondria play essential roles in amino acid, nucleobase, lipid and cofactor biosynthesis. In addition, they are involved in calcium homeostasis and control programmed cell death or apoptosis.

Over 99% of proteins required for mitochondrial function are actually encoded in the nuclear DNA and imported into mitochondria through strictly regulated import processes²⁴.

Taken together, all these factors point out the central role of mitochondria in overall energetic metabolism of cells; consequently, alterations of these pathways lead to major energetic deficits associated with severe hereditary diseases known as mitochondrial disorders^{24,25}. Hereditary mitochondrial disorders are caused by alteration of mitochondrial metabolic pathways which generates severe energetic disfunction²⁵. Their estimated prevalence ranges between 5 and 15 cases every 100.000 individuals²⁶. Mitochondrial disorders can be caused either by mutations in nuclear genes encoding for mitochondrial proteins (e.g MRC subunits or assembly factors) or can result from alterations on mtDNA (Figure 3). A list of genes and mutations directly linked to mitochondrial pathology is regularly updated at MitoMap (<https://www.mitomap.org/>).

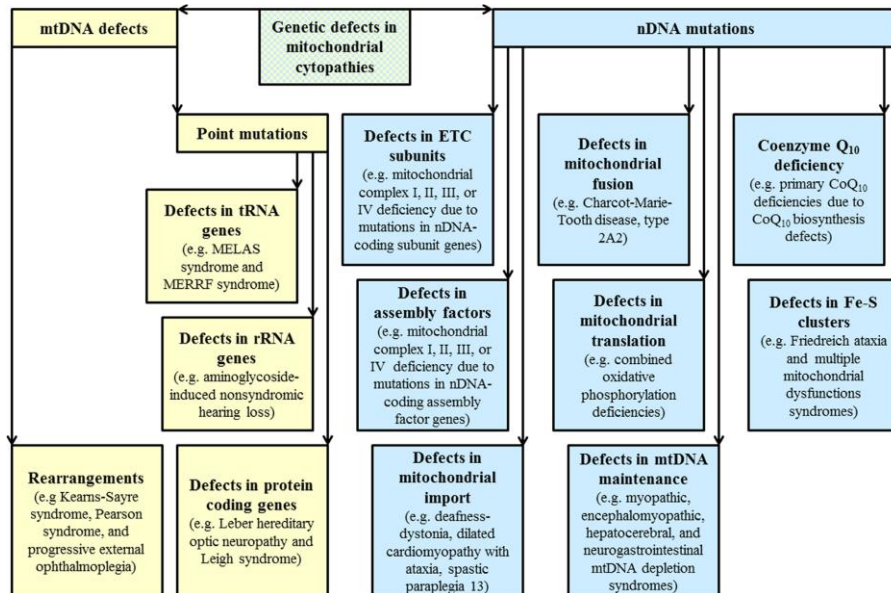


Figure 3: Simplified list of genetic defects leading to mitochondrial dysfunction (from El-Hattab *et al.*,³⁵)

mtDNA alterations are responsible for the majority of mitochondrial diseases arising in adulthood, while recessive nDNA mutations are most frequently the cause of childhood onset diseases. nDNA alterations can affect mitochondria in multiple ways: in particular, mutations on genes involved in mtDNA replication or maintenance can result in mtDNA qualitative or quantitative defects. Primary mtDNA alterations, ranging from point mutations to large deletions, show some intrinsic characteristic that distinguish them from nuclear defects. They can either be sporadic (acquired during embryogenesis) or, more frequently, maternally inherited, because only oocyte mitochondria, not the sperm, are maintained during fecundation. As each cell contains high number of mitochondria, and each mitochondrion holds dozens of mitochondrial genomes, from hundreds to thousands of mitochondrial

genomes are found in a single cell: this phenomenon is also known as polyplasmia. Consequently, wild-type and mutated mtDNA molecules can coexist: this condition, known as heteroplasmy, denotes that a clinical phenotype would appear just when the amount of mutated mtDNAs reaches a definite threshold. Besides, during mitosis mtDNA is randomly distributed to daughter cells; thus, heteroplasmic alleles can also modify their ratio during mitotic cell division in different tissues. Other environmental and epigenetic factor can finally influence the clinical manifestations of the disease. Reports on completely different phenotypes caused by mutation on the same gene or even by the same mutation are highly common, just as the frequency of reports on similar phenotypes caused by mutation on disparate genes. Moreover, mitochondrial disorders are frequently multisystemic, although brain, heart and muscle, are the most affected systems as they require a high amount of energy to function.

All these considerations, together with individual genetic background and tissue specificity, contribute to the severity of mitochondrial dysfunctions and determine the complexity of phenotypes and the extreme clinical heterogeneity associated with these diseases²⁵.

From a clinical point of view, the multi-systemic nature of mitochondrial diseases makes molecular diagnosis particularly challenging, as many different medical specialties are often involved in patient care. On the other hand, this remarkably multi-systemic nature aids in raising suspicion for the diagnosis of a mitochondrial disease.

Childhood onset defects are often more severe and commonly arise with non-specific clinical signs including hypotonia, encephalopathy, seizures, motor and developmental delay, hearing loss and hypertrichosis. Syndromic phenotypes include, amongst the others, Leigh syndrome, Alpers syndrome and Pearson syndrome (Table 2).

Syndrome	Genetics	Clinical features
<i>Childhood-onset mitochondrial diseases</i>		
Leigh syndrome	>75 genes in nDNA and mtDNA	Acute periods of neurodevelopmental regression followed by partial recovery, hypotonia, dystonia, hypopnoea, dysphagia, epilepsy, failure to thrive, encephalopathy, and basal ganglia and brainstem lesions
Alpers–Huttenlocher syndrome (AHS)	nDNA (<i>POLG</i> -related)	Intractable epilepsy, psychomotor regression and liver disease; might also include the clinical features of MCHS and MEMSA
Childhood myocerebrohepatopathy spectrum (MCHS)		Neuropathy, ataxia, hypotonia, myoclonus (spontaneous muscle contractions), choreoathetosis (the occurrence of involuntary jerky, writhing movements of muscles or muscle groups) and Parkinsonism, in addition to renal tubulopathy
Ataxia neuropathy spectrum (ANS; previously referred to as mitochondrial recessive ataxia syndrome (MIRAS) and sensory ataxia neuropathy dysarthria and ophthalmoplegia (SANDO))		Sensory axonal neuropathy with variable sensory and cerebellar ataxia
Myoclonic epilepsy myopathy sensory ataxia (MEMSA; previously referred to as spinocerebellar ataxia with epilepsy (SCAE))		Epilepsy, PEO, seizures, dysarthria, dementia, spasticity and myopathy
Sengers syndrome	nDNA (<i>AGK</i> mutations)	Congenital cataracts, hypertrophic cardiomyopathy, skeletal myopathy, exercise intolerance and lactic acidosis. Patients can present with or without mtDNA depletion in muscle

MEGDEL syndrome (also known as 3-methylglutaconic aciduria with deafness, encephalopathy and Leigh-like syndrome)	nDNA (<i>SERAC1</i> mutations)	Sensorineural hearing loss, encephalopathy, failure to thrive, hypotonia, psychomotor delay, dystonia, spasticity, hypoglycaemia, hepatopathy and lactic acidosis
Pearson syndrome	Single, large-scale mtDNA deletion or rearrangements of mtDNA (often sporadic)	Sideroblastic anaemia of childhood associated with exocrine and/or endocrine pancreatic dysfunction, pancytopenia and renal tubulopathy
Congenital lactic acidosis (CLA)	nDNA, <i>de novo</i> mtDNA point mutations or inherited mtDNA point mutations	Childhood onset, often fatal, progressive neuromuscular weakness, accumulation of lactate in the blood (acidosis), urine and/or CSF

Table 2. Clinical syndromes, inheritance pattern and phenotypic features of childhood-onset mitochondrial diseases (from Gorman *et al*²⁶). CSF, cerebrospinal fluid; mtDNA, mitochondrial DNA; nDNA, nuclear DNA

Syndromic phenotypes are more frequently documented in adult onset mitochondrial disorders, even if a large number of patients still manifest with symptoms and progression course which do not conform to a specific one.

Far from being fully exhaustive, I provide below a short list of the most frequently diagnosed mitochondrial syndromes in adulthood (Table 3).

Syndrome	Genetics	Clinical features
<i>Adult-onset mitochondrial diseases</i>		
Leber hereditary optic neuropathy (LHON)	Mutations in mtDNA, for example, m.11778G>A (<i>MT-ND4</i>), m.14484T>C (<i>MT-ND6</i>) and m.3460G>A (<i>MT-ND1</i>)	Subacute painless bilateral visual loss. Might also include dystonia, cardiac pre-excitation syndromes and LHON associated with multiple sclerosis-like symptoms (Harding syndrome)

Kearns–Sayre syndrome (KSS)	Single, large-scale mtDNA deletion (often sporadic)	PEO, pigmentary retinopathy (progressive vision impairment due to degeneration of the rod photoreceptors), CSF protein levels of >1 g per l, cerebellar ataxia, cardiac conduction abnormalities (age of onset <20 years), myopathy, diabetes mellitus, deafness, bulbar weakness and dementia
Mitochondrial myopathy, encephalopathy, lactic acidosis and stroke-like episodes (MELAS) syndrome	Mutations in mtDNA, such as m.3243A>G in <i>MT-TL1</i> , and 23 other pathogenetic variants in <i>MT-TL1</i> and in other mtDNA genes (for example, <i>MT-TF</i> , <i>MT-TV</i> and <i>MT-TQ</i>)	Stroke-like episodes. Can also include deafness, diabetes mellitus, pigmented retinopathy, cardiomyopathy, cerebellar ataxia, seizures, encephalopathy, lactic acidosis and mitochondrial myopathy
Myoclonic epilepsy with ragged red fibres (MERRF)	Mutations in mtDNA, such as m.8344A>G in <i>MT-TK</i> , and other pathogenetic variants in <i>MT-TF</i> , <i>MT-TL1</i> , <i>MT-TI</i> and <i>MT-TP</i>	Progressive myoclonic epilepsy, ataxia, weakness. Can also include pigmented retinopathy, sensorineural hearing loss, lactic acidosis, lipomata, spasticity and cardiac conduction defects (Wolff–Parkinson–White syndrome)
Neurogenic muscle weakness, ataxia and retinitis pigmentosa (NARP)	Mutations in mtDNA, such as <i>MT-ATP6</i> m.8993T>G, which is the most common variant, and m.8993T>C, a less severe variant	Early childhood onset, can remain quiescent or stable into adulthood, sensorimotor neuropathy, ataxia and pigmentary retinopathy. Can also include seizures, learning disability, dementia, proximal neurogenic muscle weakness, basal ganglia abnormalities, sensorineural hearing loss, short stature, CPEO, cardiac conduction defects, obstructive sleep apnoea and neuropsychiatric disorders ⁸ . These syndromes form a clinical continuum with Leigh syndrome
Chronic progressive external ophthalmoplegia (CPEO) ⁸⁴	<i>TYMP</i> , which encodes thymidine phosphorylase	Gastrointestinal dysmotility, muscle weakness and atrophy, neuropathy, retinopathy, hearing loss, leukoencephalopathy and depleted <i>TYMP</i> activity
	<i>POLG1</i> , which encodes α -DNA polymerase subunit γ 1	Ataxia, peripheral sensory neuropathy, Parkinsonism, premature ovarian failure, psychiatric symptoms, MELAS syndrome and epilepsy
	<i>POLG2</i> , which encodes DNA polymerase subunit γ 2	Ptosis and proximal myopathy, dystrophy, cerebellar ataxia and gastrointestinal symptoms
	<i>MPV17</i> , which encodes protein MPV17	Distal limb weakness, neuropathy, exercise intolerance, diabetes mellitus, ptosis, hearing loss, gastrointestinal dysmotility, depression and Parkinsonism

	<i>DGUOK</i> , which encodes deoxyguanosine kinase	Exercise intolerance, limb girdle weakness, muscle cramps and occasional dysphagia
	<i>TK2</i> , which encodes thymidine kinase 2	Ptosis, scapular winging, facial and proximal muscle weakness and wasting, dysphagia and respiratory deficiency
	<i>RRM2B</i> , which encodes ribonucleotide-diphosphate reductase subunit M2B	Hearing loss, bulbar dysfunction, renal disease and gastrointestinal disturbance
	<i>C10orf2</i> , which encodes Twinkle protein	Isolated PEO with or without mild proximal myopathy and exercise intolerance, fatigue, hearing loss, Parkinsonism psychiatric symptoms and cardiac involvement
	<i>SLC25A4</i> , which encodes ADP/ATP translocase 1	Indolent or mild PEO with or without ptosis, facial weakness, mild hearing loss, psychiatric symptoms and neuropathy
	<i>SPG7</i> , which encodes paraplegin	Ataxia, optic atrophy, myopathy, spastic paraparesis and cerebellar atrophy
	<i>AFG3L2</i> , which encodes AFG3-like protein 2	Ataxia, spastic paraparesis, myopathy and cerebellar atrophy
	<i>OPA1</i> , which encodes dynamin-like 120 kDa protein	Optic atrophy, early-onset visual loss, ataxia and deafness, spasticity, axonal neuropathy, diabetes mellitus, epilepsy and dementia
	<i>C20orf7</i> , which encodes mitochondrial genome maintenance exonuclease 1	Proximal muscle weakness, generalized muscle wasting, respiratory deficiency, chronic renal failure, cardiac arrhythmias and depression
	<i>DNA2</i> , which encodes DNA replication ATP-dependent helicase/nuclease DNA2	Progressive myopathy
	<i>RNASEH1</i> , which encodes ribonuclease H1	Myopathy, dysphagia and spinocerebellar signs
	<i>DNM2</i> , which encodes dynamin 2	Facial and proximal weakness, axonal neuropathy and cardiomyopathy
Mitochondrial neurogastrointestinal encephalopathy (MNGIE) syndrome	<i>TYMP</i> , <i>RRM2B</i> and <i>POLG</i>	Gastrointestinal dysmotility, muscle weakness and atrophy, PEO, neuropathy, retinopathy, hearing loss, leukoencephalopathy ² and depleted TYMP activity ²

Table 3. Clinical syndromes, inheritance pattern and phenotypic features of adult-onset mitochondrial diseases (from Gorman *et al*²⁶). CSF, cerebrospinal fluid; mtDNA, mitochondrial DNA; nDNA, nuclear

DNA; PEO, progressive external ophthalmoplegia. *Not affected in RRM2B and POLG variants.

Complex I (CI) deficiency is the most common enzymatic defect found in primary mitochondrial diseases as mutations in many of its 44 structural subunits either in many other nuclear encoded assembly and maturation factors, can damage its function²⁷, thus making CI enzymatic activity extremely vulnerable.

For the same reason, CI deficiency also shows extreme phenotypic heterogeneity and can underly a wide variety of clinical conditions, ranging from severe infantile disease to adult-onset neurodegenerative disorders, namely Leigh syndrome (OMIM entry #256000), Leber hereditary optic neuropathy (#535000), and some forms of Parkinson disease (#556500), but also cases of isolated myopathy or hypertrophic cardiomyopathy, unspecific encephalopathy and liver disease (see Fiedorczuk and Sazanov, 2018 for an updated review of pathologic conditions associated to CI deficiency)²⁸.

In particular, Leigh syndrome is the most common early onset progressive neurodegenerative disease that results from an alteration of mitochondrial energy production. It is mainly characterized by bilateral and symmetric lesions of the basal ganglia, cerebellum and brainstem in association with blood and CSF (cerebrospinal fluid) hyperlactacidemia²⁹.

If prenatal and preimplantation genetic diagnosis have given a boost to prevention of mitochondrial diseases, unfortunately, effective therapies for the vast majority of mitochondrial diseases are still lacking:

management of patients mainly relies on supportive and symptomatic therapies for organ specific complications.

The vast majority of ongoing or completed clinical trials have been performed on homogeneous groups of patients (mainly MELAS, LHON, MNGIE, primary mitochondrial myopathies). Available data are fragmentary and often ambiguous, but new approaches are going (or have recently started recruitment) to be tested patients in a clinical setting (see Hirano *et al.*³⁰ for an updated review on the topic).

Besides, new promising treatments are emerging from preclinical studies.

Translation of these promising techniques to clinical settings requires extensive pathophysiological investigations and recruitment of homogeneous cohorts of patients.

Role of NGS in mitochondrial diseases

The introduction of next generation sequencing (NGS) and massively parallel sequencing in the late 2000s has definitely upgraded the diagnostic potential for mitochondrial diseases, especially for the discovery of nuclear genes associated with mitochondrial dysfunctions, increasing the diagnostic yield up to 60% for certain conditions.

Indeed, NGS allows to analyze both mtDNA and nuclear genomes within a single assay. The off-target mtDNA sequence can be identified

bioinformatically and sensitivity of new techniques has improved up to a detection of a 10% heteroplasmy²⁶.

Undoubtedly, definite diagnosis relies on an accurate clinical characterization of patients and, in many cases, on complementary biochemical and histochemical tests on muscle biopsies or skin fibroblasts³¹.

Widely exploited biomarkers of disease such as blood lactic acid, CPK (creatine kinase), pyruvic acid, thymidine, alanine, acylcarnitine, and urinary organic acids, are mostly unspecific, but they can help to address the diagnostic workup³².

During the last few years, levels of serum FGF21 (fibroblast growth factor 21) is emerging as a promising biomarker for primary muscle-manifesting mitochondrial respiratory chain deficiencies in both adults and children³³.

Despite the wide growth of sequencing techniques and their combination with the above-mentioned complementary investigations, a lot of patient still remain undiagnosed. There are a number of underlying reasons: missing of large-scale deletions, uneven coverage of some genomic regions, such as those with high load of C and G residues, and identification of variants of uncertain significance within noncoding or regulatory regions of DNA, which represent up to 99% of genomic material, are amongst the most critical ones. In the last few years, -omics technologies are starting to take hold and, in some cases, they could be the key determinant to clarify the role of noncoding variants on splicing patterns (transcriptomic), or on tissue-specific

protein expression and metabolic pathways (proteomics and metabolomics). The development of such technologies and their mutual integration will hopefully represent major catalysts to understand still unsolved questions²⁶.

The identification of a constantly increasing amount of new causative nuclear disease genes, has also allowed to unravel novel pathogenetic mechanisms and thus has driven the development of new cellular and animal models to test potential targeted therapeutic approaches.

In this perspective, the enlargement of cohorts of mitochondrial patient with a molecular diagnosis, will provide a further breakthrough. In several countries, National clinical networks have been established to recruit and standardize patient phenotyping. The collection of clinical information and biological material from patients affected by mitochondrial diseases enables the study of their natural history and often allows to overcome drawbacks associated to the identification of rare mitochondrial diseases in isolated individuals. Already established National networks include: the German network for mitochondrial disorders (mitoNET), the nationwide Italian collaborative network of mitochondrial diseases (Mitocon), the UK MRC mitochondrial disease patient cohort study, and the North American Mitochondrial Disease Consortium (NAMDC). Nevertheless, the definite recognition of pathogenicity of new disease genes requires the identification of several individual cases from unrelated families with a similar phenotype. Sufficiently powered sample sizes cannot generally be reached by Isolated National datasets. The extension of storage of data collection from single National networks to a coordinated European network

empowers the creation of large biological banks and high-quality NGS datasets from accurately-phenotyped patients. GENOMIT consortium, which coordinates European National networks, since its establishment in 2015, allowed the identification and validation of more than 30 novel genetic disorders in patients with suspected mitochondrial disease, thus providing a genetic diagnosis for more than 300 individuals.

AIM OF THE THESIS

The work I carried throughout my PhD period has been aimed to identify and characterize disease genes associated with rare neurological disorders.

Chapter 2 is dedicated to phenotypic and molecular characterization of two patients with an atypical neuroaxonal dystrophy presentation in which a homozygous mutation within the *TFG* gene has been identified by mean of WES technology.

Chapter 3 is a report of three unrelated families with individuals affected by Leigh syndrome and carrying the same biallelic mutations in the *NDUFAF6* gene. The identification of a novel intronic variant is integrated with its functional validation through mRNA analysis.

Chapter 4 and 5 describe two cases with complex clinical phenotypes and the identification of two novel mutations in already reported disease genes, respectively *OTX2* and *DNMT1*. In the patient with *OTX2* mutation, molecular and clinical presentation remains not entirely explained by a single gene mutation and additional possible genetic modifiers were found. This case represents an example of how detailed collection of clinical data and family history in parallel to NGS data analysis is often helpful in order to identify composite genotypes sometimes associated with complicated inherited syndromes.

Additionally (see Chapter 6), I dedicated the last few months of my PhD to investigate the feasibility of a promising xenotopic therapy for Leigh syndrome and other neurological conditions associated with mitochondrial complex I deficiency, using engineered patient fibroblasts as a cellular model of disease.

References

1. Boycott KM, Vanstone MR, Bulman DE, MacKenzie AE. Rare-disease genetics in the era of next-generation sequencing: discovery to translation. *Nat Rev Genet.* 2013 Oct;14(10):681-91. doi: 10.1038/nrg3555.
2. Ng SB, Turner EH, Robertson PD, Flygare SD, Bigham AW, Lee C, Shaffer T, Wong M, Bhattacharjee A, Eichler EE, Bamshad M, Nickerson DA, Shendure J. Targeted capture and massively parallel sequencing of 12 human exomes. *Nature.* 2009 Sep 10;461(7261):272-6. doi:10.1038/nature08250.
3. van Dijk EL, Auger H, Jaszczyszyn Y, Thermes C. Ten years of next-generation sequencing technology. *Trends Genet.* 2014;30:418-426.
4. Morey M, Fernandez-Marmiesse A, Castineiras D, Fraga JM, Couce ML, Cocho JA. A glimpse into past, present, and future DNA sequencing. *Mol Genet Metab* 2013;110:3-24.
5. Klein CJ, Foroud TM. Neurology Individualized Medicine: When to Use Next-Generation Sequencing Panels. *Mayo Clin Proc.* 2017 Feb;92(2):292-305. doi: 10.1016/j.mayocp.2016.09.008. Review.
6. Metzker ML. Sequencing technologies—the next generation. *Nat Rev Genet* 2010;11:31-46.
7. Legati A, Reyes A, Nasca A, Invernizzi F, Lamantea E, Tiranti V, Garavaglia B, Lamperti C, Ardisson A, Moroni I, Robinson A, Ghezzi D, Zeviani M. New genes and pathomechanisms in mitochondrial disorders unraveled by NGS technologies. *Biochim Biophys Acta.* 2016 Aug;1857(8):1326-1335. doi: 10.1016/j.bbabbio.2016.02.022.
8. Richards S, Aziz N, Bale S, Bick D, Das S, Gastier-Foster J, Grody WW, Hegde M, Lyon E, Spector E, Voelkerding K, Rehm HL;

- ACMG Laboratory Quality Assurance Committee. Standards and guidelines for the interpretation of sequence variants: a joint consensus recommendation of the American College of Medical Genetics and Genomics and the Association for Molecular Pathology. *Genet Med*. 2015 May;17(5):405-24. doi: 10.1038/gim.2015.30.
9. Ruano L, Melo C, Silva MC, Coutinho P. The global epidemiology of hereditary ataxia and spastic paraplegia: a systematic review of prevalence studies. *Neuroepidemiology*. 2014;42(3):174-83. doi: 10.1159/000358801.
 10. Fink JK. Hereditary spastic paraplegia: clinico-pathologic features and emerging molecular mechanisms. *Acta Neuropathol*. 2013 Sep;126(3):307-28. doi: 10.1007/s00401-013-1115-8. Epub 2013 Jul 30.
 11. Crowther LM, Poms M, Plecko B. J Multiomics tools for the diagnosis and treatment of rare neurological disease. *Inherit Metab Dis*. 2018 May;41(3):425-434. doi: 10.1007/s10545-018-0154-7.
 12. de Souza PVS, de Rezende Pinto WBV, de Rezende Batistella GN, Bortholin T, Oliveira A Hereditary Spastic Paraplegia: Clinical and Genetic Hallmarks. *Cerebellum*. 2017 Apr;16(2):525-551. doi: 10.1007/s12311-016-0803-z SB1.
 13. Lo Giudice T, Lombardi F, Santorelli FM, Kawarai T, Orlacchio A. Hereditary spastic paraplegia: clinical-genetic characteristics and evolving molecular mechanisms. *Exp Neurol*. 2014 Nov;261:518-39. doi: 10.1016/j.expneurol.2014.06.011.
 14. Park SH, Zhu PP, Parker RL, Blackstone C. Hereditary spastic paraplegia proteins REEP1, spastin, and atlastin-1 coordinate microtubule interactions with the tubular ER network. *J Clin Invest*. 2010 Apr;120(4):1097-110. doi: 10.1172/JCI40979.

15. Schüle R, Wiethoff S, Martus P, Karle KN, Otto S, Klebe S, Klimpe S, Gallenmüller C, Kurzwelly D, Henkel D, Rimmele F, Stolze H, Kohl Z, Kassubek J, Klockgether T, Vielhaber S, Kamm C, Klopstock T, Bauer P, Züchner S, Liepelt-Scarfone I, Schöls L. Hereditary spastic paraplegia: Clinicogenetic lessons from 608 patients. *Ann Neurol*. 2016 Apr;79(4):646-58. doi: 10.1002/ana.24611.
16. Travaglini L, Aiello C, Stregapede F, D'Amico A, Alesi V, Ciolfi A, Bruselles A, Catteruccia M, Pizzi S, Zanni G, Loddo S, Barresi S, Vasco G, Tartaglia M, Bertini E, Nicita F. The impact of next-generation sequencing on the diagnosis of pediatric-onset hereditary spastic paraplegias: new genotype-phenotype correlations for rare HSP-related genes. *Neurogenetics*. 2018 May;19(2):111-121. doi: 10.1007/s10048-018-0545-9.
17. Kara E, Tucci A, Manzoni C, Lynch DS, Elpidorou M, Bettencourt C, Chelban V, Manole A, Hamed SA, Haridy NA, Federoff M, Preza E, Hughes D, Pittman A, Jaunmuktane Z, Brandner S, Xiromerisiou G, Wiethoff S, Schottlaender L, Proukakis C, Morris H, Warner T, Bhatia KP, Korlipara LV, Singleton AB, Hardy J, Wood NW, Lewis PA, Houlden H. Genetic and phenotypic characterization of complex hereditary spastic paraplegia. *Brain*. 2016 Jul;139(Pt 7):1904-18. doi: 10.1093/brain/aww111.
18. Lynch DS, Koutsis G, Tucci A, Panas M, Baklou M, Breza M, Karadima G, Houlden H. Hereditary spastic paraplegia in Greece: characterisation of a previously unexplored population using next-generation sequencing. *Eur J Hum Genet*. 2016 Jun;24(6):857-63. doi: 10.1038/ejhg.2015.200.
19. Shakiba M, Keramatipour M. Effect of Whole Exome Sequencing in Diagnosis of Inborn Errors of Metabolism and Neurogenetic Disorders. *Iran J Child Neurol*. 2018 Winter;12(1):7-15. Review.

20. van de Warrenburg BP, Schouten MI, de Bot ST, Vermeer S, Meijer R, Pennings M, Gilissen C, Willemsen MA, Scheffer H, Kamsteeg EJ. Clinical exome sequencing for cerebellar ataxia and spastic paraplegia uncovers novel gene-disease associations and unanticipated rare disorders. *Eur J Hum Genet*. 2016 Oct;24(10):1460-6. doi: 10.1038/ejhg.2016.42.
21. Galatolo D, Tessa A, Filla A, Santorelli FM. Clinical application of next generation sequencing in hereditary spinocerebellar ataxia: increasing the diagnostic yield and broadening the ataxia-spasticity spectrum. A retrospective analysis. *Neurogenetics*. 2018 Jan;19(1):1-8. doi: 10.1007/s10048-017-0532-6.
22. Pang SY, Teo KC, Hsu JS, Chang RS, Li M, Sham PC, Ho SL. The role of gene variants in the pathogenesis of neurodegenerative disorders as revealed by next generation sequencing studies: a review. *Transl Neurodegener*. 2017 Oct 6;6:27. doi: 10.1186/s40035-017-0098-0. eCollection 2017.
23. Synofzik M, Schüle R. Overcoming the divide between ataxias and spastic paraplegias: Shared phenotypes, genes, and pathways. *Mov Disord*. 2017 Mar;32(3):332-345. doi: 10.1002/mds.26944.
24. Fox TD. Mitochondrial protein synthesis, import, and assembly. *Genetics*. 2012 Dec;192(4):1203-34.
25. Turnbull DM, Rustin P. Genetic and biochemical intricacy shapes mitochondrial cytopathies. *Neurobiol Dis*. 2016 Aug;92(Pt A):55-63.
26. Gorman GS, Chinnery PF, DiMauro S, Hirano M, Koga Y, McFarland R, Suomalainen A, Thorburn DR, Zeviani M, Turnbull DM. Mitochondrial diseases. *Nat Rev Dis Primers*. 2016 Oct 20;2:16080. doi: 10.1038/nrdp.2016.80. Review.

27. Haack TB, Haberberger B, Frisch EM, Wieland T, Iuso A, Gorza M, Strecker V, Graf E, Mayr JA, Herberg U, Hennermann JB, Klopstock T, Kuhn KA, Ahting U, Sperl W, Wilichowski E, Hoffmann GF, Tesarova M, Hansikova H, Zeman J, Plecko B, Zeviani M, Wittig I, Strom TM, Schuelke M, Freisinger P, Meitinger T, Prokisch H. Molecular diagnosis in mitochondrial complex I deficiency using exome sequencing. *J Med Genet.* 2012 Apr;49(4):277-83. doi: 10.1136/jmedgenet-2012-100846.
28. Fiedorczuk K, Sazanov LA. Mammalian Mitochondrial Complex I Structure and Disease-Causing Mutations. *Trends Cell Biol.* 2018 Oct;28(10):835-867. doi: 10.1016/j.tcb.2018.06.006.
29. Lake NJ, Bird MJ, Isohanni P, Paetau A. Leigh syndrome: neuropathology and pathogenesis. *J Neuropathol Exp Neurol.* 2015 Jun;74(6):482-92. doi: 10.1097/NEN.000000000000195.
30. Hirano M, Emmanuele V, Quinzii CM. Emerging therapies for mitochondrial diseases. *Essays Biochem.* 2018 Jul 20;62(3):467-481. doi: 10.1042/EBC20170114. Print 2018 Jul 20. Review.
31. Greaves LC, Reeve AK, Taylor RW, Turnbull DM. Mitochondrial DNA and disease. *J Pathol.* 2012 Jan;226(2):274-86. doi: 10.1002/path.3028.
32. Haas RH, Parikh S, Falk MJ, Saneto RP, Wolf NI, Darin N, Cohen BH. Mitochondrial disease: a practical approach for primary care physicians. *Pediatrics.* 2007 Dec;120(6):1326-33.
33. Suomalainen A, Elo JM, Pietiläinen KH, Hakonen AH, Sevastianova K, Korpela M, Isohanni P, Marjavaara SK, Tyni T, Kiuru-Enari S, Pihko H, Darin N, Öunap K, Kluijtmans LA, Paetau A, Buzkova J, Bindoff LA, Annunen-Rasila J, Uusimaa J, Rissanen A, Yki-Järvinen H, Hirano M, Tulinius M, Smeitink J, Tyynismaa H. FGF-21 as a biomarker for muscle-manifesting mitochondrial respiratory chain

deficiencies: a diagnostic study. *Lancet Neurol.* 2011 Sep;10(9):806-18. doi: 10.1016/S1474-4422(11)70155-7.

Chapter 2

R106C TFG variant causes infantile neuroaxonal dystrophy “plus” syndrome

A. Catania,^{1,2} R. Battini,^{3,4} T. Pippucci,⁵ R. Pasquariello,³ M. L. Chiapparini,⁶ M. Seri,⁷ B. Garavaglia,¹ G. Zorzi,⁸ N. Nardocci,⁸ D. Ghezzi,^{1,9} V. Tiranti,¹

1 Molecular Neurogenetics Unit, IRCCS Foundation, C. Besta Neurological Institute, Via L. Temolo n. 4, 20126 Milan, Italy

2 Department of Medicine and Surgery, PhD Programme in Molecular and Translational Medicine, Milan Bicocca University, Via Cadore 48, 20900 Monza, Italy

3 IRCCS Fondazione Stella Maris, Calambrone, Pisa, Italy

4 Department of Experimental Medicine, University of Pisa, Pisa, Italy

5 Medical Genetics Unit, San'Orsola-Malpighi University Hospital, Via Giuseppe Massarenti 9, 40138 Bologna, Italy

6 Neuroradiology, Foundation IRCCS, Neurological Institute BC. Besta, Milan, Italy

7 Medical Genetics Unit, Sant'Orsola-Malpighi University Hospital, Department of Medical and Surgical Sciences, University of Bologna, Via Giuseppe Massarenti 9, 40138 Bologna, Italy

8 Child Neurology Unit, Foundation IRCCS, Neurological Institute C. Besta, Milan, Italy

9 Department of Pathophysiology and Transplantation, University of Milan, Milan, Italy

Neurogenetics (2018) 19:179–187. doi: 10.1007/s10048-018-0552-x.

Abstract

TFG (tropomyosin-receptor kinase fused gene) encodes an essential protein in the regulation of vesicular trafficking between endoplasmic reticulum and Golgi apparatus. The homozygous variant c.316C>T within TFG has been previously associated with a complicated hereditary spastic paraplegia (HSP) phenotype in two unrelated Indian families. Here, we describe the first Italian family with two affected siblings harboring the same variant, who in childhood were classified as infantile neuroaxonal dystrophy (INAD) based on clinical and neuropathological findings. Twenty years after the first diagnosis, exome sequencing was instrumental to identify the genetic cause of this disorder and clinical follow-up of patients allowed us to reconstruct the natural history of this clinical entity. Investigations on patient's fibroblasts demonstrate the presence of altered mitochondrial network and inner membrane potential, associated with metabolic impairment. Our study highlights phenotypic heterogeneity characterizing individuals carrying the same pathogenic variant in TFG and provides an insight on tight connection linking mitochondrial efficiency and neuronal health to vesicular trafficking.

Keywords: INAD-TFG .Mitochondria .Endoplasmicreticulum .Axonalspheroids

Introduction

TFG (tropomyosin-receptor kinase fused gene) encodes a regulator protein in a secretory pathway at the interface between the endoplasmic reticulum (ER) and ER-Golgi intermediate compartments [1].

Mutations in *TFG* have been described as responsible for neurological phenotypes characterized by upper or lower axonopathy, which correlate with the domain affected by the aminoacidic substitution [2].

In particular, the heterozygous c.854C > T (p.Pro285Leu) missense mutation located within the proline and glutamate (P/Q)-rich domain, which is critical for proper *TFG* subcellular localization, was described as causative for autosomal-dominant hereditary motor and sensory neuropathy with proximal dominant involvement (HMSN-P) [3, 4, 5]. The proposed pathogenic mechanism underlying this phenotype seems to involve a toxic gain of function leading to increased *TFG* inhibitory effect on unfolded protein response signaling (UPS), which is in turn responsible for ER stress enhancement [6].

In 2014 and 2016, respectively, genetic investigations in a Taiwanese family affected by Charcot Marie Tooth disease type 2 and in a large Iranian pedigree affected by HMSN-P revealed the novel c.806G > T; p.Gly269Val heterozygous missense mutation, also falling within the of the (P/Q)-rich domain protein [7, 8]. Functional studies showed that the mutation acts in a dominant negative manner by sequestering both mutant and wild-type protein in cytoplasmic aggregates and consequently disrupting ER secretory pathways [7].

The c.316C > T; p.Arg106Cys *TFG* homozygous variant was originally identified in an Indian family with two siblings affected by early-onset progressive spastic paraplegia, optic atrophy, and mixed axonal demyelinating neuropathy [9]. The same change was described in a second family from northern India exhibiting a similar clinical phenotype [10] and apparently sharing a common founder mutation. The p.Arg106Cys variant falls within the coiled-coil (CC) domain of *TFG*, and has been shown to prevent normal assembly of *TFG* complexes at ER exit sites [9].

Recently, an HSP phenotype without optic atrophy and associated with variable degrees of mixed neuropathy has further been reported in three members of a family from Sudan and caused by a homozygous mutation (c.64C > T; p.Arg22Trp) located within the PB1 (Phox and Bem1p) domain. This variant, similarly to the previously described one, seems to hinder *TFG* octamerization in vitro [11]. Furthermore, a significantly enlarged phenotypic spectrum has been recently described in association with the above-mentioned aminoacidic change [12].

We describe the first Italian consanguineous family with two siblings harboring the c.316C > T, p.Arg106Cys homozygous variant and presenting with an early-onset infantile neuroaxonal dystrophy (INAD) later evolving into complicated hereditary spastic paraplegia (HSP). We provide a 20-year clinical follow-up of the peculiar evolution of an otherwise fatal disorder and employed patient's fibroblasts to investigate pathogenic mechanisms of disease.

Materials and methods

Human subjects

The ethic board of the Scientific Institute Stella Maris (Pisa) approved the study and informed consent was obtained according to the Declaration of Helsinki from all the subjects involved.

Cell cultures

Fibroblasts were obtained from skin biopsy performed on subject II-3 at the age of 25. Two fibroblast cell lines, obtained from male healthy subjects (33 and 53 years), were used as control for all the experiments. Two additional fibroblast cell lines obtained from healthy subjects were used as control for Seahorse and Glycolysis assays. Cell lines were grown in Dulbecco's modified Eagle's high glucose medium (DMEM) as described [13]. All experiments were performed on cells at the same passage number ± 1 .

Exome sequencing and variant interpretation

WES of subject II-2 was performed at Beijing Genomics Institute (Shenzen, China) and bioinformatic analysis followed previously described pipeline [14]. Due to consanguinity, exome homozygosity mapping approach was used [15]. Runs of homozygosity (ROH) were detected from WES data with H3M2 [16], and homozygous variants within large regions of homozygosity ($ROH \geq 1.5$ Mb), which are the most likely to be identical by descent (IBD), were prioritized. Only variants predicted to affect protein function (nonsynonymous, nonsense, splicing, and small indels) were retained. Variants with a

minor allele frequency higher than 0.01 in gnomAD (<http://gnomad.broadinstitute.org/>) or in the Bologna in-house database (about 700 additional exomes) were filtered out. We then restricted the search for candidate genes to those harboring loss of function or nonsynonymous variants with CADD Phred-scaled v1.2 score greater than 20 [14, 15, 16].

Microscale oxygraphy in fibroblasts

Oxygen consumption rate (OCR) and extra-cellular acidification rate (ECAR) were measured in triplicate as described [13]. Glycolysis Stress Test (Agilent) was performed in triplicate according to manufacturer's instructions.

Cellular ATP production

Quantitative evaluation of ATP production was performed in fibroblasts using ATPlite Luminescence Assay Kit (PerkinElmer), according to the manufacturer's instructions.

Mitochondrial staining on live cells

Fibroblasts were incubated for 20 min at 37 °C with 30 nM of mitochondrial membrane potential (MMP)-dependent dye (MitoTracker Red [MTR] CMXRos; Invitrogen-Molecular Probes, Eugene, OR, USA). At least 60 reconstructions of confocal 7 z-stacks series (or 60 confocal acquisitions obtained by collapsing series of 7 Z-stacks) per line were collected and blinded processed using ImageJ software.

Mitochondrial membrane potential analysis

Patient' and controls' fibroblasts were incubated for 20 min at 37 °C with 2 μM JC-1 (Sigma-Aldrich; Merck KGaA) according to the manufacturer's protocol. One microliter of valinomycin was used as positive control. At least 50 reconstructions of confocal 3 z-stacks series (or 50 confocal acquisitions obtained by collapsing series of 3 Z-stacks) per line were collected and processed using ImageJ after background correction.

Immunocytochemistry

Fixed cells were incubated with anti-TRK fused gene antibody (Abcam) using 1:1000 dilution. For KDEL (Enzo lifesciences) and GM130 (BD lifesciences) immunostaining, we used 1:200 and 1:250 dilutions, respectively. To-pro 3 fluorescent dye was used for nuclear counterstaining.

Citrate synthase assay

Citrate synthase enzymatic activity was measured as described in [17].

Western blot

Western blot was performed as previously described [18] using 50 μg of proteins per lane. The membrane was incubated overnight first with anti-TFG (1:10000) and then with anti-GAPDH (1:5000).

Blue native polyacrylamide gel electrophoresis

Patient' and control's cells pellets were solubilized with n-Dodecyl- β -D-maltoside (DMM) at a final concentration of 1%. Twenty micrograms of proteins were separated in a precast 3–12% gradient polyacrylamide gel (NativePAGE Novex 3–12% Bis-Tris gel) and transferred to a nitrocellulose membrane. The membrane was incubated overnight with anti-TFG (1:10000) and anti-CO1 (Cytochrome c oxidase subunit 1, 1:3000) antibodies. CO1 was used as loading control and molecular weight marker.

Statistical analysis

All data are expressed as the mean \pm sd, and comparisons between the two groups were performed with Student's *t* test.

Results

Patients

Index subject (II-2, Fig. 1a) was described in 1999 [19] within a cohort of patients diagnosed with infantile neuroaxonal dystrophy (INAD): second of three siblings, he was born in Southern Italy from first-degree cousins. Delivery was uncomplicated and early developmental milestones were referred as normal until the age of 8 months, when he was diagnosed with psychomotor regression after an acute febrile episode. At 12 months, he presented with loss of trunk control and spasticity, complicated dystonia, bilateral optic atrophy, rapidly worsening dysarthria, and intellectual disability (Table 1).

Neuropsychological scores at 2 years of age corresponded to cognitive performances of an 8-month-old child, showing a multiple-domain mental retardation. Sphincter control was never achieved. Screening for neurometabolic disorders resulted in normal findings. At 11 years, sensorimotor axonal neuropathy with signs of active denervation at EMG was detected in the lower limbs. Brain MRI documented mild cerebral hemispheres and cerebellar atrophy (Fig. 1b, c) associated with brainstem and corpus callosum hypoplasia, while EEG registered abundance of cluster of fast rhythms, sometimes correlated to typical absence seizures. Altered EEG patterns tended to increase in late childhood.

Electron microscopy examination of the excisional skin biopsy performed at the age of 16 years, documented the presence of axonal spheroids in peripheral fibers (Fig. 1f), thus corroborating the clinical diagnosis of INAD.

Later at follow-up, disease progressed to a severe stiffness with tendinous retraction. Somatosensory evoked potentials (SSEPs) performed at the age of 22 were consistent with a damage of lemniscus and central pathways.

Death occurred at 25 years by an episode of urinary infection complicated by acute respiratory distress syndrome (ARDS).

His younger sister (subject II-3) was also diagnosed with INAD (Table 1). She showed a mild delay in psychomotor development since birth: at 12 months of age, she was able to sit autonomously, but with impaired trunk control and postural reflexes. Similarly to his brother,

she presented with acute psychomotor deterioration at 15 months of age, after a febrile illness, showing reduced attention span, spasticity, truncal hypotonia, and nystagmus. Occurrence and progression of clinical symptoms were steadily homogeneous with subject II-2 phenotype: loss of visual acuity apparently started before 1 year of age, progressing to an almost complete blindness in few years. Fundus oculi and visual evoked cortical potentials (VECP) examination revealed bilateral optic atrophy, while a severe intellectual disability was also documented with slowed reasoning and executive functions. Episodes of tonic-clonic seizures were reported, with EEG showing abnormal paroxysmal activity; first brain MRI (Supplementary Fig. 1d, e) and somatosensory evoked potentials (SSEPs) showed features overlapping with her brother. Electrophysiological studies on upper and lower limbs were consistent with a diagnosis of motor-sensory axonal neuropathy, as well.

By the age of 4 years, she had already developed a severe spastic tetraparesis with axial hypotonia, inexhaustible torsional nystagmus, and nearly absent verbal communication.

Our last clinical evaluation performed at 29 years, showed a complete anarthria, absence of voluntary movements, severely impaired verbal comprehension, myoclonus, dysphagia, and psychosis, with episodes of agitation and pathological laughter and crying. Autonomic dysfunctions (abundant night sweats, drooling, and disordered urination) and signs of extrapyramidal involvement were also detected, with positive bilateral cogwheel phenomenon at wrists.

Follow-up brain MRI showed advanced cerebral and cerebellar atrophy (Supplementary Fig. 1).

Identification of TFG pathogenic variant

Karyotype analysis on subject II-2 revealed a normal male chromosomal karyotype and ruled out X-fragile syndrome. Genetic analysis of *PLA2G6*, the most frequent genetic cause of INAD [20], was negative.

Then, whole exome sequencing (WES) analysis was performed on subject II-2. After annotation and filtering steps, we identified 3 missense variants fulfilling prioritization criteria, of which 2 were in genes, *SI* (NM_001041:c.3598C>T;p.P1200S) and *TFG* (NM_01195478:c.316C>T;p.R106C), linked to autosomal recessive disorders in the Online Mendelian inheritance in Man (OMIM, www.omim.org) catalog, while the third was in *MFNI* (NM_033540:c.1207G>A;p.E403K). Pathogenicity of *SI* and *MFNI* variants was excluded based on clinical dissimilarity and segregation inconsistency, respectively.

Hence, we focused on the variant within *TFG*, already reported as responsible for SPG57 syndrome [9]. In the large population variant database gnomAD (www.gnomad.broadinstitute.org), the variant allele ([rs587777175](https://www.ncbi.nlm.nih.gov/variation/view/variant_proxy/rs587777175)) has never been observed in the homozygous state and only 11 times in the heterozygous state, always in subjects of European descent. This variant was further validated by Sanger sequencing and identified in the affected sister in a homozygous condition as well.

Unaffected parents were both heterozygous c.316C>T carriers (Fig. 1a).

Characterization of TFG patient's fibroblasts

Western blot analysis performed with anti-TFG antibody evidenced a doublet band (55 and 50 kDa, respectively) with a predominant upper one (Supplementary Fig. 3a), as previously reported [21].

Densitometry analysis failed to show any difference in patient TFG levels compared to controls (Supplementary Fig. 2). Together with the evidence of a normal expression pattern of TFG in patient's cells at immunofluorescence analysis (Supplementary Fig. 3), these data indicated that the presence of the R106C variant did not modify TFG amount.

As demonstrated by several in vitro studies, TFG recombinant protein assembles in an octameric cup-like structure, which in turn is able to polymerize to form larger structures [1, 21].

To evaluate TFG assembly in patient's and control's fibroblasts, proteins were resolved under native conditions by blue native polyacrylamide gel electrophoresis (BN-PAGE). Control's fibroblasts showed the presence of a band of around 500 kDa, dimensionally consistent with the octameric TFG complex, and a higher molecular weight band, which could correspond to a bigger TFG assembly product. Only the lower band with a dramatically reduced intensity was detected in patient's fibroblasts (Supplementary Fig. 2d). Since the total amount of the protein seems to be unaltered in the patient under

denaturing conditions, a possible explanation for our results could be that the missing fraction of the mutant protein organizes in abnormal aggregates, which are not accessible to the antibody under native conditions.

To further understand the impact of the variant on protein localization, we compared the anti-TFG immunostaining with the staining obtained using Mitotracker red as specific marker of mitochondria, anti-KDEL, and anti-GM-130 antibodies as specific markers of endoplasmic reticulum and Golgi apparatus, respectively. We did not observe any significant co-localization of TFG protein with these sub-cellular compartments but demonstrated that the protein showed a punctate and evenly distributed cytoplasmic pattern, with a slightly more pronounced tendency to cluster in the perinuclear region (Supplementary Fig. 3a–f), which was similar in patient's and control's fibroblasts.

Characterization of mitochondrial network and functionality

Based on published results obtained in primary murine neurons overexpressing different TFG variants, which demonstrated alteration of the mitochondrial morphology [10], we decided to investigate mitochondrial network integrity in mutant patient's fibroblasts. Analysis of Mitotracker red staining images (Fig. 2a, b) showed a significant reduction of Feret's diameter (Fig. 2c), an index of mitochondrial elongation, and an increased organelle average circularity (Fig. 2d) in patient's fibroblasts as compared to control, thus indicating that the filamentous connection was altered in favor of a fragmented network.

To determine if these structural abnormalities were associated with altered mitochondrial functionality, we evaluated mitochondrial respiratory chain (MRC) function, but failed to show any significant difference of oxygen consumption rate (OCR) in basal conditions, between mutant and controls' cells (not shown). While OCR is an indicator of mitochondrial respiration, ECAR (extra-cellular acidification rate) is proportional to the production of lactic acid, reflecting the rate of anaerobic glycolysis. Since OCR/ECAR ratio was significantly decreased in mutant cells (Fig. 3a), we evaluated glycolysis to confirm the presence of a metabolic imbalance. In basal conditions, glycolysis assay showed only a slight increase of glycolytic parameters in patient's fibroblasts, while in conditions of cellular stress and higher energetic demand (evaluated calculating glycolytic capacity and reserve), glycolysis appeared to be significantly increased in comparison to controls (Fig. 3b).

Mitochondrial ATP production was only slightly decreased in mutant cells without reaching statistical significance (data not shown). We speculated that the observed impairment of mitochondrial energy production is well compensated by the anaerobic boost, at least in basal conditions.

Citrate synthase (CS) activity (a mitochondrial mass marker) assessment excluded reduction of mitochondrial number in patient's cells (Fig. 3c).

Therefore, hypothesizing that the observed metabolic imbalance could be attributable to mitochondrial membrane potential (MMP)

dissipation, we used JC1 potential-sensitive fluorescent probe to assess MMP in cultured cells. JC1 assay confirmed a strong reduction of MMP in patient's fibroblasts, as evidenced by the significant imbalance in red to green ratio (Fig. 3d).

Discussion

In the last few years, reports expanding clinical spectrum associated with the same pathogenic variant are rapidly growing, thanks to the accelerated pace of disease-causing variants enabled by next generation sequencing (NGS) technologies.

So far, two families of Indian ancestry harboring c.316C>T homozygous variant in *TFG* have been described, both affected by a phenotype encompassing progressive spastic paraplegia, optic atrophy, and mixed neuropathy [9, 10]. Genetic data suggested that both families shared a common founder allele originating in India [10].

Our report describes the first Italian family with two siblings, harboring the same variant, both presenting with a clinical syndrome fulfilling the clinic-pathological diagnostic criteria for INAD [19], but displaying, overtime, a clinical course consistent with a complicated HSP phenotype.

Early onset of the disease with rapid motor and cognitive deterioration, truncal hypotonia associated with tetraparesis, early appearance of visual acuity loss, seizures, and cerebellar signs are cardinal diagnostic features of INAD. Electromyographic signs of denervation, cerebellar atrophy at brain MRI, fast rhythms on EEG, and detection of axonal

spheroids in skin biopsy [19] supported the diagnosis. Altogether, our results indicate *TFG* as a potential causative gene for a broader INAD clinical spectrum with additional symptoms and suggest screening of the gene in patients with a complicated non-canonical HSP clinical picture. Similarly, mutations in *PLA2G6*, the main INAD causative gene, have recently been described in patients affected by complicated HSP [22, 23]: the emerging evidence that mutations of genes typically associated with HSP or INAD can underpin a continuous clinical spectrum spanning both diseases, may suggest that common pathways could be involved in their pathogenesis, and should further encourage clinicians to carefully consider these results in the diagnostic workup of patients affected by these pathological entities.

TFG is undoubtedly required for ER structure maintenance [9] and regulation of vesicle trafficking from the endoplasmic reticulum to Golgi intermediate compartment (ERGIC) [1, 24, 25]. ER organization and vesicular trafficking could also impact on mitochondrial structure and function, thus determining the fate of neuronal cells. Preliminary studies on murine hippocampal neurons overexpressing two mutant *TFG* proteins carrying the p. R106C or the R106H respectively [10] already suggested a disruption of mitochondrial morphology characterized by increased fragmentation and reduced continuity, which was more severe in the presence of the p. R106C variant. Moreover, siRNA mediated depletion of *TFG* in mammalian cells determines clustering of mitochondria around the microtubules [9].

Our study suggests that, even though *TFG* does not co-localize with mitochondria and protein levels are not affected by the R106C change,

mitochondrial network appears fragmented and less interconnected in patient's fibroblasts, in parallel with a perturbation of the mitochondria inner membrane potential. Despite a normal mitochondrial content and OXPHOS functionality, dissipation of MMP probably results in less efficient ATP production, leading to a compensatory boost of anaerobic metabolism, especially in conditions of increased energetic demand.

Although further studies are required to fully elucidate the pathogenic mechanism triggered by R106C *TFG* variant, especially in the nervous system, our report provides additional insights on the relevance of mitochondria functionality in the pathophysiology of *TFG*-related disease.

Acknowledgements

We are grateful to the patients and their family for their participation and contribution in this study. We also thank Dr. Giaccone for helping with the biopsy report and images.

Funding information

This study received support from the Mariani Foundation of Milan.

Compliance with ethical standards

The ethic board of the Scientific Institute Stella Maris (Pisa) approved the study and informed consent was obtained according to the Declaration of Helsinki from all the subjects involved.

Conflict of interest

The authors declare that they have no conflict of interest.

References

1. Johnson A, Bhattacharya N, Hanna M, Pennington JG, Schuh AL, Wang L, Otegui MS, Stagg SM, Audhya A (2015) TFG clusters COPII-coated transport carriers and promotes early secretory pathway organization. *EMBO J* 34(6):811–827. <https://doi.org/10.15252/embj.201489032>
2. Yagi T, Ito D, Suzuki N (2016) TFG-related neurologic disorders: new insights into relationships between endoplasmic reticulum and neurodegeneration. *J Neuropathol Exp Neurol* 75(4):299–305. <https://doi.org/10.1093/jnen/nlw009>
3. Ishiura H, Sako W, Yoshida M, Kawarai T, Tanabe O, Goto J, Takahashi Y, Date H, Mitsui J, Ahsan B, Ichikawa Y, Iwata A, Yoshino H, Izumi Y, Fujita K, Maeda K, Goto S, Koizumi H, Morigaki R, Ikemura M, Yamauchi N, Murayama S, Nicholson GA, Ito H, Sobue G, Nakagawa M, Kaji R, Tsuji S (2012) The TRK-fused gene is mutated in hereditary motor and sensory neuropathy with proximal dominant involvement. *Am J Hum Genet* 91(2):320–329. <https://doi.org/10.1016/j.ajhg.2012.07.014>
4. Lee SS, Lee HJ, Park JM, Hong YB, Park KD, Yoo JH, Koo H, Jung SC, Park HS, Lee JH, Lee MG, Hyun YS, Nakhro K, Chung KW, Choi BO (2013) Proximal dominant hereditary motor and sensory neuropathy with proximal dominance association with mutation in the TRK-fused gene. *JAMA Neurol* 70(5):607–615. <https://doi.org/10.1001/jamaneurol.2013.1250>
5. Alavi A, Shamshiri H, Nafissi S, Khani M, Klotzle B, Fan JB, Steemers F, Elahi E (2015) HMSN-P caused by p.Pro285Leu mutation in TFG is not confined to patients with far east ancestry. *Neurobiol Aging* 36(3):1606.e1–1606.e7. <https://doi.org/10.1016/j.neurobiolaging.2014.11.021>
6. Yagi T, Ito D, Suzuki N (2014) Evidence of TRK-fused gene (TFG1)

function in the ubiquitin-proteasome system. *Neurobiol Dis* 66:83–91.
<https://doi.org/10.1016/j.nbd.2014.02.011>

7. Tsai PC, Huang YH, Guo YC, Wu HT, Lin KP, Tsai YS, Liao YC, Liu YT, Liu TT, Kao LS, Yet SF, Fann MJ, Soong BW, Lee YC (2014) A novel TFG mutation causes Charcot-Marie-Tooth disease type 2 and impairs TFG function. *Neurology* 83(10):903–912.
<https://doi.org/10.1212/WNL.0000000000000758>
8. Khani M, Shamshiri H, Alavi A, Nafissi S, Elahi E (2016) Identification of novel TFG mutation in HMSN-P pedigree: emphasis on variable clinical presentations. *J Neurol Sci* 369:318–323.
<https://doi.org/10.1016/j.jns.2016.08.035>
9. Beetz C, Johnson A, Schuh AL, Thakur S, Varga RE, Fothergill T, Hertel N, Bomba-Warczak E, Thiele H, Nürnberg G, Altmüller J, Saxena R, Chapman ER, Dent EW, Nürnberg P, Audhya A (2013) Inhibition of TFG function causes hereditary axon degeneration by impairing endoplasmic reticulum structure. *Proc Natl Acad Sci U S A* 110(13):5091–5096.
<https://doi.org/10.1073/pnas.1217197110>
10. Harlalka GV, McEntagart ME, Gupta N, Skrzypiec AE, Mucha MW, Chioza BA, Simpson MA, Sreekantan-Nair A, Pereira A, Günther S, Jahic A, Modarres H, Moore-Barton H, Trembath RC, Kabra M, Baple EL, Thakur S, Patton MA, Beetz C, Pawlak R, Crosby AH (2016) Novel genetic, clinical, and pathomechanistic insights into TFG-associated hereditary spastic paraplegia. *Hum Mutat* 37(11):1157–1161.
<https://doi.org/10.1002/humu.23060>
11. Elsayed LE, Mohammed IN, Hamed AA, Elseed MA, Johnson A, Mairey M, Mohamed HE, Idris MN, Salih MA, El-Sadig SM, Koko ME, Mohamed AY, Raymond L, Coutelier M, Darios F, Siddig RA, Ahmed AK, Babai AM, Malik HM, Omer ZM, Mohamed EO, Eltahir HB, Magboul NA, Bushara EE, Elnour A, Rahim SM, Alattaya A, Elbashir

- MI, Ibrahim ME, Durr A, Audhya A, Brice A, Ahmed AE, Stevanin G (2016) Hereditary spastic paraplegias: identification of a novel SPG57 variant affecting TFG oligomerization and description of HSP subtypes in Sudan. *Eur J Hum Genet* 25(1):100–110. <https://doi.org/10.1038/ejhg.2016.108>
12. Tariq H, Naz S (2017) TFG associated hereditary spastic paraplegia: an addition to the phenotypic spectrum. *Neurogenetics* 18(2): 105–109. <https://doi.org/10.1007/s10048-017-0508-6>
 13. Invernizzi F, D'Amato I, Jensen PB, Ravaglia S, Zeviani M, Tiranti V (2012) Microscale oxygraphy reveals OXPHOS impairment in MRC mutant cells. *Mitochondrion* 12(2):328–335. <https://doi.org/10.1016/j.mito.2012.01.001>
 14. Magini P, Pippucci T, Tsai IC, Coppola S, Stellacci E, Bartoletti-Stella A, Turchetti D, Graziano C, Cenacchi G, Neri I, Cordelli DM, Marchiani V, Bergamaschi R, Gasparre G, Neri G, Mazzanti L, Patrizi A, Franzoni E, Romeo G, Bordo D, Tartaglia M, Katsanis N, Seri M (2014) A mutation in PAK3 with a dual molecular effect deregulates the RAS/MAPK pathway and drives an X-linked syndromic phenotype. *Hum Mol Genet* 23(13):3607–3617
 15. Pippucci T, Benelli M, Magi A, Martelli PL, Magini P, Torricelli F, Casadio R, Seri M, Romeo G (2011) EX-HOM (EXome HOMozygosity): a proof of principle. *Hum Hered* 72:45–53
 16. Magi A, Tattini L, Palombo F, Benelli M, Gialluisi A, Giusti B, Abbate R, Seri M, Gensini GF, Romeo G, Pippucci T (2014) H3M2: detection of runs of homozygosity from whole-exome sequencing data. *Bioinformatics* 30:2852–2859
 17. Bugiani M, Invernizzi F, Alberio S, Briem E, Lamantea E, Carrara F, Moroni I, Farina L, Spada M, Donati MA, Uziel G, Zeviani M (2004) Clinical and molecular findings in children with complex I deficiency.

Biochim Biophys Acta 1659:136–147

18. Tiranti V, Galimberti C, Nijtmans L, Bovolenta S, Perini MP, Zeviani M (1999) Characterization of SURF-1 expression and Surf-1p function in normal and disease conditions. *Hum Mol Genet* 8:2533–2540. <https://doi.org/10.1093/hmg/8.13.2533>
19. Nardocci N, Zorzi G, Farina L, Binelli S, Scaioli W, Ciano C, Verga L, Angelini L, Savoirdo M, Bugiani O (1999) Infantile neuroaxonal dystrophy: clinical spectrum and diagnostic criteria. *Neurology* 52(7):1472–1478
20. Morgan NV, Westaway SK, Morton JE, Gregory A, Gissen P, Sonek S, Cangul H, Coryell J, Canham N, Nardocci N, Zorzi G, Pasha S, Rodriguez D, Desguerre I, Mubaidin A, Bertini E, Trembath RC, Simonati A, Schanen C, Johnson CA, Levinson B, Woods CG, Wilmot B, Kramer P, Gitschier J, Maher ER, Hayflick SJ (2006) PLA2G6, encoding a phospholipase A2, is mutated in neurodegenerative disorders with high brain iron. *Nat Genet* 38(7): 752–754 Erratum in: *Nat Genet* 2006 Aug;38(8):957
21. Witte K, Schuh AL, Hegermann J, Sarkeshik A, Mayers JR, Schwarze K, Yates JR 3rd, Eimer S, Audhya A (2011) TFG-1 function in protein secretion and oncogenesis. *Nat Cell Biol* 13(5):550–558. <https://doi.org/10.1038/ncb2225>
22. Ozes B, Karagoz N, Schüle R, Rebelo A, Sobrido MJ, Harmuth F, Synofzik M, Pascual SIP, Colak M, Ciftci-Kavaklioglu B, Kara B, Ordóñez-Ugalde A, Quintáns B, Gonzalez MA, Soysal A, Zuchner S, Battaloglu E (2017) PLA2G6 mutations associated with a continuous clinical spectrum from neuroaxonal dystrophy to hereditary spastic paraplegia. *Clin Genet* 92(5):534–539. <https://doi.org/10.1111/cge.13008>
23. Chen YJ, Chen YC, Dong HL, Li LX, Ni W, Li HF, Wu ZY (2018) Novel PLA2G6 mutations and clinical heterogeneity in Chinese cases with

- phospholipase A2-associated neurodegeneration. *Parkinsonism Relat Disord* 49:88–94. <https://doi.org/10.1016/j.parkreldis.2018.02.010>
24. Kanadome T, Shibata H, Kuwata K, Takahara T, Maki M (2017) The calcium-binding protein ALG-2 promotes endoplasmic reticulum exit site localization and polymerization of Trk-fused gene (TFG) protein. *FEBS J* 284(1):56–76. <https://doi.org/10.1111/febs.13949>
25. Hanna MG, Block S, Frankel EB, Hou F, Johnson A, Yuan L, Knight G, Moresco JJ, Yates JR 3rd, Ashton R, Schekman R, Tong Y, Audhya A (2017) TFG facilitates outer coat disassembly on COPII transport carriers to promote tethering and fusion with ER-Golgi intermediate compartments. *Proc Natl Acad Sci U S A* 114(37):E7707–E7716. <https://doi.org/10.1073/pnas.1709120114>.

Figures and Tables:

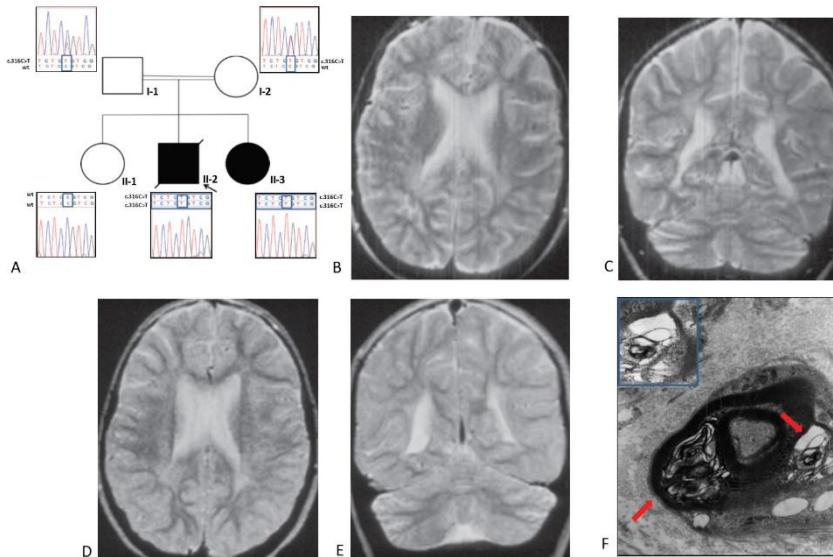


Figure 1: Family description and clinical studies. **a** Family pedigree with the identified TFG variant. The proband is pointed out by black arrow. **b–e** Brain MRI, T2-weighted images, of subject II-2 (**b** and **c**) and of subject II-3 (**d** and **e**), obtained at the ages 11 years and 5 months and 4 years and 2 months, respectively. The neuroradiological findings are nearly identical showing lateral ventricles and cerebral hemispheric sulci mild enlargement and a slight hyperintensity in the posterior periventricular white matter. Note the mild hemispheric cerebellar atrophy in both cases. **f** Electron microscopy examination of skin biopsy from subject II-2. Arrows point out areas of axonal dystrophy and swelling. Upper left inset shows higher magnification of axonal spheroids

	II-3	II-2 (Index Patient)	Beetz et al 2013 Index Patient	Harlaka et al 2016 Patient 1	Harlaka et al 2016 Patient 2
Age at onset	Birth	8 mo	8 mo	12 mo	8mo
Symptoms at onset	psychomotor retardation and regression	psychomotor regression	Spasticity	motor delay	motor delay
Age of last follow up evaluation	29 y	25 y	12 y	10 y	5 y
Standing position achieved	Never	Never	11 months	1 y	Never
Visual loss noticed	< 1 y	1 y	2.5 y	18 mo	18 mo
Nationality	Italian	Italian	Indian	Indian	Indian
Main complicating symptoms (1-II)					
Cognitive impairment	Y	Y	Doubtful	N	N
Dysphagia	Y	Y	NR	NR	NR
Epilepsy	Y (tonic-clonic epilepsy)	Y (Absence seizures)	N	N	N
Visual loss	Bilateral Optic atrophy	Bilateral Optic atrophy	Bilateral Optic atrophy	Bilateral Optic atrophy	Bilateral Optic atrophy
Extrapyramidal involvement	Y	NR	NR	NR	NR
Cerebellar signs	Y	Y	N	NR	NR
Psychosis	Y	NR	N	N	N
Neuropathy	Y (axonal motor-sensory)	Y (axonal smotor-sensory)	Y (mixed axonal and demyelinating motor-sensory)	Y (axonal motor-sensory)	NR
Dysarthria	Severe progressing to anarthria	Severe progressing to anarthria	NR	N	N
Facioskeletal abnormalities	N	Microcrania	N	NR	NR
Nystagmus	Y (torsional)	NR	N	Y (roving)	Y (roving)
Autonomic dysfunctions	Y	NR	N	NR	NR
Sleep disturbances	Y	NR	NR	NR	NR
Instrumental exams (1-III)					
EEG	Abnormal	Abnormal	/	/	/
Cerebral and cerebellar atrophy	Y	Y	N	N	/
Brainstem atrophy	Y	Y	N	N	/
VECP	Altered	Altered	/	/	/
SSEPs	Altered	Altered	/	/	/
EMG	Axonal neuropathy	Axonal neuropathy with signs of active denervation	Axonal demyelinating neuropathy	Axonal neuropathy	/
Muscle biopsy	/	Chronic denervation	/	/	/
Sural nerve biopsy	/	Diffuse axonal damage	/	/	/
Skin biopsy	/	Axonal spheroids	/	/	/

Y yes, N no, NR not reported, / not evaluated or unavailable

Table 1: Comparison of phenotypes. Schematic comparison of major (1-I), complicating (1-II) clinical findings, and main MRI and neurophysiological findings (1-III) between subjects II-3, II-2, and

previously reported patients [3, 4] carrying c.316C>T homozygous variant in TFG gene

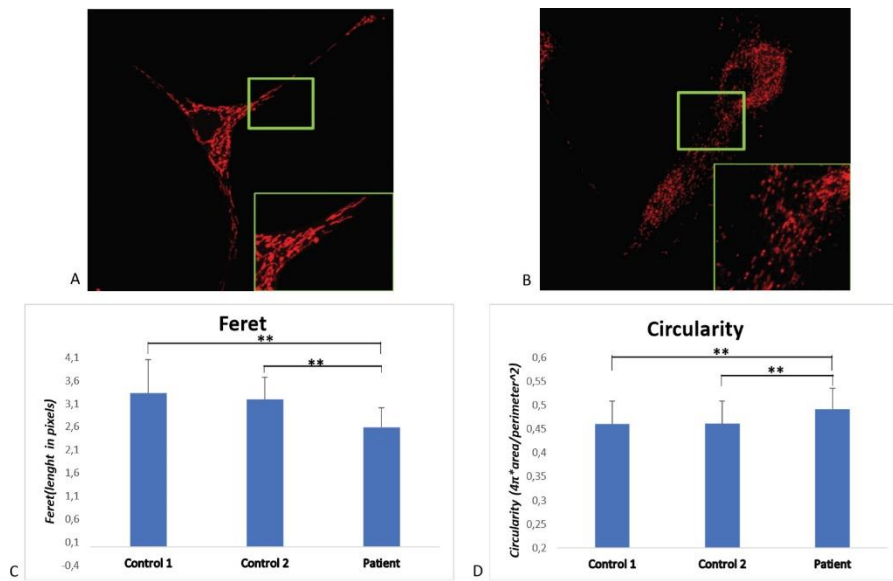


Figure 2: Characterization of mitochondrial network. Representative images of controls' (a) and patient's 1 fibroblasts (b) after incubation with MitoTracker Red. $\times 3$ magnification views are shown in order to give emphasis to morphological differences in mitochondrial network. Images were analyzed using ImageJ software. Mean Feret (c) and average circularity (d) of control and patient fibroblast. Error bars represent mean \pm s.d. Comparisons between groups were performed with paired t test (** $p < 0.01$)

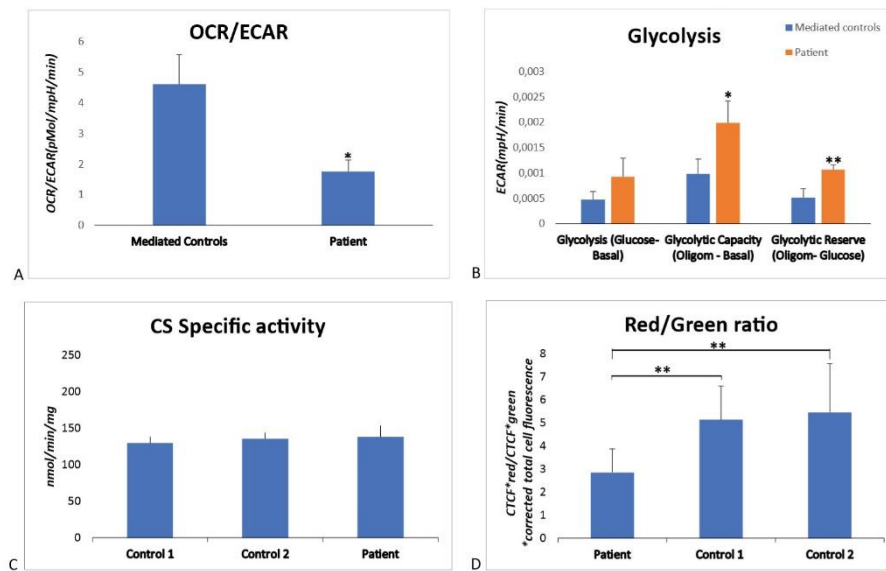
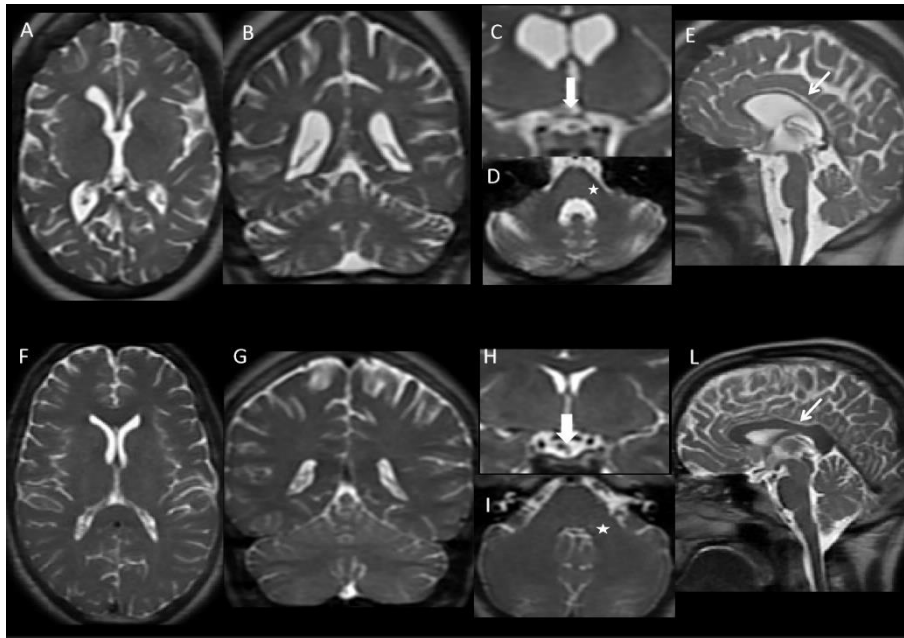
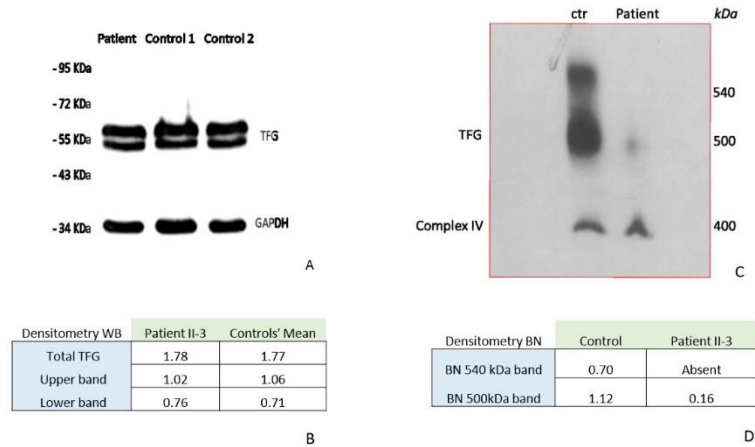


Figure 3: Characterization of mitochondrial functionality. **a** Mean OCR/ECAR ratio evaluated by seahorse assay (four independent experiments). **b** Mean basal Glycolysis, glycolytic capacity, and glycolytic reserve evaluated using Seahorse XF Glycolysis Stress Test Kit (three independent experiments). Four different fibroblast cell lines were used as control. Comparisons between groups were performed with paired *t* test (**p* < 0.05; ***p* < 0.01). **c** Quantification of citrate synthase (CS) activity (mean of three replicates) in two different control fibroblast lines and patient fibroblast. **d** Mean of red to green ratio measured using ImageJ software after incubation with JC-1 probe. Error bars represent mean ± s.d. Comparisons between groups were performed with paired *t* test (***p* < 0.01)

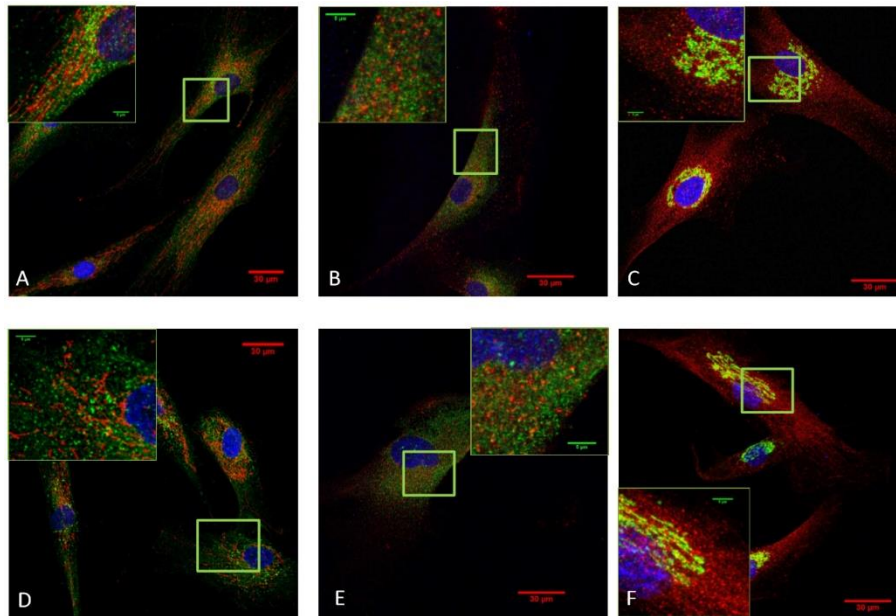
Supplementary material



Supplementary Figure 1 Follow-up brain MRI of subject II-3. **a–e** Subject II-3. Axial (**a**, **d**) and coronal (**b**) FAST T2-weighted images show reduction of the supratentorial white matter, lateral ventricle enlargement, and large subarachnoid spaces as the effect of diffuse atrophy, middle cerebellar peduncle hypoplasia (star), and enlargement of the IV ventricle. Coronal image (**c**) shows possible hypoplasia of the optic chiasm (white arrow). **e** Sagittal image reveals thin corpus callosum (thin white arrow) and small brainstem. FAST imaging was required due to low patient compliance to the MRI exam. **f–i** Subject 2 (healthy control, matched for age) for comparison. Normal axial, coronal, and sagittal FAST T2-weighted images.



Supplementary Figure 2 TFG expression and assembly in patient's fibroblasts. **a:** Patient and controls protein samples resolved in 10% SDS/PAGE gel after incubation with anti-TFG antibody. GAPDH was used as loading control. **b:** Densitometric analysis of WB. **c:** Blue native gels stained for TFG protein and CO1 (Cytochrome c oxidase subunit 1) used as loading control. **d:** Densitometric analysis of BN. Numbers of kilodaltons are given on left of gels. WB, western blot; BN, blue native



Supplementary Figure 3 Sub-cellular distribution of TFG in patient's fibroblasts. Control (**a, b, c**) and patient (**d, e, f**) fixed fibroblasts after double staining with Mitotracker red (**a-d**), KDEL antibody (green in **b-e**), GM130 antibody (green in **c-f**), and TFG-specific antibody (green in **a-d**, red in **b, c, e, f**). To-Pro3 fluorescent dye (blue) was used for nuclear counterstaining. Original magnification of all images is $\times 63$. Higher magnification views of the indicated regions (boxed) are also shown. The scale bars represent 30 μm (main) and 5 μm (inset).

Chapter 3

Compound Heterozygous Missense and Deep Intronic Variants in NDUFAF6 Unraveled by Exome Sequencing and mRNA Analysis

Alessia Catania¹, Anna Ardisson², Daniela Verrigni³, Andrea Legati¹, Aurelio Reyes⁴, Eleonora Lamantea¹, Daria Diodato³, Davide Tonduti², Valentina Imperatore⁶, Anna Maria Pinto^{6,7}, Isabella Moroni², Enrico Bertini³, Alan Robinson⁴, Rosalba Carrozzo³, Massimo Zeviani⁴, and Daniele Ghezzi^{1,8}

1 Molecular Neurogenetics, Foundation IRCCS Neurological Institute Besta, Milan, Italy

2 Child Neurology Unit, Foundation IRCCS Neurological Institute Besta, Milan, Italy

3 Department of Molecular and Translational Medicine DIMET, University of Milan-Bicocca, Milan, Italy

4 Unit of Muscular and Neurodegenerative Disorders, Laboratory of Molecular Medicine, “Bambino Gesù” Children’s Hospital, IRCCS, Rome, Italy

5 Medical Research Council - Mitochondrial Biology Unit, University of Cambridge, Cambridge, UK

6 Medical Genetics, Department of Medical Biotechnology, University of Siena, Policlinico “Santa Maria alle Scotte”, Siena, Italy

7 Medical Genetics, Azienda Ospedaliero-Universitaria Senese, Siena, Italy

8 Department of Pathophysiology and Transplantation, University of Milan, Milan, Italy

J Hum Genet. 2018 May;63(5):563-568. doi: 10.1038/s10038-018-0423-1.

Abstract

Biallelic mutations in *NDUFAF6* have been identified as responsible for cases of autosomal recessive Leigh syndrome associated with mitochondrial complex I deficiency. Here, we report two siblings and two unrelated subjects with Leigh syndrome, in which we found the same compound heterozygous missense (c.532G>C:p.A178P) and deep intronic (c.420+784C>T) variants in *NDUFAF6*. We demonstrated that the identified intronic variant creates an alternative splice site, leading to production of an aberrant transcript.

A detailed analysis of whole exome sequencing data together with functional validation based on mRNA analysis may reveal pathogenic variants even in non-exonic regions

Introduction

Leigh syndrome is an early onset progressive neurodegenerative disease with an invariably devastating clinical course. The neuropathology of Leigh syndrome is characterized by bilateral, symmetrical necrotic lesions in deep gray matter structures. The most common cause of Leigh syndrome is a defect in oxidative phosphorylation.¹ The NADH dehydrogenase (ubiquinone) complex I assembly factor 6 (*NDUFAF6*, previously known as *C8ORF38*) gene encodes a mitochondrial protein, highly conserved across eukaryotes, which plays an essential role in the early assembly stages of mitochondrial respiratory chain complex I.² Biallelic missense mutations within *NDUFAF6* have been associated with cases of Leigh syndrome due to mitochondrial complex I deficiency.³⁻⁵ In a very recent paper about molecular and enzymatic assays for diagnosis in Leigh

syndrome cases, NDUFAF6 was one of the most frequently mutated nuclear genes and was invariably associated with reduced complex I activity.⁶

Recently, Bianciardi *et al.*⁷ described a patient presenting Leigh syndrome and mitochondrial complex I deficiency associated with a pathogenic heterozygous missense variant in NDUFAF6 (c.532G>C:p.A178P) and an almost monoallelic expression of the mutated allele at transcriptional level; an autosomal recessive model of inheritance was hypothesized, but the second pathogenic mutation remained unidentified.⁷ Upon identification in our laboratory of two siblings and a singleton unrelated subject, all affected by Leigh syndrome and harbouring the same heterozygous missense mutation (c.532G>C:p.A178P), here we provide evidence that the second allelic mutation consists of a deep intronic variant present in all affected individuals, including the previously published case.⁷ Through mRNA analysis we demonstrated that the identified intronic mutation is responsible for the formation of an alternative splice site, leading to altered mRNA splicing.

Materials and Methods

Informed consents for biological sample collection and genetic studies were obtained from all the subjects involved in the study (Siblings A1 and A2 and their parents; patient B, previously described by Bianciardi *et al.*⁷; patient C and his parents), in agreement with the Declaration of Helsinki.

Extraction of genomic DNA from peripheral blood was performed using standard methods. A targeted-NGS using a custom panel containing genes responsible for mitochondrial disorders⁸ was performed on DNAs from patients A1 and B, while clinical exome sequencing using a commercial kit with genes associated with inherited diseases (TrusightOne, Illumina) was performed in patient C. Whole exome sequencing (WES) analysis and variant calling/prioritization were conducted on DNAs from patients A1 and A2, as previously described.⁸ Libraries were prepared with the Nextera Rapid Exome Capture kit (FC-140-1001, Illumina), and sequencing was performed on an Illumina MiSeq platform. Variants identified by NGS were validated by Sanger sequencing and resolved on a 3130xl Genetic Analyzer (Applied Biosystems).

The identified mutations were validated by employing the following pairs of primers, respectively:

Exon 3b F: 5'-ATTTTGAGGTGGTGATTTCAAAG-3';

R: 5'GGAAGGCTTTAGTGGTAAACTGG-3';

Exon 5 F: 5'-AATGGAAACCTATGGGCTAGAG-3';

R: 5'TGAGCTTCTTGAAGTGGGATG-3'.

For RNA purification and cDNA retrotranscription we used RNeasy mini kit (QIAGEN) and GoTaq 2-Step RT-qPCR System (Promega), respectively, according to the manufacturers' protocols.

For cDNA amplification (from exon 3 to exon 7) and sequencing we used the following primer pair:

3F: 5'-CTGAGAAAACAATTGGACTGATG-3';

7R: 5'TCTCACATTTTTATCTTGGTTCCTC-3'.

For deep sequencing of NDUFAF6 transcript, PCR products were processed with Nextera XT DNA sample preparation kit (Illumina). Next Generation Sequencing (NGS) was performed on an Illumina MiSeq instrument. Filtered reads were then aligned using BWA and visualized with Integrating Genomics Viewer (IGV).

Tag SNPs were selected using the SNPinfo web server (<https://snpinfo.niehs.nih.gov>), based on the HapMap CEU (Utah residents with Northern and Western European ancestry) and Tuscani populations. Specific primers were designed (available upon request) and SNPs were assessed by Sanger sequencing. Information about SNPs frequencies was obtained from public databases: dbSNP, Genome Aggregation Database (gnomAD).

For the nonsense-mediated mRNA decay (NMD) assay, patients and control fibroblasts were grown in complete DMEM and incubated for 12 h with puromycin (100 µg/ml). Total RNA was extracted after 4 and 8 hours of recovery in puromycin free medium from treated and untreated paired cultures.

Results

Case reports

We report an Italian family in which two siblings were diagnosed with Leigh syndrome (Family A, Fig. 1A). The older sibling (patient A1) presented psychomotor regression at 21 months of age; neurological evaluation at 30 months showed ataxic gait and fine tremor. Cognitive

functions were preserved. He presented a Leigh syndrome pattern at brain MRI. Biochemical analysis showed an isolated respiratory chain complex I deficiency in muscle and fibroblasts (42% and 38% of the controls' mean, respectively; Suppl. Table S1). The disease was slowly progressive: at 4½ years he presented with drooling, dysarthria, dysmetria, tremor, severe ataxic gait and hypertonia. His younger sister (patient A2) showed psychomotor delay at the age of 12 months and then limb dysmetria, trunk titubation, and ataxic gait. Cognitive functions were preserved. MRI disclosed a Leigh syndrome pattern. Plasma lactate and pyruvate levels were slightly increased. A detailed clinical description of these cases is reported in the supplementary material.

Patient B was described in detail by Bianciardi et al.⁷ Briefly, he developed motor and language disturbances by the age of 3.5 years progressing to severe gait impairment, dysarthria and early occurrence of dystonic movements. Brain MRI showed necrotic damage of the putamina, gradually extending to dentate nuclei and anterior caudate nuclei. Evaluation of mitochondrial respiratory chain revealed decreased complex I activity on fibroblasts (~25% of the controls' mean), while enzymatic activity was normal on muscle homogenate (Suppl. Table S1).

Patient C is an 11 year-old Italian boy, first child of unrelated parents. Psychomotor developmental milestones were referred as normal. He presented at 5 years of age with gait unsteadiness and motor coordination problems. These symptoms gradually worsened, configuring over time an extrapyramidal syndrome; cognitive function

was preserved. Brain MRI disclosed involvement of the putamen bilaterally, stable over time. Extensive metabolic screening was normal as well as mtDNA analysis. A detailed clinical description of this case is reported in the supplementary material.

Molecular studies

WES was performed on patients A1 and A2. Variants annotation and filtering steps focused on variants shared by both siblings and affecting mitochondrial genes led to the identification of the heterozygous missense variant c.532G>C:p.A178P in NDUFAF6 (NM_152416.3) in both siblings; the same mutation (rs201088736) had been already reported as pathogenic by Bianciardi et al.⁷ Analysis of WES data also revealed the presence of an additional heterozygous intronic variant (NM_152416.3:c.420+784C>T) in NDUFAF6 in both affected siblings (Fig. 1A-B). It corresponds to rs749738738 in dbSNP database, and is reported with an extremely low allele frequency (0.003% in gnomAD). The missense and the intronic variants, validated by Sanger sequencing, were inherited from the unaffected father and mother, respectively (Fig. 1A).

In order to assess the effects of the intronic variant, RNA was extracted from fresh blood samples of family A members and retrotranscribed into cDNA. Through amplification and sequencing of the NDUFAF6 transcript (Fig. 1C-D), we detected an additional transcript in samples of both siblings and their mother (Suppl. Fig. S1): this corresponded to alternative splicing isoforms (e.g. ENST00000520757.1 or XM_005250791.1), retaining an extra 124 nucleotide-long exon (exon 3b; Fig. 1B) and predicted to undergo premature non-sense mediated

decay on public databases, because of the creation of a premature stop codon. Interestingly, the alternative splicing acceptor site is placed 11 nucleotides downstream the rs749738738 variant and in silico predictions gave higher scores for creating an acceptor site to the mutant sequence (Suppl. Table S2).

We also assessed and eventually confirmed the presence of the same intronic variant on DNA of patient B, already reported to be heterozygous for the paternally inherited c.

532G>C:p.A178P mutation.⁷ In accordance with a recessive pattern of transmission, segregation analysis confirmed a maternal origin for the intronic variant.

Similarly, direct sequencing revealed the c.420+784C>T intronic variant in an additional case, patient C, in which an independent genetic analysis using a clinical exome panel had identified the c.532G>C:p.A178P heterozygous variant. The two variants were inherited from the parents (Fig. 1). Increased expression of the alternative splicing isoform of the transcript (retaining exon 3b) was confirmed on RNA purified from patient B's fibroblasts as well.

A further analysis of NDUFAF6 transcripts using an NGS approach confirmed that, although expressed at low levels also in control subjects, the alternative isoform is overrepresented in the samples from individuals harboring the intronic variant (patients A1 and B, and the mother of siblings A1 and A2) compared to subjects lacking this variant (control subjects and the father of siblings A1 and A2) (Fig. 2).

Notably, in the patients we observed a predominant expression of the mutated allele harboring the missense mutation c.532G>C in fibroblasts and, partly, in blood (Fig. 1D, Fig. 2). A non-sense mediated decay (NMD) assay performed on fibroblasts from both patients A1 and B and a control individual did not show any detectable difference in RNA sequence profiles between treated and untreated samples.

The identification of two extremely rare variants in three unrelated families from Italy displaying a similar clinical presentation raised the possibility of unreported/unknown relationship between the families and common founder alleles. All the families originate from Southern Italy, although from different regions (2 from Campania, 1 from Abruzzo). We performed a haplotype analysis using 7 tagSNPs present in the NDUFAF6 genomic region. All the patients showed the same haplotype (Suppl. Table S3) indicating that they likely harbor common NDUFAF6 alleles rather than having had independent mutational events. Analysis of the variants identified by targeted-NGS confirmed this finding, with shared NDUFAF6 haplotypes amongst patients; however it revealed a quite different variants profile in surrounding genes present on chromosome 8 (Suppl. Table S4), suggesting not recent founder occurrence.

Discussion

We identified compound heterozygous missense and deep intronic variants in three different families with a typical recessive NDUFAF6 - related disease characterized by Leigh syndrome. Complementation studies, previously performed on patient B,⁷ already proved that NDUFAF6 impairment was the cause of the disease. In accordance with

in silico predictions, our transcript data suggest that the intronic variant promotes the alternative splicing event, thus enhancing expression of the non-functional altered isoform of the gene at the expense of the canonical one.

An NMD assay, together with the amplification of the aberrant transcript in standard conditions, excludes the hypothesis of a relevant NMD involvement on the alternative NDUF6F6 isoform, at least in fibroblasts. Nevertheless, several NDUF6F6 transcripts which could be variably expressed in different tissues have been reported² and may be differently affected by the intronic variant and otherwise subjected to NMD. In line with this hypothesis, different expression of the two alleles was reported by Bianciardi et al.⁷ in blood, fibroblasts, urine and brush RNA samples from patient B. These data could thus suggest the existence of trans-splicing factors which determine a tissue-specific switch between the alternative spliced isoform and the canonical isoform.

The fact that we identified three unrelated cases with the same, peculiar combination of extremely rare NDUF6F6 variants may be casual. Otherwise we may speculate that one of these variants is hypomorphic (possibly the splicing variant which allows the formation of a quote of wild type transcript) and does not lead to disease, at least Leigh syndrome, in the homozygous state but only when associated with a severe mutation which in turn is too deleterious/embryolethal in the homozygous state. Homozygosity or various compound heterozygosity of splicing defect, missense changes or nonsense mutations have been found in the previously reported patients with NDUF6F6 mutations³⁻⁶,

and the affected nucleotides are located throughout the gene hampering an easy identification of obvious genotype-phenotype correlations.

The clinical presentation of the NDUFAF6 -mutant cases here reported is a Leigh syndrome with early childhood onset (1-5 years) and stable or slowly progressive course, associated with isolated cerebellar or extrapyramidal signs depending on affected cerebral structures; cognitive involvement and seizures were not detected/reported. MRI pattern was characterized by striatal and dentate nuclei involvement. Patient C presented isolated putamina involvement that was stable over time, and a relatively mild phenotype compared to other patients. Only in patient A2 putamen alterations were not observed, but she performed a single MRI at disease onset and additional data about radiological course were not available.

Reports on mutations located outside the coding regions and associated with human diseases are rapidly growing. In this study we confirmed that WES data analysis should take into account all rare variants, including those with poorly predictable effect on transcript/protein. Moreover, we underline that mRNA analysis is a complementary strategy, extremely useful to integrate WES and demonstrate the deleterious impact of identified variants, especially those affecting splicing and stability of transcripts.

Acknowledgments

This work was supported by the Telethon Grant GGP15041; the Pierfranco and Luisa Mariani Foundation (to DG); the MRC-QQR (2015-2020) grant; the ERC advanced grant FP7-322424, the NRJ-Institut de France grant (to MZ); the Italian Ministry of Health (Ricerca Corrente 2016-2017 to DG, EB and RC).

The “Cell lines and DNA Bank of Genetic Movement Disorders and Mitochondrial Diseases” of the Telethon Network of Genetic Biobanks (grant GTB12001J) and the EuroBioBank Network supplied biological specimens.

References

1. Dahl H-H. Getting to the nucleus of mitochondrial disorders: identification of respiratory chainenzyme genes causing Leigh syndrome. *Am J Hum Genet.* 1998; 63:1594–1597. [PubMed: 9837811]
2. McKenzie M, Tucker EJ, Compton AG, Lazarou M, George C, Thorburn DR, Ryan MT. Mutations in the gene encoding C8orf38 block complex I assembly by inhibiting production of the mitochondria-encoded subunit ND1. *J Mol Biol.* 2011; 414:413–426. [PubMed: 22019594]
3. Pagliarini DJ, Calvo SE, Chang B, Sheth SA, Vafai SB, Ong S-E, et al. A mitochondrial protein compendium elucidates complex I disease biology. *Cell.* 2008; 134:112–123. [PubMed: 18614015]
4. Kohda M, Tokuzawa Y, Kishita Y, Nyuzuki H, Moriyama Y, Mizuno Y, et al. A comprehensive genomic analysis reveals the genetic landscape of mitochondrial respiratory chain complex deficiencies. *PLoS Genet.* 2016; 12:e1005679. [PubMed: 26741492]

5. Fang F, Liu Z, Fang H, Wu J, Shen D, Sun S, et al. The clinical and genetic characteristics in children with mitochondrial disease in China. *Sci China Life Sci.* 2017; 60:746–757. [PubMed: 28639102]
6. Ogawa E, Shimura M, Fushimi T, Tajika M, Ichimoto K, Matsunaga A, et al. Clinical validity of biochemical and molecular analysis in diagnosing Leigh syndrome: a study of 106 Japanese patients. *J Inherit Metab Dis.* 2017; 40:685–693. [PubMed: 28429146]
7. Bianciardi L, Imperatore V, Fernandez-Vizarra E, Lopomo A, Falabella M, Furini S, et al. Exome sequencing coupled with mRNA analysis identifies NDUFAF6 as a Leigh gene. *Molec Genet Metab.* 2016; 119:214–222. [PubMed: 27623250]
8. Legati A, Reyes A, Nasca A, Invernizzi F, Lamantea E, Tiranti V, et al. New genes and pathomechanisms in mitochondrial disorders unraveled by NGS technologies. *Biochim Biophys Acta.* 2016; 1857:1326–1335. [PubMed: 26968897]

Figures and Tables:

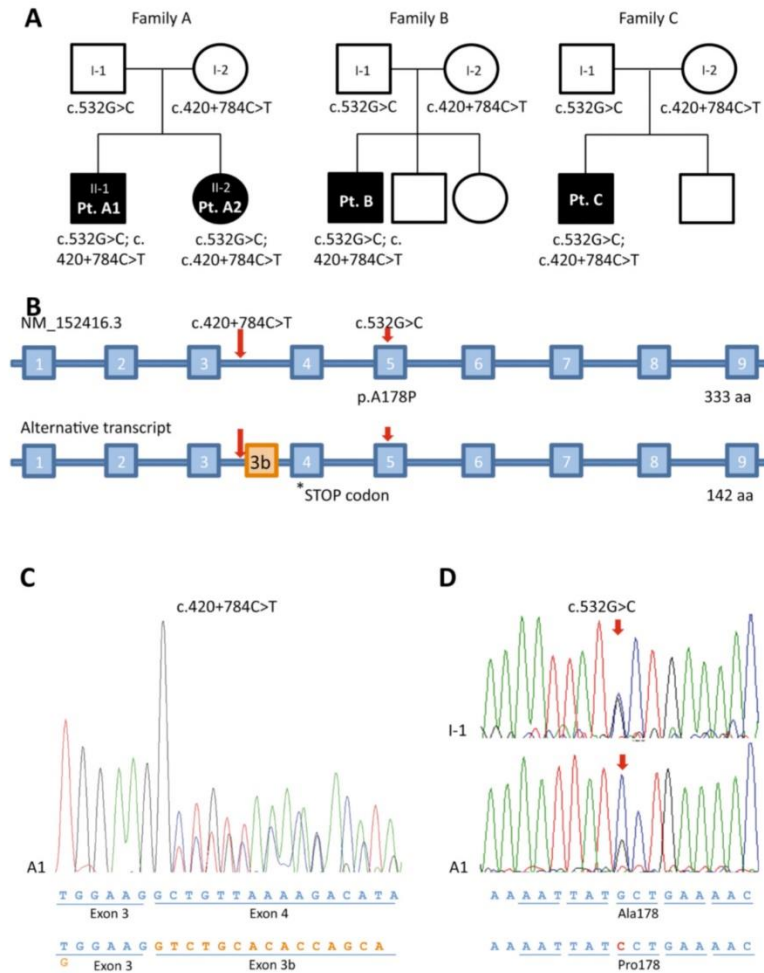


Figure 1. Pedigrees and genetic studies A. Pedigrees of the families A, B, C showing the identified NDUFAF6 variants. Black symbols indicate the affected siblings. B. Schematic structure of NDUFAF6 NM_152416.3 transcript (upper panel) and alternative splicing isoform (bottom panel). The retention of a string of 124 nucleotides located within intron 3 (exon 3b, orange box) generates a premature stop codon within exon 4 (arrow). C. Sanger sequence of NDUFAF6 cDNA

obtained from patient A1 blood RNA, showing two distinct sequences starting from the end of exon 3, that correspond to the NM_152416.3 transcript (junction exon 3-exon 4) and an alternative transcript retaining exon 3b (junction exon 3-exon 3b). D. Sanger sequence of NDUFAF6 cDNA obtained from blood samples of patient A1 (bottom panel) and his father (I-1, upper panel), showing a region within exon 5 which encompasses the heterozygous missense mutation.

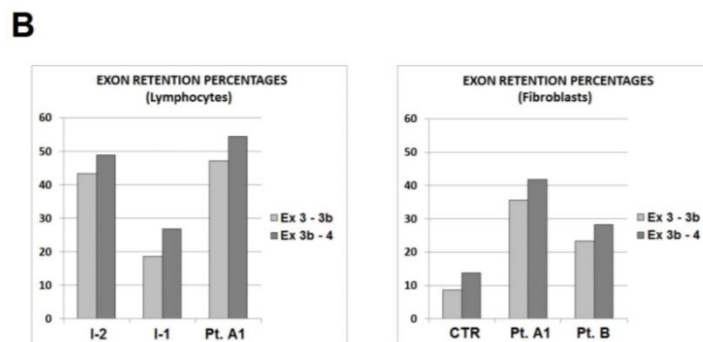
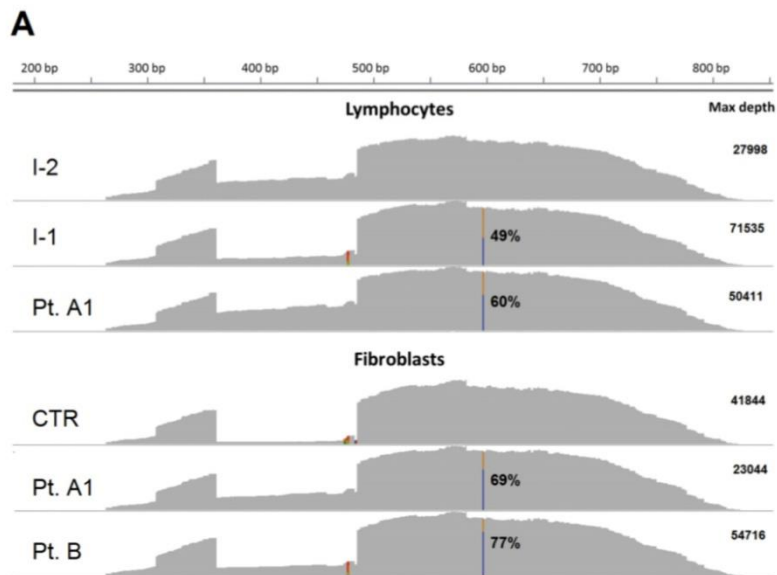


Figure 2. NGS coverage analysis A. Profiles of depth of coverage obtained through NGS on NDUFAF6 transcript PCR products. RNA was extracted from lymphocytes of Patient A1 (Pt. A1) and his parents (I-1; I-2), and from fibroblasts of patients A1, B and a control sample (CTR). B. Quantification of exon 3b retention. Graphs of the coverage ratio (in percentage) between the NDUFAF6 alternative isoform containing exon 3b and the canonical isoform, calculated for all the samples analyzed by NGS (the two bars correspond to the junctions exon 3-exon 3b and exon 3b-exon 4).

Supplementary Information: includes detailed case reports, 4 supplementary tables and 1 supplementary figure.

Case reports

Patient A1, now 5 years old, was born after uncomplicated pregnancy and delivery. Early development was referred as normal. At 21 months of age, after a febrile illness, he presented psychomotor regression, losing autonomous gait in about 4 months, whereas other acquired skills and cognitive functions were preserved. After 2 months he recovered autonomous deambulation but neurological signs became evident. Brain MRI at onset disclosed slight bilateral T2-hyperintensities in putamina, dentate nuclei and superior cerebellar peduncles. He was first evaluated at 30 months of age, showing ataxic gait and fine tremor. A second MRI -9 months after onset- showed the additional involvement of caudate nuclei. Fundus oculi, electroneuronography, electroretinogram, visual and brainstem auditory evoked potentials were normal. Blood routine exams, amino acids, lactate and pyruvate – plasma levels, and urinary organic acids were normal. Suspecting a mitochondrial disease, a muscle-cutaneous biopsy was performed: an isolated complex I deficiency in muscle and fibroblasts was documented (42% and 38% of the controls' mean, respectively, Suppl. Tab. S1). Treatment with coenzyme Q10 and riboflavin was started. Clinical evolution slowly worsened: at last neurological evaluation -at 4 years and 6 months- he presented with drooling, dysarthria, dysmetria, tremor, severe ataxic gait and hypertonia. Transient worsening of the neurological conditions and marked fatigability were subsequently

reported in association with infectious illnesses. Serial biochemical assays were normal, except for the last one that showed elevated plasma levels of lactate (2818 $\mu\text{mol/l}$, n.v. 580–2100 $\mu\text{mol/l}$) and pyruvate (181 $\mu\text{mol/l}$, n.v. 55-145 $\mu\text{mol/l}$). A third MRI -at 3 years and 6 months- confirmed a Leigh syndrome pattern and showed enlarged bilateral T2-hyperintensities in caudate and putamen that also appeared hypotrophic.

Patient A2, now 3 years old, is the younger sister of patient A1; she was born after uncomplicated pregnancy and delivery. Her early development was referred as normal, but since 1 year of age motor delay was reported. She was evaluated for the first time at 19 months of age: autonomous gait was not achieved, and she showed limb dysmetria and trunk titubation, while cognitive functions were preserved. Brain MRI disclosed bilateral T2-hyperintensities in dentate nucleus and superior cerebellar peduncle. Neurophysiological studies were normal. Lactate and pyruvate plasma levels were mildly elevated (2293 $\mu\text{mol/l}$, n.v. 580–2100 $\mu\text{mol/l}$ and 146 $\mu\text{mol/l}$, n.v. 55-145 $\mu\text{mol/l}$ respectively). Clinical evolution was moderately favorable, as she achieved autonomous gait at 24 months albeit with ataxic features. At the last clinical follow up -at 33 months of age- neurological evaluation confirmed the presence of cerebellar signs.

Patient B was described in detail in Bianciardi et al. 2016. Biochemical evaluation of the respiratory chain complexes in muscle and fibroblasts is reported in Suppl. Tab. S1.

Patient C is an 11 year-old boy, first child of unrelated parents born by cesarean section for uterine inertia. His psychomotor developmental milestones were referred to be normal. He presented at 5 years of age with gait unsteadiness and motor coordination problems. These symptoms gradually worsened, configuring over time an extrapyramidal syndrome. The last neurological examination revealed drooling, dysarthria, oculomandibular dystonia, extrapyramidal hypertonia and a mild camptocormic gait; cognitive functions were preserved. The first brain MRI was performed at 7 years of age and showed bilateral T2-hyperintense lesions of the putamen which appeared hypotrophic; these lesions remained stable at exams performed 3 years later. Extensive metabolic screening, including lysosomal enzymes, amino acids and lactate in plasma and CSF, urinary organic acids and oligosaccharides, were normal.

The activities of mitochondrial respiratory chain complexes on muscle homogenate were reported as normal but no biological specimen was available for further analysis; analysis of the mitochondrial DNA was normal.

Supplementary Table S1: Biochemical analysis of respiratory chain complex activities

		cI/CS	cII/CS	cIII/CS	cIV/CS	CS*
Muscle	Pt A1	42%	100%	116%	104%	191
	Pt B	72%	81%	96%	87%	227
		cI %	cII %	cIII %	cIV %	CS*
Fibroblasts	Pt A1	38%	133%	140%	122%	169
	Pt B #1	18%	100%	99%	127%	194
	Pt B #2	32%	89%	97%	106%	181

All enzymatic activities are normalized for citrate synthase (CS) activity and expressed as percentage of the mean control value. Values under the control range are in red bold. Biochemical assay on fibroblasts from patient B was repeated twice (#1 and #2).

* nmol/min mg (n.v. muscle 80-210; n.v. fibroblasts 80-150)

Supplementary Table S2: *in silico* predictions of the intronic variant effect on splicing

Tool	Analysed motif/sequence	Score for wild type	Analysed motif/sequence	Score for mutant
HSF ^a : potential splice site	acctcttcagGT	91.47	atctcttcagGT	93.32
HSF ^a : enhancers	/	/	tacatc	new site: 88.26
Spliceport ^b	acctcttcagGTCT G	0.333001	atctcttcagGTCTG	0.657623
BDGP splice predictor ^c	cagtgtacacctcttc agGTCTGCACAC CA	0.94	cagtgtacatctcttcag GTCTGCACACCA	0.97

The reported scores were obtained using different bioinformatic tools:

^a <http://www.umd.be/HSF3>

^b <http://spliceport.cbc.umd.edu>

^c http://www.fruitfly.org/seq_tools/splice.html

Supplementary Table S3: haplotype analysis of the tag SNPs

Chr	Coordinate	<i>NDUFAF6</i>	Reference	Pt A1	Pt B	Pt C	dbSNP ID	MAF%*
8	96038252	IVS1	G	C/G	C/G	C/G	rs10113282	49
8	96041267	IVS1	G	G/G	G/G	G/G	rs2599718	9
8	96042890	IVS1	A	A/G	A/G	A/G	rs10098197	12
8	96046094	IVS2	A	G/A	G/A	G/A	rs2678823	23
8	96048588	c.420+784C>T	C	C/T	C/T	C/T	rs749738738	0.003**
8	96049339	IVS3	T	T/T	T/T	T/T	rs2678827	27
8	96057827	c.532G>C	G	G/C	G/C	G/C	rs201088736	0.01**
8	96058218	IVS5	A	A/A	A/A	A/A	rs2678836	9
8	96065878	IVS8	G	A/G	A/G	A/G	rs9297952	33

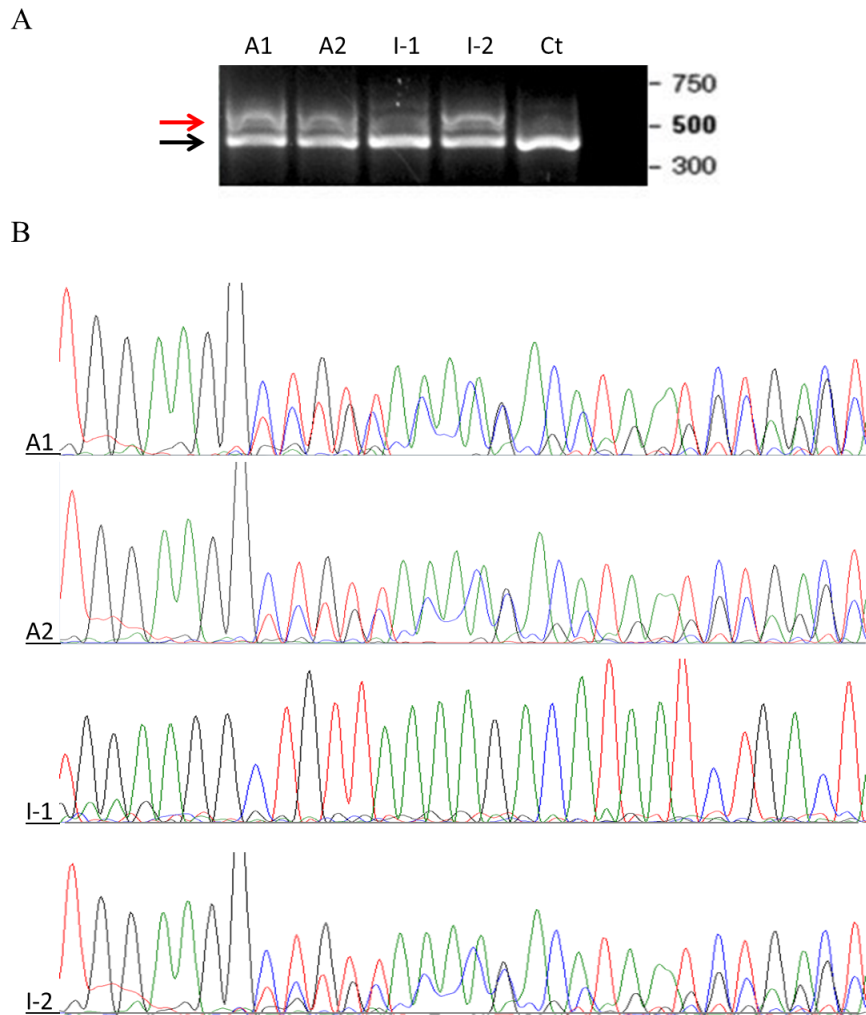
*: minor allele frequency from 1000 Genomes; **: minor allele frequency from gnomAD. Pt: patient, IVS: Intervening sequence. The two *NDUFAF6* mutations identified in the patients are in red.

Supplementary Table S4: haplotype analysis of variants on chromosome 8

Ch r	Coordin ate	Gene	Referen ce	Pt A1	Pt B	Pt C	dbSNP ID	MAF % *
8	74888494	TMEM70	C	T/T	C/T	C/C	rs2306486	21
8	74888616	TMEM70	G	G/G	G/C	G/G	rs8075	17
8	74888857	TMEM70	C	G/G	C/G	C/C	rs12548461	21
8	74888893	TMEM70	G	G/G	G/C	G/G	rs975915	17
8	74891164	TMEM70	A	A/A	A/G	A/A	rs75674446	18
8	74891200	TMEM70	A	A/A	A/G	A/A	rs73687119	25
8	74893821	TMEM70	A	A/A	A/G	A/A	rs1053079	25
8	74893850	TMEM70	C	C/C	C/G	C/C	rs1053077	25
8	74893880	TMEM70	C	T/T	T/T	C/C	rs7108	46
8	94935937	PDP1	T	T/C	C/C	C/C	rs4735258	50
8	96047621	NDUFAF6	G	G/C	G/C	G/C	rs6651271	10
8	96047933	NDUFAF6	C	C/G	C/G	C/G	rs6651272	10
8	96053782	NDUFAF6	GCT	GCT/ G	GCT/ G	GCT/ G	rs3510457 8	78
8	96057827	NDUFAF6	G	G/C	G/C	G/C	rs2010887 36	0
8	96070181	NDUFAF6	T	C/C	C/C	C/C	rs2678832	92
8	97243720	UQCRB	G	G/A	G/A	G/G	rs2292835	26
8	12555156 7	NDUFB9	C	C/T	C/T	C/C	rs7010411	28

*: minor allele frequency from 1000 Genomes. In red the missense mutation c.532G>C.

Supplementary Figure S1



Supplementary Figure S1: *NDUF6* transcript analysis in family

A

A. Agarose gel electrophoresis of cDNA amplified with *NDUF6* 3F-7R primers, showing the expected amplicon (453 nucleotides from NM_152416.3; black arrow) and the presence of a higher band (red arrow) in patients A1, A2 and their mother I-2, which corresponds to a transcript about 100-150 nt longer than the canonical isoform. Ct: cDNA from a control subject.

B. Electropherograms of the PCR amplicons reported in panel A. The alternative splicing isoform is also detectable on electropherograms, and the inserted sequence corresponds to an extra 124 nucleotide-long exon (exon 3b) present in *NDUFAF6* isoforms such as XM_005250791.1 and ENST00000520757.1.

Chapter 4

Homozygous variant in *OTX2* and possible genetic modifiers identified in a patient with combined pituitary hormone deficiency, ocular involvement, myopathy, ataxia and mitochondrial impairment.

Alessia Catania^{a,*}, Andrea Legati ^{a,*}, Lorenzo Peverelli ^{a,b}, Lorenzo Nanetti^a, Silvia Marchet ^a, Nadia Zanetti ^a, Costanza Lamperti ^a, Daniele Ghezzi ^{a,c}

^aUnit of Medical Genetics and Neurogenetics, Fondazione IRCCS Istituto Neurologico Carlo Besta

^bNeuromuscular and Rare Diseases Unit, Department of Neuroscience Fondazione IRCCS Ca' Granda Ospedale Maggiore Policlinico

^cDepartment of Pathophysiology and Transplantation, University of Milan, Milan, Italy

*: Equal contribution.

SUBMITTED

Abstract:

Here we report on a singleton patient affected by a complicated congenital syndrome characterized by growth delay, retinal dystrophy, sensorineural deafness, myopathy, ataxia, combined pituitary hormone deficiency, associated with mitochondrial impairment. Targeted clinical exome sequencing led to the identification of a homozygous missense variant in *OTX2*. Since only dominant mutations within *OTX2* have been associated with cases of syndromic microphthalmia, retinal dystrophy with or without pituitary dysfunctions, this represents the first report of an *OTX2* recessive mutation. Part of the phenotype, including ataxia, myopathy and multiple mitochondrial respiratory chain defects, seemed not related to *OTX2*. Further analysis of NGS data revealed additional candidate variants: a homozygous variant in *LETM1*, and heterozygous rare variants in *AFG3L2* and *POLG*. All three genes encode mitochondrial proteins and the last two are known to be associated with ataxia, a neurological sign present also in the father of the proband.

With our study we aim to encourage the integration of next generation sequencing (NGS) data with a detailed analysis of clinical description and family history in order to unravel composite genotypes sometimes associated with complicated phenotypes.

Keywords:

OTX2; *LETM1*; *AFG3L2*; *POLG*; complex congenital syndromes; NGS.

Introduction

In the last decade, the development of new next generation sequencing (NGS) technologies such as whole genome/exome sequencing, has rapidly offered a growing opportunity to provide large-scale and high sensitivity genomic screening allowing the identification of new pathogenic variants associated with rare inherited diseases and overcoming most of the limitations of a candidate-gene based approach to diagnostics. Even though, complex congenital phenotypes in singleton cases, thus without a clear Mendelian inheritance pattern, still represent one of the main pitfalls of these techniques. A close interaction between clinicians and geneticists is fundamental in order to allow a proper evaluation of the NGS data, especially considering the growing number of reports about cases with intricate clinical presentation and composite genetic basis.

In this report we describe a singleton patient affected by a complicated congenital syndrome characterized by growth delay, retinal dystrophy, sensorineural deafness, myopathy, ataxia, combined pituitary hormone deficiency, associated with mitochondrial impairment. Genetic and clinical data were deeply investigated in order to find genotype-phenotype correlations.

Materials and methods

Clinical, genetic and histo/biochemical evaluations were performed upon acquisition of informed consent from all the subjects involved in this study, as required by the Ethical Committee of the Fondazione IRCCS Istituto Neurologico Carlo Besta, in accordance with the Helsinki Declaration.

All members of the family who participated in the study took a complete neurologic examination. For the index case electroencephalography, neurophthalmologic and endocrine examinations, brain MRI, histological and biochemical evaluations on quadriceps muscle biopsy and electrophysiological studies (electroencephalography, electromyography, and brainstem evoked potentials) were performed. Brain MRI and neuropsychological evaluation were performed on the father as well.

Quadriceps muscle biopsy was obtained from subject III-2. Muscle morphology and histochemistry were performed as previously described¹. Respiratory chain complex activities were measured using standard spectrophotometric methods in muscle homogenate².

Total DNA was extracted from muscle biopsy of the proband and used for mitochondrial DNA (mtDNA) analyses, i.e. Southern blot and sequencing. Genomic DNA was extracted from peripheral blood samples, employing standard techniques. The TruSight One Sequencing Panel (Illumina®) that provides comprehensive coverage of 4.813 clinically relevant genes, was used for the preparation of the library then NGS was performed on MiSeq platform. The called variants were analyzed through a series of filtering steps as previously described³. Phenolyzer (<http://phenolyzer.wglab.org>), a bioinformatics tool focusing on discovering genes based on user-specific disease/phenotype terms, was used for prioritization of the heterozygous variants linked to “ataxia”. All selected variants identified by NGS were validated by Sanger sequencing.

Clinical description

The index subject (III-2), now 34 years old, is the second of two siblings born from first degree Italian cousins. Facial dysmorphic features, namely low set ears, micrognathia, divergent strabismus and bilateral ptosis, were evident at birth. After normal acquisition of autonomous gait at 10 months of age, during early childhood she developed a progressive speech impairment associated with severe sensorineural hypoacusia which required hearing aid since 5 years of age, congenital bilateral cataract, growth delay and cognitive impairment. She presented an early, slowly progressive myopathy with facial hyposthenia, diffuse skeletal muscle hypotrophy (particularly prominent in distal upper limbs) associated with gait ataxia and poor coordination. During the following years, a combined pituitary hormone deficiency (CPHD) was also detected, leading to early menopause, severely reduced bone density and generalized osteoporosis.

First brain MRI was performed at age of 8, disclosing cerebral cortical atrophy (particularly evident in frontal lobes), associated with hypoplasia of the cerebellum, mostly evident in the cerebellar vermis, shrunken pituitary gland and slightly sharpened optic tracts. Electromyography confirmed the presence of myopathic abnormalities without signs of neuropathy. Auditory evoked potentials revealed a marked bilateral brainstem dysfunction. Electroencephalography displayed normal findings.

Under the hypothesis of a mitochondrial encephalomyopathy, she underwent a muscle biopsy when she was 11. Histological examination suggested neurogenic muscle atrophy associated with mitochondrial dysfunction as multiple ragged-red fibers with increased fiber

anisometry and basophilia were detected. COX-negative fibers and subsarcolemmal accumulation of oxidative enzymes on ragged-red fibers were revealed by histoenzymatic analysis (Figure 1). Isolated fibers exhibited increased acid phosphatase activity and esterase positivity. Furthermore, biochemical assays evidenced a reduced activity of all mitochondrial respiratory complexes with the exception of complex II (Figure 1).

Clinical conditions very slowly worsened overtime: last neurologic and physical examination, performed at the age of 34, revealed decreased BMI, horizontal nystagmus, severe limb dysmetria and ataxic gait with myopathic features. Hypophonia and dysarthria were also documented, together with generalized amyotrophy, reduced deep tendon reflexes in upper limbs and absence on lower limbs. Considering her general conditions and acoustic-articulatory defects, a complete neuropsychological battery couldn't be administered, but basic testing revealed intellectual disability and marked executive dysfunctions, defective verbal denomination and behavioral disturbances with emotional lability. Repeated panic attacks were also reported by parents. Ophthalmologic evaluation disclosed an exo-hypertropia, diplopia, signs of past bullous keratopathy, tight bilateral myosis conditioning difficulties in clear visualization of fundus oculi.

Her father (II-1), now 78 years old, developed during his fifties a progressively worsening gait impairment, which required the use of a walking aid for medium-long distance walking. Clinical evaluation at 9 years of follow up revealed ataxic, slowed down and wide based gait associated with limb incoordination and mild dysdiadochokinesia. Speech was mildly dysarthric. A comprehensive neuropsychological

battery revealed defective attentive and executive functions and weakened visual memory. Moderate limb apraxia appeared at imitation of nonmeaningful gestures. He also displayed signs of mild asymptomatic neuropathy, with absence of tendon reflexes and distal-impaired vibratory sensation. Muscle trophism and strength were normal. Anamnesis also revealed the presence of history of anxiety, phobic behavior and panic attacks responsive to therapy with serotonin reuptake inhibitors and benzodiazepines. His brain MRI showed brain atrophy and moderate cerebellar atrophy, particularly prominent in vermis. Under the hypothesis of a genetic origin of the adult onset ataxic syndrome, mutational analysis of *FTAX* and *SCA6* genes were performed, resulting in normal findings.

Results

Karyogram analysis of the proband (III-2) revealed a normal female chromosomal karyotype.

Evaluation of mtDNA from subject III-2 muscle by Southern blot analysis ruled out the presence of mtDNA macrodeletions, while mtDNA sequencing excluded the presence of MELAS or MERRF associated variants, revealing the presence of a single homoplasmic variant (m.14687A>G), located in *MT-TE*, the gene encoding for the mitochondrial tRNA(Glu). It was homoplasmic also in the asymptomatic mother. The m.14687A>G variant is predicted to be likely benign, being found in 241 full length mitochondrial sequences in MitoMap (<https://www.mitomap.org>), despite in 2003 it was reported as causative of myopathy with lactic acidosis and retinopathy

in a 16 year-old patient⁴. Taken together these findings did not support a causative role for this mtDNA variant.

Thereafter, we performed clinical exome sequencing on the index subject DNA. In light of parental consanguinity, NGS data were processed and analyzed based on an autosomal recessive mode of inheritance, focusing our search on rare (MAF<0.1%), predicted pathogenic homozygous variants. With this approach we found two homozygous missense variants, located within the *OTX2* and *LETMI* genes (Figure 2). The homozygous missense change c.844T>A, p.Cys282Ser (rs764205900) in *OTX2* (Orthodenticle homeobox 2) falls within the last exon of the gene, is present in all validated isoforms of the protein and involves an amino acid residue highly conserved across species. It segregated with the disease as parents were found to harbor the mutation in the heterozygous state, while their healthy daughter was wild type in both alleles (Figure 2). This variant is predicted deleterious by SIFT (sift.jcvi.org) and probably damaging by Polyphen and is reported with an extremely low frequency on GnomAD (2×10^{-5}).

A second rare homozygous variant was identified in *LETMI*; it is the c.881G>A nucleotide change, causing the missense substitution p.Arg294Gln. It segregated with the disease being heterozygous in the parents and in the unaffected sister (Figure 2). This variant is reported with an extremely low frequency on GnomAD (2×10^{-5}) and predicted deleterious by SIFT and probably damaging by Polyphen.

Based on the clinical picture of the proband's father, we considered the possibility of a double diagnosis, and hypothesized a dominant model of inheritance underlying the ataxic signs. Moreover, we considered ataxic signs probably associated with the mitochondrial impairment,

which is not attributable with certainty to *OTX2* or *LETMI* variants. Running a new analysis of NGS data, we focused on genes possibly involved in autosomal dominant inherited ataxia (Supplementary table 1): candidate genetic variants in two genes, namely *AFG3L2* and *POLG*, were identified (Figure 2). Interestingly, both encode for mitochondrial proteins.

The variant found in *AFG3L2* (c.2167G>A; p.Val723Met) is reported in public SNP database (rs139469785) with a low frequency (2×10^{-3} on ExAC), classified as “likely pathogenic” in ClinVar (based on population studies and in silico predictions) and predicted deleterious by SIFT/probably damaging by Polyphen. The amino acid change p.Val723Met is conservative but occurs in a well-conserved residue across species (Figure 2). The variant was heterozygous on DNA from the father, and absent in the mother and in the sister.

The latter analysis of NGS data also revealed the presence of a heterozygous variant in *POLG* (c.1898A>G/p.Lys633Arg), extremely rare on public databases (rs568913937; 4×10^{-6} on GnomAD). In the same amino acid position, two additional variants have been reported, namely p.Lys633Thr (rs568913937) and p.Lys633Asn (rs761467007); all three missense changes are predicted benign/tolerated. The *POLG* heterozygous variant was inherited from the father and present also in the unaffected sister (Figure 2).

Discussion

In this report we describe a deep genetic analysis carried out in a patient affected by a complex neuro-endocrine syndrome. We identified a homozygous variant within *OTX2* as the main genetic cause of the

clinical picture, in particular combined pituitary hormone deficiency, syndromic microphthalmia and retinal dystrophy, a condition previously associated only with single heterozygous *OTX2* mutations. Further analysis of NGS data revealed the presence of additional variants in candidate genes which may contribute to explain the complicated phenotype of this subject and additional symptoms possibly not related to *OTX2* impairment.

OTX2 encodes for a nuclear protein belonging to the homeobox family, which is essential for regulation of genes involved in forebrain and craniofacial development during embryonic stages and for long term maintenance of adult retina⁵. Besides, *OTX2* protein plays essential roles in dopaminergic neurons differentiation, pineal and anterior pituitary development, also acting as a transactivator of gonadotropin-releasing hormone in the hypothalamus⁶.

Autosomal dominant mutations within *OTX2* have been associated with cases of syndromic microphthalmia, retinal dystrophy with or without pituitary dysfunctions and combined pituitary hormone deficiency (OMIM 600037). Until now, pathogenic homozygous mutations of *OTX2* have never been reported. Most relevant clinical features of the index subject phenotype are consistent with biological functions of *OTX2* protein and with phenotypic expression of reported cases of patients carrying dominant *OTX2* mutations, namely severe optic damage, microcephaly, pituitary dysfunctions, neurodevelopmental and growth delay. For this reason, the *OTX2* homozygous variant we identified can be considered the main genetic cause of the clinical presentation in our proband, despite a different (recessive vs. dominant) inheritance. Reports on inherited diseases with a similar clinical

phenotype determined by dominant or recessive mutations falling within the same gene are rapidly increasing during the last few years. *OTX2* variants mainly act by a mechanism of haploinsufficiency, reducing protein transactivation activity on target genes with or without a dominant negative effect on gene expression⁷. In mouse models the complete absence of *Otx2* causes a severe developmental impairment with defective axis conversion. We may speculate that the missense p.Cys282Ser change leads to the synthesis of a hypomorphic protein, causing an incomplete *OTX2* deficiency similar to *OTX2* haploinsufficiency. The temporal and tissue- limited expression of *OTX2* hampered any functional studies on available biological specimens (blood, muscle) from the proband to test this hypothesis. Furthermore, although never reported in association with *OTX2* mutations, the presence of sensorineural deafness as a relevant sign in the clinical phenotype could be explained by the already established crucial role of *OTX2* in mammalian cochlear development⁸. Indeed, cochlear and vestibular abnormalities have been reported in *Otx1* and *Otx2* (mouse orthologs of *OTX2*) knock-down mutants, and a rescue of the phenotype is described upon expression of human *OTX2* cDNA⁹. Additionally, cases of children with apparently conductive hearing loss lacking one copy of the *OTX2* gene have been described¹⁰. On the other hand, severe sensorineural deafness could be considered a typical manifestation of complex phenotypic spectrum caused by major mitochondrial dysfunction. Despite some experimental evidences emphasize the potential role of exogenous *OTX2* in mitochondrial respiratory chain function and regulation¹¹, severe cerebellar atrophy associated with clinically prominent ataxia together with myopathy and

multiple mitochondrial respiratory chain defects, don't appear to be immediately correlated to *OTX2* mutation and/or biological function. In addition to *OTX2* variant, another homozygous missense change was identified in *LETMI*. Monoallelic deletions of *LETMI* are found in patients affected by Wolf-Hirschhorn syndrome, a congenital malformation syndrome associated with a hemizygous deletion of chromosome 4p16.3, as a result of haploinsufficiency phenotype¹². Phenotypic dissimilarity reasonably rule out a major involvement of the p.Arg294Gln *LETMI* variant in the development of the syndromic condition detected in our patient. However, *LETMI* encodes for a mitochondrial $\text{Ca}^{2+}/\text{H}^{+}$ antiporter¹³, thus we cannot exclude a link between the identified *LETMI* variant and the mitochondrial defects observed in the proband, also considering growing evidence derived from model organisms suggesting that reduced *LETMI* expression is associated with some mitochondrial dysfunctions¹⁴. Very recently researchers have recognized an important role for LETM1 in mitochondrial ribosome function, thus being essential in mitochondrial translation machinery. Additionally, fibroblasts from WHS patients displayed clear abnormalities in mitochondrial morphology, mtDNA organization and a remodeling of oxidative metabolism¹⁵. The emerging importance of LETM1 in mitochondrial morphology maintenance and function, suggests a possible role of the p.Arg294Gln variant in the determination or worsening of at least a portion of our patient's symptoms, and may contribute to the severe mitochondrial dysfunction revealed by studies on muscle biopsy of our proband. Nevertheless, haploinsufficiency of *LETMI* has been proposed as an underlying pathomechanism mainly for seizures in Wolf-Hirschhorn

syndrome¹⁶, but epileptic signs are not part of the complex picture in our proband.

In addition to homozygous variants we identified heterozygous variants in *AFG3L2* and *POLG*, shared by the proband and her father and linked to ataxia and mitochondrial dysfunction. *AFG3L2* encodes for a well-known mitochondrial protein involved as a catalytic subunit in m-AAA protease, which plays an essential role in misfolded protein degradation, ribosome assembly¹⁷, and mitochondrial dynamics through proteolytic regulation of OPA1¹⁸. Monoallelic *AFG3L2* mutations have been associated with cases of spinocerebellar ataxia, genetically designated as SCA28¹⁹. The phenotype of subject II-1 is quite consistent with clinical presentation of SCA28 patients. Besides, conditional *Afg3l2* mouse models restricted to Purkinje cells exhibit fragmentation of mitochondrial network and strongly impaired activities of mitochondrial respiratory chain complexes, possibly attributable to defective protein synthesis²⁰. Even though this aspect has never been systematically tested on humans, muscle biopsies from SCA28 patients have shown histological abnormalities with COX deficient and ragged red fibers, and profound reorganization of mitochondrial distribution within altered fibers²¹. *AFG3L2* mutations have been reported also in cases of progressive external ophthalmoplegia (PEO) and multiple mtDNA deletions²². It is important to mention some considerations concerning the *AFG3L2* variant c.2167G>A/p.Val723Met; its allelic frequency in public databases is much higher than estimated prevalence of SCA28 cases on overall population and the missense change is located in a C-terminal region, more distal than any previously known mutation. Even

assuming that the defective mitochondrial respiratory chain activity observed on subject III-1 muscle could be at least partially explained by the above described *AFG3L2* variant, it is unlikely that p.Val723Met alone could fully justify the severe mitochondrial damage. Muscle from the father (II-1) was not available to confirm this point.

Recessive and dominant variants in *POLG* have been associated with several hereditary syndromes encompassing severe cases of mtDNA depletion syndromes, cases of isolated PEO, cases of Sensory Ataxic Neuropathy, Dysarthria and Ophthalmoparesis (SANDO phenotype) and cases of SpinoCerebellar Ataxia with Epilepsy (SCAE phenotype) (OMIM 203700, 613662, 607459, 157640, 258450). However, ataxia was typically present in recessive *POLG* cases. All *POLG* related syndromes are associated with extensive alterations of mitochondrial function²³, as a direct consequence of its essential role in mitochondrial DNA replication machinery²⁴. The presence of the *POLG* variant even in the unaffected sister (III-1) casts doubt about its pathogenic role. Nevertheless, the existence of possible risk factor variants in *POLG* has been recently proposed in a panel study of a group of patients with dominant cerebellar ataxia²⁵.

We may speculate that *POLG* p.Lys633Arg could contribute to clinical presentation of both II-1 (who also displays a mild sensory ataxic neuropathy) and III-2 subjects, acting as an interplayer in the determination of mitochondrial impairment, possibly together with *AFG3L2*, *LETMI* or other unidentified variants. The role of biallelic *LETMI* variants as causative for human diseases and/or for mitochondrial dysfunction as well as the possible pathogenic effect of

p.Val723Met in *AFG3L2* and p.Lys633Arg in *POLG* need the identification of further cases in order to be fully elucidated.

Even though the contribution of each variant to the phenotype is far from being clarified, with our study we aim to encourage the integration of NGS data with a detailed analysis of clinical description and family history, in order to unravel composite genotypes sometimes associated with complicated phenotypes. Dissecting overlapping phenotypes and preventing misleading expansion of phenotypic spectrum are diagnostic challenges for researchers involved in the field of rare disorders.

Acknowledgements

Funding: This work was supported by the Pierfranco and Luisa Mariani Foundation, the Telethon Grant GGP15041.

Conflict of interest

The authors declare that they have no conflict of interest.

References

1. Sciacco M, Bonilla E. Cytochemistry and immunocytochemistry of mitochondria in tissue sections. *Methods Enzymol* 1996; 264:509–21.
2. Bugiani M, Invernizzi F, Alberio S, Briem E, Lamantea E, Carrara F, Moroni I, Farina L, Spada M, Donati MA, Uziel G, Zeviani M. Clinical and molecular findings in children with complex I deficiency. *Biochim Biophys Acta* 2004;1659:136–47.
3. Legati A, Reyes A, Nasca A, Invernizzi F, Lamantea E, Tiranti V, Garavaglia B, Lamperti C, Ardisson A, Moroni I, Robinson A, Ghezzi D, Zeviani M. New genes and pathomechanisms in mitochondrial disorders unraveled by NGS technologies. *Biochim*

- Biophys Acta. 2016 Aug;1857(8):1326-1335. doi: 10.1016/j.bbabi.2016.02.022.
4. Bruno C, Sacco O, Santorelli FM, Assereto S, Tonoli E, Bado M, Rossi GA, Minetti C. Mitochondrial myopathy and respiratory failure associated with a new mutation in the mitochondrial transfer ribonucleic acid glutamic acid gene. *J Child Neurol.* 2003 Apr;18(4):300-3.
 5. Beby F, Lamonerie T. The homeobox gene *Otx2* in development and disease. *Exp Eye Res.* 2013 Jun;111:9-16. doi: 10.1016/j.exer.2013.03.007. doi: 10.1016/j.exer.2013.03.007.
 6. Dateki S, Kosaka K, Hasegawa K, Tanaka H, Azuma N, Yokoya S, Muroya K, Adachi M, Tajima T, Motomura K, Kinoshita E, Moriuchi H, Sato N, Fukami M, Ogata T. Heterozygous orthodontic homeobox 2 mutations are associated with variable pituitary phenotype. *J Clin Endocrinol Metab.* 2010 Feb;95(2):756-64. doi: 10.1210/jc.2009-1334.
 7. Mortensen AH, Schade V, Lamonerie T, Camper SA. Deletion of *OTX2* in neural ectoderm delays anterior pituitary development. *Hum Mol Genet.* 2015 Feb 15;24(4):939-53. doi: 10.1093/hmg/ddu506.
 8. Vendrelli V, López-Hernández I, Durán Alonso MB, Feijoo-Redondo A, Abello G, Gálvez H, Giráldez F, Lamonerie T, Schimmang T *Otx2* is a target of N-myc and acts as a suppressor of sensory development in the mammalian cochlea. *Development.* 2015 Aug 15; 142(16):2792-800. doi: 10.1242/dev.122465.
 9. Morsli H, Tuorto F, Choo D, Postiglione MP, Simeone A, Wu DK. *Otx1* and *Otx2* activities are required for the normal development of the mouse inner ear. *Development.* 1999;126:2335-2343.
 10. Brisset S, Slamova Z, Dusatkova P, Briand-Suleau A, Milcent K, Metay C, Simandlova M, Sumnik Z, Tosca L, Goossens M, Labrune P, Zemankova E, Lebl J, Tachdjian G, Sedlacek Z. Anophthalmia,

- hearing loss, abnormal pituitary development and response to growth hormone therapy in three children with microdeletions of 14q22q23. *Mol Cytogenet.* 2014 Feb 28;7(1):17. doi: 10.1186/1755-8166-7-17.
11. Kim HT, Kim SJ, Sohn YI, Paik SS, Caplette R, Simonutti M, Moon KH, Lee EJ, Min KW, Kim MJ, Lee DG, Simeone A, Lamonerie T, Furukawa T, Choi JS, Kweon HS, Picaud S, Kim IB, Shong M, Kim JW. Mitochondrial Protection by Exogenous Otx2 in Mouse Retinal Neurons. *Cell Rep.* 2015 Nov 3;13(5):990-1002. doi: 10.1016/j.celrep.2015.09.075.
 12. Endele S, Fuhry M, Pak SJ, Zabel BU, Winterpacht A. LETM1, a novel gene encoding a putative EF-hand Ca²⁺-binding protein, flanks the Wolf-Hirschhorn syndrome (WHS) critical region and is deleted in most WHS patients. *Genomics.* 1999 Sep 1;60(2):218-25.
 13. Jiang D, Zhao L, Clapham DE. Genome-wide RNAi screen identifies Letm1 as a mitochondrial Ca²⁺/H⁺ antiporter. *Science.* 2009 Oct 2;326(5949):144-7. doi: 10.1126/science.1175145.
 14. Hart L, Rauch A, Carr AM, Vermeesch JR, O'Driscoll M. LETM1 haploinsufficiency causes mitochondrial defects in cells from humans with Wolf-Hirschhorn syndrome: implications for dissecting the underlying pathomechanisms in this condition. *Dis Model Mech.* 2014; 7(5):535-45. doi: 10.1242/dmm.014464.
 15. Durigon R, Mitchell AL, Jones AW, Manole A, Mennuni M, Hirst EM, Houlden H, Maragni G, Lattante S, Doronzio PN, Dalla Rosa I, Zollino M, Holt IJ, Spinazzola A. LETM1 couples mitochondrial DNA metabolism and nutrient preference. *EMBO Mol Med.* 2018 Sep;10(9). pii: e8550. doi: 10.15252/emmm.201708550.
 16. Zhang X, Chen G, Lu Y, Liu J, Fang M, Luo J, Cao Q, Wang X. Association of mitochondrial letm1 with epileptic seizures. *Cereb Cortex.* 2014; 24(10):2533-40. doi: 10.1093/cercor/bht118.

17. Koppen M, Metodiev MD, Casari G, Rugarli EI, Langer T. Variable and tissue-specific subunit composition of mitochondrial m-AAA protease complexes linked to hereditary spastic paraplegia. *Molec. Cell. Biol.* 2007, 27: 758-767. doi: 10.1523/JNEUROSCI.4677-07.2008.
18. Maltecca F, Aghaie A, Schroeder DG, Cassina L, Taylor BA, Phillips SJ, Malaguti M, Previtali S, Guénet JL, Quattrini A, Cox GA, Casari G. The mitochondrial protease AFG3L2 is essential for axonal development. *J Neurosci.* 2008 Mar 12;28(11):2827-36. doi: 10.1523/JNEUROSCI.4677-07.2008.
19. Di Bella D, Lazzaro F, Brusco A, Plumari M, Battaglia G, Pastore A, Finardi A, Cagnoli C, Tempia F, Frontali M, Veneziano L, Sacco T, Boda E, Brussino A, Bonn F, Castellotti B, Baratta S, Mariotti C, Gellera C, Fracasso V, Magri S, Langer T, Plevani P, Di Donato S, Muzi-Falconi M, Taroni F. Mutations in the mitochondrial protease gene AFG3L2 cause dominant hereditary ataxia SCA28. *Nat Genet.* 2010 Apr;42(4):313-21. doi: 10.1038/ng.544.
20. Almajan ER, Richter R, Paeger L, Martinelli P, Barth E, Decker T, Larsson NG, Kloppenburg P, Langer T, Rugarli EI. AFG3L2 supports mitochondrial protein synthesis and Purkinje cell survival. *J Clin Invest.* 2012 Nov;122(11):4048-58. doi: 10.1172/JCI64604.
21. Svenstrup K, Nielsen TT, Aidt F, Rostgaard N, Duno M, Wibrand F, Vinther-Jensen T, Law I, Vissing J, Roos P, Hjermand LE, Nielsen JE. SCA28: Novel Mutation in the AFG3L2 Proteolytic Domain Causes a Mild Cerebellar Syndrome with Selective Type-1 Muscle Fiber Atrophy. *Cerebellum.* 2017 Feb;16(1):62-67. doi: 10.1007/s12311-016-0765-1.
22. Gorman GS, Pfeiffer G, Griffin H, Blakely EL, Kurzawa-Akanbi M, Gabriel J, Sitarz K, Roberts M, Schoser B, Pyle A, Schaefer AM, McFarland R, Turnbull DM, Horvath R, Chinnery PF, Taylor RW.

- Clonal expansion of secondary mitochondrial DNA deletions associated with spinocerebellar ataxia type 28. *JAMA Neurol.* 2015 Jan;72(1):106-11. doi: 10.1001/jamaneurol.2014.1753.
23. Béreau M, Anheim M, Echaniz-Laguna A, Magot A, Verny C, Goideau-Sevrain M, Barth M, Amati-Bonneau P, Allouche S, Aygnac X, Bédard-Millet AL, Guyant-Maréchal L, Kuntzer T, Ochsner F, Petiot P, Vial C, Omer S, Sole G, Taieb G, Carvalho N, Tio G, Kremer S, Acquaviva-Bourdain C, de Camaret BM, Tranchant C. The wide POLG-related spectrum: An integrated view. *J Neurol Sci.* 2016 Sep 15;368:70-6. doi: 10.1016/j.jns.2016.06.062.
24. Lestienne, P. Evidence for a direct role of the DNA polymerase gamma in the replication of the human mitochondrial DNA in vitro. *Biochem. Biophys. Res. Commun.* 1987, 146: 1146-1153.
25. Coutelier M, Coarelli G, Monin ML, Konop J, Davoine CS, Tesson C, Valter R, Anheim M, Behin A, Castelnovo G, Charles P, David A, Ewencyk C, Fradin M, Goizet C, Hannequin D, Labauge P, Riant F, Sarda P, Sznajder Y, Tison F, Ullmann U, Van Maldergem L, Mochel F, Brice A, Stevanin G, Durr A; SPATAX network. A panel study on patients with dominant cerebellar ataxia highlights the frequency of channelopathies. *Brain.* 2017 Jun 1;140(6):1579-1594. doi: 10.1093/brain/awx081.

Figures

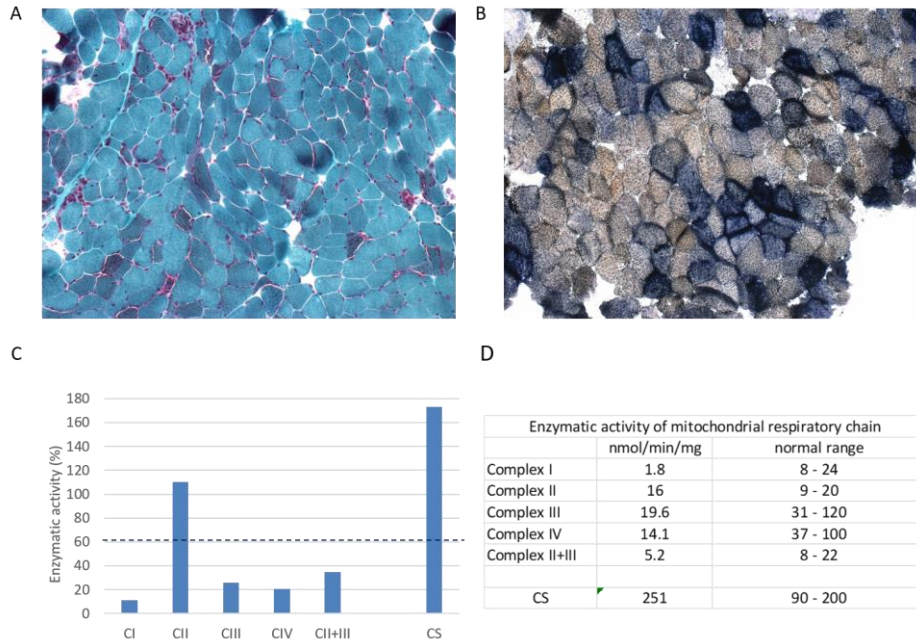


Figure 1: Histo- and biochemical analysis of the proband's muscle biopsy A: Gomori trichrome staining highlights the presence of several ragged red fibers, rare basophil accumulations in subsarcolemmal position, and some hypotrophic fibers. B: Cytochrome *c* oxidase (COX) and succinate dehydrogenase (SDH) double staining shows an altered oxidative enzymatic activity, with mitochondrial accumulation at the periphery of some fibers, reduced COX activity in many muscular cells and increase of SDH activity in some ragged blue fibers. C-D: Biochemical analysis of mitochondrial respiratory chain complex activities in muscle from the proband. Enzyme activities, normalized for citrate synthase (CS) activity, are expressed as percentages of the control mean. cI, cII, cIII, cIV: complex I, II, III, IV. The dotted line indicates the lower values in the control range.

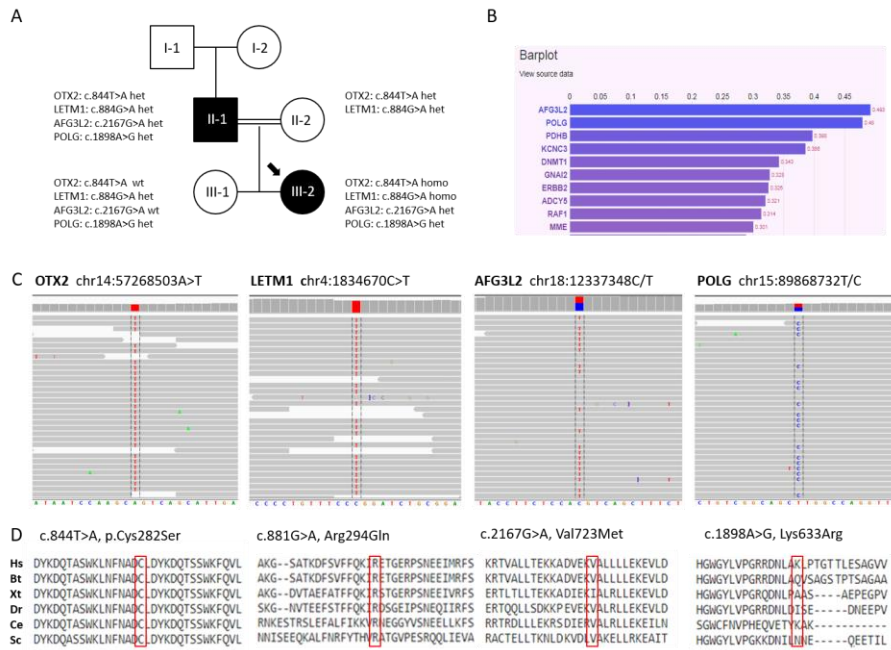


Figure 2: Pedigree and genetic findings A: Family pedigree with the identified variants. Black symbols indicate affected subjects; an arrow indicates the proband. B: Prioritization of genes related to “ataxia” from index subject (III-2) WES data (Software: Phenolyzer) C: Snapshots from IGV software of the variants identified in the proband by clinical exome sequencing. D: Phylogenetic alignment of the human protein region containing the substitutions found in the proband. Altered residues in the affected subject are boxed in red. Abbreviations are as follows: Hs, *H. sapiens*; Bt, *B. taurus*; Xt, *X. tropicalis*; Dr, *D. rerio*; Ce, *C. elegans*; Sc, *S. cerevisiae*.

Supplementary material:

Supplementary Table 1: Prioritization analysis of index subject (III-2) WES data with genes related to “ataxia” and corresponding variants.

<i>Chr</i>	<i>Coordinate</i>	<i>Variant</i>	<i>Gene</i>	<i>Genotype</i>	<i>HGVSc</i>	<i>HGVSp</i>	<i>dbSNP ID</i>	<i>GnomAD MAF</i>	<i>ACMG criteria*</i>	<i>Disease #OMIM</i>	<i>Comments</i>
18	12337348	C>C/T	<i>AFG3L2</i>	het	c.2167G>A	p.Val723Met	rs139469785	0.01%	Likely pathogenic	614487 AR 610246 AD	Segregation (I-1 het; III-1 wt); conserved aa
15	89868732	T>T/C	<i>POLG</i>	het	c.1898°>G	p.Lys633Arg		4.117e-6	VUS	203700 AR 613662 AR 607459 AR 157640 AD 258450 AR	Segregation (I-1 het; III-1 het); not conserved aa
3	58414328	C>C/T	<i>PDHB</i>	het	c.806G>A	p.Arg269His	rs769187141	0.001%	VUS	614111 AR	Phenotype and inheritance not compatible
19	50826453	T>T/G	<i>KCNC3</i>	het	c.1757°>C	p.His586Pro		absent	VUS	605259 AD	NGS artifact; not conserved aa
19	10270746	GA>G/G	<i>DNMT1</i>	hom	c.1044-8delT		rs3079962 (merged with rs796846833)	0.008% (36%)	VUS	604121 AD 614116 AD	Intronic, polyA stretch, highly polymorphic region (Clinvar: benign)
3	50293617	T>T/C	<i>GNAI2</i>	het	c.465-7T>C			absent	VUS	192605 AD	NGS artifact; Intronic
17	37868568	T>T/C	<i>ERBB2</i>	het	c.1022-7T>C		rs757367899	absent	VUS	211980 613659 137800	NGS artifact; Intronic
3	123023037	T>T/G	<i>ADCY5</i>	het	c.2443-7°>C			absent	VUS	606703 AD	NGS artifact, Intronic
3	12632480	A>A/G	<i>RAF1</i>	het	c.1194-7T>C			absent	VUS	615916 AD 611554 611553 AD	NGS artifact, Intronic
3	154857984	C>C/T	<i>MME</i>	het	c.860C>T	p.Thr287Met	rs202094946	4.088e-5	VUS	617018 AD 617017 AR, AD	conserved aa (Probably dam/tolerated)

*: *Illumina Interpreter*; *HGVSc*, *HGVSp*: *Human Genome Variation Society's standard sequence variation nomenclature*; *VUS*: *variant of uncertain significance*; *MAF*: *minor allele frequency*

Chapter 5

A novel dominant mutation in *DNMT1* underlying a case of cerebellar ataxia, deafness and narcolepsy syndrome (ADCA-DN).

Preliminary data

Introduction

As already mentioned in the general introduction, and eventually illustrated in chapter 4, in some cases establishing pathogenicity of novel variants identified by WES (whole exome sequencing) reveals quite puzzling, even when they are associated with known disease genes. I will briefly present below an explanatory example from my personal work during these years.

Autosomal dominant cerebellar ataxia (ADCA) are a group of heterogeneous clinical conditions characterized by frequent association of progressive ataxia with a plethora of different neurological symptoms. They can underly a broad genetic background with a large group of ADCA causing loci still to be determined¹

We have recently identified a novel mutation within a known disease gene, namely *DNMT1*, underlying a typical case of autosomal-dominant cerebellar ataxia, deafness and narcolepsy (ADCA-DN).

Molecular studies have started very recently and results are still exploratory.

Case report and exploratory results

The patient, now 65 years old, presented with in his early fifties with a slowly progressive hypoacusia, ataxia and dysarthric speech. A brain RMN documented the presence of vermian cerebellar atrophy associated with mild cortical atrophy (Figure 1).

Family history revealed that his mother, who had died some years earlier, also developed in her adulthood a complex syndrome characterized by a diffuse axonal polyneuropathy, deafness, ataxia and severe cognitive decline with psychosis. Severe hypoacusia in the maternal grand-mother and uncle was also reported. Index patient's father and younger brother were unaffected.

At the time of follow up the patient has also developed a progressive decline of some frontal lobe functions (executive functions, phonemic fluency and planning) associated with psychosis, urinary urgency, mixed axonal polyneuropathy and lymphedema.

Under the hypothesis of an autosomal dominant disease, we performed an exome sequencing analysis on our patient, revealing a novel heterozygous variant in *DNMT1* located in exon 21 (c.1794C>T, p.Arg598Trp). The nucleotide change causes an aminoacidic substitution predicted deleterious by most commonly used variant predictor bioinformatic tools (sift.jcvi.org; <http://genetics.bwh.harvard.edu/pph2/>).

DNMT1 is a key DNA methyltransferase with essential roles in methylation pattern maintenance during chromosome replication and repair. The encoded protein is composed by a catalytic C-terminal region and a regulatory N-terminal region. All disease-causing mutations fall within exons 20 and 21, which encode a small domain of the N-terminal region, called RFTS (replication foci targeting sequence), essential for enzymatic dimerization and binding to DNA hemimethylated CpG sites².

Heterozygous mutations of *DNMT1* have been associated with two human pathological phenotypes, namely hereditary sensory autonomic neuropathy with dementia and hearing loss (HSAN1E; OMIM#614116); and cerebellar ataxia, deafness, and narcolepsy (ADCA-DN; OMIM#604121). More recently, these diseases are being considered as a continuum of a common neurodegenerative spectrum often characterized by overlapping clinical or subclinical features³.

ADCA-DN develops as an adult onset (30-40 ys old) progressive cerebellar ataxia associated with hearing loss, cognitive decline with possible psychotic symptoms and narcolepsy/cataplexy. Sensory neuropathy, optic atrophy and depression are more variable associated clinical features⁴.

It has been associated with a strong alteration of normal genomic methylation patterns⁵.

Besides, ADCA-DN shares some common phenotypic traits of mitochondrial encephalomyopathies, and also, many experimental evidences have formerly suggested the involvement of a mitochondrial dysfunction in the pathogenesis of the disease

While nuclear DNA (nDNA) methylation is widely established and extensively studied, methylation of mitochondrial DNA (mtDNA) still raises a lot of questions amongst researchers. The main explanations for this controversy lie in the low amount of methylated cytosines found in mtDNA and in the bias created by differential sensitivity and reproducibility of experimental techniques employed to assess mtDNA methylation levels².

For all these reasons, with the collaboration of the Department of Pathophysiology and Transplantation (Università degli Studi di Milano), we extracted total DNA from patient lymphocytes and fibroblast and analysis of mtDNA methylation was performed as described in Novielli *et al.* 2017⁶.

Site-specific methylation analysis of normally hypermethylated mtDNA regions (in 3 mtDNA genes: *MTCO1*, *MTTF*, *MTND6* and in the Dloop region) didn't reveal any statistically significant difference between patient and control mtDNA (Table 1).

DNMT1 involvement in mitochondrial methylation and its possible location inside mitochondria is still a matter of debate².

Further work will be necessary in order to understand pathophysiological mechanisms underlying the disease and to clarify the potential involvement of altered mitochondrial dysfunction in the pathogenesis. Hence, an enlargement of the case record would be valuable for collection of multiple biological samples. We also envisage to determine expression levels and location of mutated protein in patient fibroblasts and to perform both global and site-specific (e.g. LINE, Alu, specific genes) methylation analysis of nuclear DNA.

References:

1. Mundwiler A, Shakkottai VG. Autosomal-dominant cerebellar ataxias. *Handb Clin Neurol*. 2018;147:173-185. doi: 10.1016/B978-0-444-63233-3.00012-9.
2. Maresca A, Zaffagnini M, Caporali L, Carelli V, Zanna C. DNA methyltransferase 1 mutations and mitochondrial pathology: is mtDNA methylated? *Front Genet*. 2015 Mar 12;6:90. doi: 10.3389/fgene.2015.00090.
3. Baets J, Duan X, Wu Y, Smith G, Seeley WW, Mademan I, McGrath NM, Beadell NC, Khoury J, Botuyan MV, Mer G, Worrell GA, Hojo K, DeLeon J, Laura M, Liu YT, Senderek J, Weis J, Van den Bergh P, Merrill SL, Reilly MM, Houlden H, Grossman M, Scherer SS, De Jonghe P, Dyck PJ, Klein CJ. Defects of mutant DNMT1 are linked to a spectrum of neurological disorders. *Brain*. 2015 Apr;138(Pt 4):845-61. doi: 10.1093/brain/awv010.
4. Winkelmann J, Lin L, Schormair B, Kornum BR, Faraco J, Plazzi G, Melberg A, Cornelio F, Urban AE, Pizza F, Poli F, Grubert F, Wieland T, Graf E, Hallmayer J, Strom TM, Mignot E. Mutations in DNMT1 cause autosomal dominant cerebellar ataxia, deafness and narcolepsy. *Hum Mol Genet*. 2012 May 15;21(10):2205-10. doi: 10.1093/hmg/dds035.
5. Kernohan KD, Cigana Schenkel L, Huang L, Smith A, Pare G, Ainsworth P; Care4Rare Canada Consortium, Boycott KM, Warman-Chardon J, Sadikovic B. Identification of a methylation profile for DNMT1-associated autosomal dominant cerebellar ataxia, deafness, and narcolepsy. *Clin Epigenetics*. 2016 Sep 5;8:91. doi: 10.1186/s13148-016-0254-x.
6. Novielli C, Mandò C, Tabano S, Anelli GM, Fontana L, Antonazzo P, Miozzo M, Cetin I. Mitochondrial DNA content and methylation in fetal

cord blood of pregnancies with placental insufficiency. *Placenta*. 2017
Jul;55:63-70. doi: 10.1016/j.placenta.2017.05.008

Figures and tables:

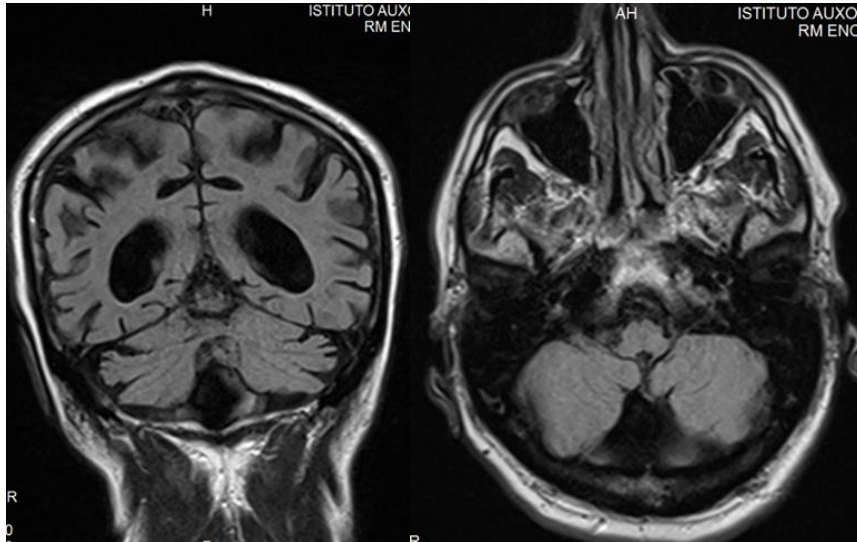


Figure 1: Brain MRI, T1 weighted images of ADCA-DN patient. Note lateral ventricles and cortical sulci enlargement (left) and prominent vermian cerebellar atrophy.

Gene	Sample	% methylation	n° CpG analyzed
mtCO1	patient	2%	2 CpG
	control	2%	
mtTF	patient	2%	3 CpG
	control	3%	
mt Dloop	patient	2%	7 CpG
	control	3%	
mtND6	patient	3%	1 CpG
	control	3%	

Table 1: Site specific methylation analysis on mtDNA of index patient. mtCO1 (mitochondrial cytochrome oxidase subunit 1); mtTF (mitochondrial tRNA for phenylalanine); mtND6 (mitochondrial NADH:Ubiquinone Oxidoreductase Core Subunit 6).

Chapter 6

Xenotopic transfection with alternative dehydrogenases as a potential therapy for mitochondrial CI deficiency: preliminary results and perspectives

Paper in preparation

Background

For the vast majority of mitochondrial diseases targeted and effective treatments are missing so far. The exceptional genetic and phenotypic heterogeneity of mitochondrial disorders, the yet poorly understood underlying mechanisms, are presumably among the main reasons why the development of valid treatments for mitochondrial diseases has proved to be so challenging. Besides, common identification of isolated affected individuals or families hampers the collection of sufficiently large groups of patients to plan clinical trials with an appropriate statistical power.

As previously mentioned, mitochondrial CI deficiency is the most commonly identified molecular alteration found in mitochondrial diseases¹.

Complex I or CI (NADH:ubiquinone oxidoreductase) pumping activity generates about 40% of the proton gradient across the mitochondrial inner membrane².

Mammalian CI is a 44 subunits complex containing a catalytic core of 14 subunits, which have homologues in prokaryotes and are strictly

conserved across evolution: 7 of them are encoded by the nuclear DNA (nDNA), the remaining by mitochondrial DNA (mtDNA). From a structural point of view the catalytic core has the shape of an L with two main domains: seven hydrophilic subunits build the matrix arm, which contains all the redox cofactor and the Q-binding site and is responsible for electron transfer activity; seven hydrophobic subunits, which form the intermembrane segment, contain the proton pumping modules. Mammalian CI also possesses 30 “accessory” subunits playing a role in its assembly, stability and regulation. Besides, several additional non-structural proteins have been identified as key players in assembly and maturation processes.^{3,4}

Mutations in many of its 44 structural subunits or other assembly factors, can damage its enzymatic activity¹, thus making CI function extremely vulnerable. A disruption in CI activity unavoidably causes metabolic disturbances (derived from lack of CI dependent NADH oxidation which perturbs upstream NAD⁺ reducing metabolic pathways), accumulation of toxic compounds and ROS (radical oxygen species) due to defective electron transfer which further damage membranes and mtDNA.

Despite the progresses in understanding the molecular basis of conditions associated to CI deficiency, treatment options are still extremely limited: indeed, Leber hereditary optic neuropathy is the first mitochondrial disease for which therapy with high dose idebenone has recently been approved by the European Medicine Agency, even if under strict clinical criteria)⁵.

Besides, the most recent therapeutic efforts did not result in a significant improvement when translated to clinics: a relevant exception are the encouraging preliminary results obtained from allotopic expression of *ND4* mtDNA gene in group of LHON patients (see Hirano *et al.*⁶).

The development of reliable experimental models of disease is the essential pre-requisite to enable the evaluation of potential treatment efficacy and safety tests. Even though a detailed description of available cellular and animal models of CI deficiency is beyond the scope of this thesis, the recent progress in the development of reliable experimental models is encouraging^{7,8}.

NDUFS4 mutations, associated with Leigh syndrome due to CI deficiency, have received a particular attention. Pathogenic homozygous variants usually lead to absence of *NDUFS4* protein and undetectable mature form CI with the appearance of an intermediate 830 kDa subcomplex: *NDUFS4* incorporation in CI is one of the last steps of CI assembly and plays an important role in functional stabilization of its hydrophilic arm. Patient skin fibroblasts (and more recently, fibroblast-derived induced pluripotent stem cells- iPSc) are the most widely studied in vitro models of CI deficiency. Patient fibroblasts typically display a reduced mitochondrial membrane potential and a metabolic switch towards glycolysis as an attempt of the cell to partially compensate the defective OXPHOS system. Besides the increase of cellular ROS levels, also mitochondrial morphology can be affected resulting in a fragmented network.

One of the most extensively employed animal model of CI deficiency is the *Ndufs4* *-/-* double KO, which develops a fatal

encephalomyopathic phenotype closely resembling the human one. Furthermore, other *Ndufs4*^{-/-} tissue-specific and conditional mouse models have been generated⁸⁻¹⁰.

During the last few years, multiple experimental approaches are being tested on the above-mentioned preclinical models. Amongst other strategies designed to counteract metabolic and oxidative consequences of CI deficiency (see Hirano *et al*⁹, for a comprehensive review on this subject), the research community has shown a growing interest on enzyme replacement therapy, which could functionally bypass a defective mitochondrial protein and reveals as a promising approach for a number of mitochondrial diseases. Many non-mammalian species express several types of respiratory chain bypassing enzymes¹¹. In case of CI deficiencies, trans-kingdom gene replacement therapy with alternative NADH dehydrogenases (NDH-2) could represent an effective tool to bypass a defective CI activity and thus holds potential for representing an active therapy for the widest subgroup of patients affected by mitochondrial diseases. However, it is mandatory to first evaluate possible side-effects and to determine long-term efficacy of replacement therapy.

The recent creation of national and international consortia appears promising to give a boost to research in this field and to facilitate not only the recruitment of patients affected by mitochondrial diseases eligible for clinical trials, but also to build a fruitful collaboration aimed at establishing accurate experimental models to test the efficacy of emerging therapies.

Within this research field, in the framework of GENOMIT international program, I dedicated the last few months of my PhD to the characterization of biological and biochemical properties of plants enzymes which have been proven potentially effective to improve electron flow through mitochondrial respiratory chain in a cellular model of CI deficiency. Preliminary results are briefly summarized below.

Abstract

Complex I (CI) deficiency is the most common cause of mitochondrial disorders associated to respiratory chain defects. Successful attempts to rescue CI function by introducing an exogenous NADH dehydrogenase, as the ScNDI1 from *Saccharomyces cerevisiae*, were reported, although with drawbacks deriving from the evidence of a competition with CI. Differently from ScNDI1, that is permanently active in yeasts which lack CI, plant alternative NADH dehydrogenases (NDH-2) naturally support the oxidation of NADH only when the CI is metabolically inactive and conceivably when the concentration of matrix NADH exceeds a certain threshold. Therefore, we questioned the feasibility of CI rescue by NDH-2 from *Arabidopsis thaliana* (At) in human CI defective fibroblasts. We showed that, other than ScNDI1, two different NDH-2 addressed to the matrix (AtNDA2 and AtNDB4) were able to rescue CI defect in human fibroblasts. Nevertheless, we further demonstrated that, as opposed to our initial hypothesis, when expressed in human fibroblasts AtNDA2 competes with CI, thus modifying metabolic efficiency in control cells. In conclusion, despite

their potential to revert CI defects, our data provide the evidence that plant NDH-2 should be regarded with caution as possible therapeutic tools for human mitochondrial diseases.

Introduction

Human NADH: ubiquinone oxidoreductase or complex I (CI) is the largest complex of the respiratory chain, with a mass of 980 kDa and 44 different subunits encoded by both mitochondrial and nuclear genomes. CI catalyses the consecutive transfer of two electrons, one per time, to a ubiquinone pool for each molecule of NADH oxidized. NADH oxidizing activity of CI is tightly controlling intra-mitochondrial metabolism, and electron transfer is coupled to both heat and ATP generation. Electron transfer is associated with the pumping of 4H⁺ across the inner mitochondrial membrane, which sustains part of the mitochondrial membrane potential¹². The 44 subunits are arranged in three functional modules: the N module involved in oxidizing NADH, the Q module involved in reducing ubiquinone and the P module dedicated to the proton translocation¹³. A number of mutations in nuclear and in mitochondrial genes coding for many of the 44 subunits, as well as in genes coding for assembly or regulatory factors, have been shown to result in CI deficiency¹. Therefore, CI deficiency can result in a combination of abnormalities: impaired oxidation of NADH to NAD⁺, which alters the NADH/NAD⁺ ratio and leads to lactic acidosis, release of electrons that are not correctly channelled to the ubiquinone generating ROS, and loss of proton

pumping activity, which reduces mitochondrial potential, hence lowering ATP synthesis.

In microbes, fungi, plants and also in some metazoan phyla (but not in arthropods or vertebrates), two key steps of mitochondrial respiratory chain (ubiquinone reduction and ubiquinol oxidation) can diverge from mammals, as they express bypassing enzymes belonging to two main classes: alternative NADH dehydrogenases (NDH-2) and alternative oxidases (AOXs).

NDH-2 can functionally replace NADH oxidizing activity of CI, transferring electrons from NADH directly to ubiquinone, while AOXs can be a functional substitute of complexes III and IV (CIV, being able to transfer electrons from a ubiquinol pool directly to oxygen).

These enzymes possess some key properties that distinguish them from other mitochondrial complexes: they are single or oligo subunit, non-proton pumping enzymes, as energy they convey during their activation does not support mitochondrial potential; they are not inhibited by OXPHOS inhibitors (e.g. rotenone and cyanide) and, in contrast with other mitochondrial complexes, they are not transmembrane but are either associated to the inner or the outer mitochondrial membrane^{14,15}.

In *Saccharomyces cerevisiae* CI is absent and replaced by ScNDII protein. In an attempt to rescue CI deficiency, Yagi and collaborators introduced the type II NAD(P)H dehydrogenase from yeast, ScNDI1, in mammalian cells with impaired CI. This resulted in the recovery of NADH oxidation and reduction of ROS production in a variety of CI defective cell cultures harbouring mutations in either *ND4*, *ND5* or *NDUFA1*^{16,17}. Cells with CI deficiency acquired the ability to grow in

a non-fermentable medium, as galactose, upon transfection with ScNDI1. ScNDI1 has proven beneficial also in fly models of CI deficiency¹⁸.

This concept was further developed in gene therapy approaches in mice and rats. CI bypass established by ScNDI1 was demonstrated to be well tolerated. ScNDI1 protected rat neurons against the specific CI inhibitor, rotenone, rescued CI deficiency¹⁹⁻²¹, and has shown potential therapeutic effects in a murine model of Parkinson disease²².

However, when inserted in control HEK293 cells, ScNDI1 caused a decrease of the P/O for the CI-dependent respiration from a value of 2.5 to 1.8²³, showing that ScNDI1 is active even in presence of a fully functional CI, therefore competing with it for the oxidation of NADH. Such competition could compromise energy production and lower mitochondrial potential taking over residual activity of CI *in vivo*, thus potentially leading to dramatic and unpredictable metabolic consequences.

Unlike *Saccharomyces cerevisiae*, which lacks CI, many plants have NDH-2, which naturally coexist with CI. They oxidize NADH only in specific physiologic conditions, probably depending on substrate availability, considering that some alternative dehydrogenases from plants have shown a 3 to 10 folds higher Km for NADH than plant CI in native conditions²⁴⁻²⁶, or hypothetically on the presence of specific matrix compartmentalized NADH pools.

Arabidopsis Thaliana, in particular, expresses different isoforms of NDH-2 associated either to the inner or to the outer mitochondrial membrane.

The intrinsic role of these alternative systems could be to maintain a redox balance and a proper turn-over of mitochondrial metabolism, continuing to oxidize substrates when the metabolic demand is modified. This is particularly manifest during daylight exposition for plants, when OXPHOS is inhibited by the extensive mobilization of cytosolic ADP by the photosynthetic process: actually, it was shown that activation/expression of NDH-2 takes place in physiologic conditions lowering CI activity¹¹.

Thus, the plant enzyme is expected to naturally take over for NADH oxidation only when CI is prevented to work, providing a mechanism to mitigate the redox imbalance in cells with defective CI, without competing with its endogenous residual activity.

A very similar strategy based on the expression of the tunicate *Ciona intestinalis* alternative oxidase (AOX) has been previously shown to exert beneficial effects in counteracting the consequences of complexes III or IV respiratory chain deficiency in human cells and animal models.²⁷

Taken together, all these considerations open a way to forecast xenotopic transfection of genes encoding for plant's NDH-2 as an effective treatment for syndromes associated with CI deficiency, as these enzymes should be active only when electron transfer from NADH through CI is impaired.

Therefore, we decided to evaluate the potential benefit of introducing alternative dehydrogenases AtNDA2, and AtNDB4 from *Arabidopsis thaliana* (At) in a CI defective patient fibroblast cell line carrying a homozygous mutation in *NDUFS4* gene and compared it to ScNDI1

from *Saccharomyces cerevisiae* (ScNDI1). Moreover, we assessed kinetic and biochemical effects of one of these proteins (AtNDA2) on control fibroblasts.

Materials and methods

Cell transfection and selection:

For the evaluation of the above-described therapeutic strategy on cellular models, we focused on control and CI defective human fibroblasts.

Transfection and selection of the cell lines have been carried out by the group of Holger Prokisch in Munich, within the frame of the joint European project GENOMIT (see above). Fibroblasts obtained from skin biopsies, have been transfected with constructs containing six different NDH-2 genes fused with human mitochondrial targeting signal (MTS) and a blasticidin resistance sequence. Transfection has been performed using a lentiviral vector from Invitrogen™ according to the manufacturer's protocols (ViraPower™ HiPerform™).

Assessment of transduction efficacy and selection of transfected cell lines were performed using the results of qPCR (not shown) and Seahorse analysis (Figure 1). Seahorse essays were performed as previously described²⁹.

In light of seahorse results showing a rescue of oxygen consumption rates (OCR), we decided to focus on AtNDA2, AtNDB4 and ScNDI1 transfected 79787 cell lines and a control cell line (NHDF) transfected with the same constructs.

The CI defective cell line (79787) belongs to a patient affected by Leigh syndrome carrying the homozygous frameshift mutation c462delA (pLys154fs) within *NDUFS4*, located in 5q11 and encoding for a CI subunit close to the catalytic region of NADH-quinone oxidoreductase. Mutation results in the synthesis of a truncated protein. Indeed, the absence of *NDUFS4* protein was previously reported in fibroblasts derived from patients harbouring the same *NDUFS4* homozygous mutation²⁸.

Selected NDH-2 enzymes are: ScNDI1, the internal NDH-2 of *Saccharomyces cerevisiae*; AtNDB4, an *Arabidopsis thaliana* NDH-2 localized at the external side of inner mitochondrial membrane (IMM); AtNDA2, another *Arabidopsis thaliana* NDH-2 localized at the internal side of IMM.

ScNDI1, but not AtNDA2 and AtNDB4 expression, has been also confirmed by Western Blot results (not shown), since specific antibodies for *Arabidopsis thaliana* NDH-2 were not available.

Cells were grown in complete high-glucose DMEM supplemented with GlutaMAX. Selective growth of transfected cells was maintained by adding blasticidin 5 µgr/ml to DMEM.

Enzymatic activity assay and determination of kinetic parameters:

Collection and permeabilization of fibroblast pellets were performed as previously described³¹.

Spectrophotometric analysis of NADH:quinone oxidoreductase specific activity was performed on a Cary 60 spectrophotometer equipped with a 18-cell holder maintained at 37 °C.

Measures of NADH:quinone oxidoreductase specific activity were performed in medium A containing 10 mM KH_2PO_4 (pH 7.2) and 1 mg/mL BSA at wavelengths of 340 nm–380 nm to assess NADH oxidation using an extinction coefficient of 4.87 as previously described^{30,31}.

The sample compartment was kept open in order to allow manual stirring of the cuvette content after each addition. For K_m determination, samples (8-20 μL) were added to water, incubated for 1 minute before mixing with a buffer solution containing 10 mM KH_2PO_4 (pH 7.2) and 1 mg/mL BSA. Rotenone (8 μM), KCN (650 μM), DCQ (50 μM) were sequentially added to the cuvettes before starting the reaction with the substrate NADH (at concentrations ranging from 0.3 to 150 μM) and following the reaction kinetics. A comparative assay was performed without rotenone, in order to quantify the amount of rotenone resistant NADH:quinone oxidoreductase activity. Data collection is ongoing, all the measurements will be repeated at least three times.

K_m and V_{max} were estimated using an online available tool (<http://www.ic50.tk/kmymax.html>) using the Michaelis-Menten model.

Proteins were measured according to Bradford³².

ADP/O assay:

Subconfluent fibroblasts (75 cm^2 flask) were trypsinized and the pellet was washed once with 1 mL PBS. The oxygen uptake was measured with an optic fibre equipped with an oxygen-sensitive fluorescent terminal sensor (Optode device: FireSting O2, Bionef, Paris, France).

The optic fibre was fitted to a printed cap ensuring the closure of the quartz-cell yet allowing micro-injections (0.6 mm hole diameter) for concurrent measurement of oxygen uptake (optodic signal) with mitochondrial potential (determined by the fluorescence change of 100 nM rhodamine). Cells were added to 750 μ L of buffer consisting of 0.25 M sucrose, 15 mM KCl, 30 mM KH_2PO_4 , 5 mM MgCl_2 , 1 mM EGTA, pH 7.4, followed by the addition of rhodamine and 0.01% w/v digitonin. The permeabilized cells were successively added followed by the addition of mitochondrial substrates (6.25 mM glutamate/malate or 6.25 mM succinate) and two consecutive injections of ADP (40 nmol) to ensure state 3 (phosphorylating) conditions or ATP (40 nmol) in order to estimate ATP recycling due to ATPases activity. The reaction was followed until state 4 (the respiratory rate after all the ADP has been phosphorylated to form ATP) was reached back and maintained. Respiratory control index (state 3/state 4 ratio) and ADP/O ratios were further calculated. All the assays were repeated at least three times. Protein content was measured according to Bradford³².

Statistical analysis:

All data are expressed as the mean \pm SD, and comparisons between groups performed using Student's *t* test.

Preliminary results

Expression of NDH-2 dehydrogenases does not affect growth of cultured human fibroblasts

ScNDI1, AtNDA2 and AtNDB4 transfected control fibroblasts (NHDF) and CI-defective fibroblasts (79787) exhibited comparable growth rates when compared to the corresponding untransfected control, both in glucose and glucose-deprived media (not shown).

At-NDA2 and At-NDB4 rescue NADH:quinone oxidoreductase activity of NDUFS4 mutant fibroblasts

In order to assess the potential of the alternative NADH dehydrogenases to rescue mitochondrial respiratory chain activity, we measured NADH:quinone oxidoreductase specific activity by spectrophotometry in control cells and *NDUFS4* mutated fibroblasts before and after transfection by ScNDI1, AtNDA2 and AtNDB4, showing that all the 3 dehydrogenases were able to rescue the CI defect (Table 1).

We could also observe that, while AtNDA2 and AtNDB4 restored CI activity to levels comparable to the ones observed in control cells, ScNDI1 transfected cells exhibited levels of NADH:quinone oxidoreductase activity much higher than untransfected controls (Table 1).

AtNDA2 competes with CI when expressed in human fibroblasts

In view of expression profile and location within plant mitochondria³³, we selected a control cell line transfected with AtNDA2 to test for a possible competition between CI and plant NDH-2, and studied the ADP/O ratio with different substrates, the latter being supposedly decreased if NADH, normally oxidized by the proton-motive CI, is diverted to AtNDA2. ADP/O calculation is usually performed on isolated mitochondria in order to eliminate contaminating cytosolic

ATPases activity. ATPases increase ADP recycling, allowing for a continuous stimulation of the mitochondrial ATP synthase and respiration, thus affecting state 4 establishment. For this work, taking into consideration the scarcity of material and the slow growth rate of fibroblasts, we decided to perform the assays using permeabilized cells. As expected, the observed ADP/O values were underestimated comparing to the ones measured on purified mitochondria (about 2.5 for NADH related substrates and 1.5 for succinate, respectively)-see Hinkle *et al.*³⁴ for a complete review on this topic.

Nevertheless, we were able to determine a possible interference of AtNDA2 with functional mitochondrial respiratory chain, by estimating the ADP/O ratios for glutamate/malate in the same control cell line either non-transfected or AtNDA2-transfected (Figure 2).

Transfected cells showed ADP/O values lowered by half (0.43 ± 0.08) in comparison to control cells (0.9 ± 0.1). Moreover, respiratory control index, calculated as the ratio between state 3 and state 4, which represents a numeric estimation of mitochondrial coupling efficiency, is also clearly lowered in transfected cells under glutamate-malate stimulation (Figure 3).

These data suggest that AtNDA2 interferes with mitochondrial respiratory chain in control cells, competing with the activity of CI. Because the NDH-2 do not possess proton pumping activity, thus their function is uncoupled to energy production.

A further validation of these results come from ADP/O data obtained with succinate, substrate of CII. Indeed, ADP/O ratios for succinate

were not significantly different for control and transfected cells, 0.43 ± 0.05 and 0.39 ± 0.02 , respectively

Nevertheless, under succinate stimulation we observed a reduction of respiratory control index in transfected cells, as well (Figure 3). This observation could be attributed to the metabolic conversion of a fraction of succinate to glutamate, which later enters the oxidation machinery proceeding through CI and AtNDA2.

We also repeated the same assays adding ATP instead of ADP: the low OXPHOS stimulation scores we observed in both cell lines under such experimental conditions, provides a supplementary confirmation that the difference we detected is not significantly affected by ATPase mediated ATP recycling to ADP (data not shown).

A further evidence of the possibility of a competition between CI and AtNDA2, comes from calculation of K_m for NADH in both cell lines (Figure 4).

CI affinity for NADH was estimated in control cells considering only rotenone sensitive internal NADH:quinone oxidoreductase activity, while, to evaluate AtNDA2 affinity for NADH, we exclusively analysed rotenone insensitive activity in AtNDA2-transfected control cells. We obtained preliminary values of 2.7 ± 0.4 and 9.7 ± 3.3 for CI and AtNDA2 activity, respectively. Hence, when transfected in human cells, K_m of AtNDA2 for NADH appear to be about 3 folds higher than CI affinity for NADH: this gap is probably inadequate to prevent a competition for the substrate within physiological range of NADH concentration inside the cells.

Discussion

CI is the largest complex of the respiratory chain, consisting of 44 different subunits encoded by nDNA and mtDNA. These subunits are assembled in a precise order by a plethora of assembly factors³⁵. Thus, pathogenic mutations in genes encoding either for structural subunits or for assembly factors, can result in the enzymatic impairment of CI, often with a poorly understood tissue-specificity and time-dependency.

Besides, CI deficiency may arise as a consequence of mutations in genes encoding proteins involved in mitochondrial translation, in iron-sulfur cluster assembly, in coenzyme Q₁₀ biosynthesis, and mtDNA-depletion associated genes^{9,36}.

This could explain why CI deficiency is the far most common finding in mitochondrial disorders.

In terms of therapeutic approach, having a unique treatment applicable to all CI deficiencies, regardless of the genetic cause, would be desirable. Yagi and coll. inserted the monomeric NADH dehydrogenase of yeast, ScNDI1, in CI-deficient cells²³. ScNDI1 is a non-proton pumping enzyme able to transfer electrons from NADH to CoQ. Upon ScNDI1 expression, CI-deficient cells recovered the ability to oxidize excess NADH, and even though the mitochondrial potential was not restored, the overall electron flux through the other respiratory chain complexes improved, as proven by the ability of ScNDI1-expressing cells to grow in galactose media¹⁷. ScNDI1 was thus employed in a gene therapy approach on a rat model of Leber's hereditary optic neuropathy,

showing *in vivo* the potential of rescuing CI deficiency^{20,22}. Moreover, the yeast protein was well tolerated by the immune system of the rat.

Despite the apparent beneficial effect of ScNDI1, it was observed that the yeast protein affected the P/O value for the CI-dependent oxidation of NADH when inserted in control mammalian cells. In particular, P/O value with glutamate/malate decreased from 2.5 to 1.8, indicating a competition between ScNDI1 and CI for the oxidation of NADH²³. Lowered P/O values suggest a reduction of ATP synthesis in control cells after ScNDI1 transfection: this data raise questions about its feasibility for long term treatments in patient affected by CI deficiency, where prevalence of ScNDI1 over residual CI activity could worsen metabolic disturbances and OXPHOS energetic yield.

Therefore, we looked for other monomeric NDH-2, more likely to complement a defective CI activity without competing with the endogenous CI. Plant enzymes naturally coexist with CI and it was suggested that plant NDH-2 support the NADH oxidation only when its concentration in the mitochondrial matrix exceeds a specific threshold^{11,37}, or possibly when a specific matrix pool is reduced. For these reasons, we focused on two candidate NADH dehydrogenases: AtNDA2, and AtNDB4 from *Arabidopsis thaliana*.

These *A. Thaliana* NDH-2 showed a substrate preference for NADH over NADPH and their catalytic activity is Ca²⁺ independent, similarly to CI. AtNDA2 is naturally found in the mitochondrial inner membrane, facing the matrix^{24,38}, but there are evidences of an additional peroxisomal localization³⁹. AtNDB4 instead, faces the intermembrane space. To target these proteins specifically to the mitochondrial matrix

of the mammalian cells in order to allow them to oxidize the excess of NADH produced uniquely by defective CI, the plant-specific mitochondrial targeting sequence (MTS) was replaced with the human one.

Thus, we expressed AtNDA2 and AtNDB4 in CI defective fibroblasts belonging to a patient carrying a pathogenic mutation in the nuclear gene *NDUFS4* and measured the bioenergetic parameters in transfected cell lines. Both enzymes were able to rescue the biochemical defect in patient cell line, restoring key mitochondrial respiration parameters evaluated by seahorse analysis. Functional expression of plant NDH-2 was further suggested by complementation of defective CI on spectrophotometric essays, since both enzymes were able to re-establish NADH:quinone oxidoreductase activity close to control values. Besides, they did not affect cell growth both in standard culture conditions and in case of glucose deprivation, when cells are forced to switch on OXPHOS for energy production. This observation could be dependent on a lack of competition with CI, ensuring that NDH-2 do not disperse mitochondrial potential in normal conditions, or, if competition exists, the absence of any apparent effect on cellular growth could be due to inadequate strength of competition, aberrant location of transfected NDH-2 or poor expression levels in proportion to CI.

Due to its original location within the inner surface of the inner mitochondrial membrane, AtNDA2 was chosen as the ideal candidate to be integrated into the human respiratory machinery and was expressed in human control fibroblasts. Based on above-mentioned

considerations, in order to test the hypothesis that CI and AtNDA2 were not competing for the oxidation of NADH, the effect of its expression on the ADP/O ratio was evaluated on transfected cells and compared to non-transfected controls: the ADP/O ratio of transfected cells treated with a NADH related substrate (glutamate-malate) was lowered by half when compared to control cells, and not significantly changed with an alternative substrate (succinate). These results indicate that AtNDA2 is active also when transfected in control cells and competes with CI for electron transfer from NADH to quinone. This observation matches with the preliminary evaluation of AtNDA2 affinity for NADH in transfected fibroblasts. Indeed, rotenone resistant NADH oxidase activity in AtNDA2-control cells has an apparent K_m of 9.7 μM for NADH which is slightly more than 3 folds higher than affinity of CI for NADH evaluated in control cells (2.7 μM).

Previous studies on plant mitochondria had calculated rotenone resistant NADH oxidase activity of the inner membrane to be up to 10 folds higher than K_m of CI^{26,38,40}, although other authors later reported a considerably lower value of 13.9 μM ⁴¹, which is close to our preliminary results.

Likewise, reported data on apparent K_m of CI for NADH are quite heterogeneous, ranging from values of 2 to 20⁴²⁻⁴⁵.

As repeatedly remarked in the past, the development of a specific method to evaluate kinetic properties of Complex I has been a recurrent challenge for researchers⁴⁶⁻⁴⁸.

The observed intergroup variability mainly depends on methodological heterogeneity (e. g. sample preparation, category of quinone-analogues

employed as electron acceptors, difficulty to accurately estimate enzymatic activity when dealing with extremely low concentration of the substrate etc).

Besides, kinetics properties of these enzymes have been mainly estimated on isolated mitochondria/sub mitochondrial preparations and on different cell lineages, while we studied permeabilised cell preparations, which are unavoidably contaminated to some extent by soluble NADH dehydrogenases activities. Moreover, AtNDA2 compartmentation within the inner surface of mitochondrial membrane or its association to a supramolecular complex (enzyme malic/specific quinone pool/AOXs) under native conditions, could contribute to its distinctive kinetic properties for NADH and to prevent competition with CI, thus ensuring AtNDA2 activity only in specific physiological circumstances.

However, even considering the possibility that we underestimated the real K_m values, AtNDA2 and CI affinity for the same substrate fall within a similar order of magnitude suggesting the existence of a competition in human cells, thus confirming our ADP/O data.

We are now finalizing the experiments to validate these preliminary data. We are also planning to extend biochemical analysis to AtNDB4 protein.

In parallel, since a specific antibody for AtNDA2 is now available, we are performing Western Blots to quantify the expression level of the plant peptide in transfected cells.

In order to better characterize transcription and expression levels of the transfected constructs, a multi-omics (proteomics, transcriptomics and metabolomics) analysis is simultaneously being conducted in Helmholtz Center, Munich.

In conclusion, we showed that transfection of plant NDH-2 is able to rescue CI defect *in vitro*. However, AtNDA2, the most promising candidate as based on its properties in plants, exhibits competing activity with human CI, thus raising concerns for its application to human therapy. This indicates that transfected enzyme does not complement CI but prevails over it for NADH oxidation also in control cells: consequences of this uncoupling effect are unpredictable *in vivo*, and risk to get deleterious in patients affected by CI deficiency both in terms of energetic production and metabolic dysfunctions. A lot of translational work still has to be done in the nearest future, from genetic manipulation of the transfected plant product to possibly modify its enzymatic properties, to the generation of an animal model to test its effects *in vivo*.

Nevertheless, we have moved an important step towards a deeper comprehension of potential advantages and drawbacks of trans-kingdom replacing therapy for respiratory chain defects.

References

1. Haack TB, Haberberger B, Frisch EM, Wieland T, Iuso A, Gorza M, Strecker V, Graf E, Mayr JA, Herberg U, Hennermann JB, Klopstock T, Kuhn KA, Ahting U, Sperl W, Wilichowski E, Hoffmann GF, Tesarova M,

Hanskova H, Zeman J, Plecko B, Zeviani M, Wittig I, Strom TM, Schuelke M, Freisinger P, Meitinger T, Prokisch H. Molecular diagnosis in mitochondrial complex I deficiency using exome sequencing. *J Med Genet.* 2012 Apr;49(4):277-83. doi: 10.1136/jmedgenet-2012-100846.

2. Papa S, Martino PL, Capitanio G, Gaballo A, De Rasmio D, Signorile A, Petruzzella V. The oxidative phosphorylation system in mammalian mitochondria. *Adv Exp Med Biol.* 2012; 942:3-37.

3. Carroll J, Fearnley IM, Shannon RJ, Hirst J, Walker JE. Analysis of the subunit composition of complex I from bovine heart mitochondria. *Mol Cell Proteomics.* 2003 Feb;2(2):117-26.

4. Fiedorczuk K, Sazanov LA. Mammalian Mitochondrial Complex I Structure and Disease-Causing Mutations. *Trends Cell Biol.* 2018 Oct;28(10):835-867. doi: 10.1016/j.tcb.2018.06.006.

5. Carelli V1, Carbonelli M, de Coo IF, Kawasaki A, Klopstock T, Lagrèze WA, La Morgia C, Newman NJ, Orssaud C, Pott JWR, Sadun AA, van Everdingen J, Vignal-Clermont C, Votruba M, Yu-Wai-Man P, Barboni P. International Consensus Statement on the Clinical and Therapeutic Management of Leber Hereditary Optic Neuropathy. *J Neuroophthalmol.* 2017 Dec;37(4):371-381. doi: 10.1097/WNO.0000000000000570.

6. Hirano M, Emmanuele V, Quinzii CM. Emerging therapies for mitochondrial diseases. *Essays Biochem.* 2018 Jul 20;62(3):467-481. doi: 10.1042/EBC20170114. Print 2018 Jul 20. Review.

7. Roestenberg P, Manjeri GR, Valsecchi F, Smeitink JA, Willems PH, Koopman WJ. Pharmacological targeting of mitochondrial complex I deficiency: the cellular level and beyond. *Mitochondrion.* 2012 Jan;12(1):57-65. doi: 10.1016/j.mito.2011.06.011.

8. Paule Bénit, Emmanuel Dassa, Sophie Lebon, Irina Giurgea and Pierre Rustin Mitochondrial respiratory chain complex I defects: Clinical, molecular, biochemical aspects and therapeutic prospect. *Complex I and Alternative Dehydrogenases*, 2007: ISBN: 978-81-7895-300-7
9. Scheffler IE. Mitochondrial disease associated with complex I (NADH-CoQ oxidoreductase) deficiency. *J Inherit Metab Dis*. 2015 May;38(3):405-15. doi: 10.1007/s10545-014-9768-6.
10. Breuer ME, Willems PH, Smeitink JA, Koopman WJ, Nootboom M. Cellular and animal models for mitochondrial complex I deficiency: a focus on the NDUFS4 subunit. *IUBMB Life*. 2013 Mar;65(3):202-8. doi: 10.1002/iub.1127. Epub 2013 Feb 3. Review.
11. Rasmusson AG, Geisler DA, Møller IM. The multiplicity of dehydrogenases in the electron transport chain of plant mitochondria. *Mitochondrion*. 2008 Jan;8(1):47-60. Review.
12. Ripple MO, Kim N, Springett R. Mammalian complex I pumps 4 protons per 2 electrons at high and physiological proton motive force in living cells. *J Biol Chem*. 2013;288(8):5374-80.
13. Brandt U. Energy converting NADH:quinone oxidoreductase (complex I). *Annu Rev Biochem*. 2006;75:69-92.
14. Cannino G1, El-Khoury R, Pirinen M, Hutz B, Rustin P, Jacobs HT, Dufour E. Glucose modulates respiratory complex I activity in response to acute mitochondrial dysfunction. *J Biol Chem*. 2012 Nov 9;287(46):38729-40. doi: 10.1074/jbc.M112.386060.
15. McDonald AE1, Gospodaryov DV2 Alternative NAD(P)H dehydrogenase and alternative oxidase: Proposed physiological roles in animals. *Mitochondrion*. 2018 Feb 6. pii: S1567-7249(17)30107-1. doi: 10.1016/j.mito.2018.01.009.

16. Bai Y, Hajek P, Chomyn A, Chan E, Seo BB, Matsuno-Yagi A, et al. Lack of complex I activity in human cells carrying a mutation in MtDNA-encoded ND4 subunit is corrected by the *Saccharomyces cerevisiae* NADH-quinone oxidoreductase (NDI1) gene. *J Biol Chem*. 2001;276(42):38808-13.
17. Bai Y, Hu P, Park JS, Deng JH, Song X, Chomyn A, et al. Genetic and functional analysis of mitochondrial DNA-encoded complex I genes. *Ann N Y Acad Sci*. 2004;1011:272-83.
18. Cho J, Hur JH, Graniel J, Benzer S, Walker DW. Expression of yeast NDI1 rescues a *Drosophila* complex I assembly defect. *PLoS One*. 2012;7(11):e50644. doi: 10.1371/journal.pone.0050644.
19. Marella M, Seo BB, Thomas BB, Matsuno-Yagi A, Yagi T. Successful amelioration of mitochondrial optic neuropathy using the yeast NDI1 gene in a rat animal model. *PloS one*. 2010;5(7):e11472.
20. Marella M, Seo BB, Flotte TR, Matsuno-Yagi A, Yagi T. No immune responses by the expression of the yeast Ndi1 protein in rats. *PloS one*. 2011;6(10):e25910.
21. Chadderton N, Palfi A, Millington-Ward S, Gobbo O, Overlack N, Carrigan M, et al. Intravitreal delivery of AAV-NDI1 provides functional benefit in a murine model of Leber hereditary optic neuropathy. *Eur J Hum Genet*. 2013;21(1):62-8.
22. Barber-Singh J, Seo BB, Matsuno-Yagi A, Yagi T. Protective Role of rAAV-NDI1, Serotype 5, in an Acute MPTP Mouse Parkinson's Model. *Parkinsons Dis*. 2010 Dec 6;2011:438370. doi: 10.4061/2011/438370.
23. Seo BB, Matsuno-Yagi A, Yagi T. Modulation of oxidative phosphorylation of human kidney 293 cells by transfection with the internal rotenone-insensitive NADH-quinone oxidoreductase (NDI1) gene of

Saccharomyces cerevisiae. *Biochimica et biophysica acta*. 1999;1412(1):56-65.

24. Michalecka AM, Svensson AS, Johansson FI, Agius SC, Johanson U, Brennicke A, Binder S, Rasmusson AG. Arabidopsis genes encoding mitochondrial type II NAD(P)H dehydrogenases have different evolutionary origin and show distinct responses to light. *Plant Physiol*. 2003 Oct;133(2):642-52.

25. Rasmusson AG, Soole KL, Elthon TE. Alternative NAD(P)H dehydrogenases of plant mitochondria. *Annu Rev Plant Biol*. 2004;55:23-39.

26. Moller IM, Palmer JM. Direct evidence for the presence of a rotenone-resistant NADH dehydrogenase on the inner surface of the inner membrane of plant mitochondria. *Physiologia Plantarum*. 1982;54(3):267-74.

27. El-Khoury R, Kemppainen KK, Dufour E, Szibor M, Jacobs HT, Rustin P. Engineering the alternative oxidase gene to better understand and counteract mitochondrial defects: state of the art and perspectives. *Br J Pharmacol*. 2014 Apr;171(8):2243-9. doi: 10.1111/bph.12570.

28. Anderson SL, Chung WK, Frezzo J, Papp JC, Ekstein J, DiMauro S, Rubin BY. A novel mutation in *NDUFS4* causes Leigh syndrome in an Ashkenazi Jewish family. *J Inher Metab Dis*. 2008 Dec;31 Suppl 2:S461-7. doi: 10.1007/s10545-008-1049-9.

29. Kremer LS, Prokisch H. Identification of Disease-Causing Mutations by Functional Complementation of Patient-Derived Fibroblast Cell Lines. *Methods Mol Biol*. 2017;1567:391-406. doi: 10.1007/978-1-4939-6824-4_24.

30. Chretien D, Benit P, Chol M, et al. Assay of mitochondrial respiratory chain complex I in human lymphocytes and cultured skin fibroblasts. *Biochem Biophys Res Commun* 2003;301:222-4.

31. Bénit P, Goncalves S, Philippe Dassa E, Brière JJ, Martin G, Rustin P. Three spectrophotometric assays for the measurement of the five respiratory chain complexes in minuscule biological samples. *Clin Chim Acta*. 2006 Dec;374(1-2):81-6.
32. Bradford MM. A rapid and sensitive method for the quantitation of microgram quantities of protein utilizing the principle of protein-dye binding. *Anal Biochem*. 1976 May 7;72:248-54.
33. Elhafez D, Murcha MW, Clifton R, Soole KL, Day DA, Whelan J. Characterization of mitochondrial alternative NAD(P)H dehydrogenases in Arabidopsis: intraorganelle location and expression. *Plant Cell Physiol*. 2006 Jan;47(1):43-54
34. Hinkle PC. P/O ratios of mitochondrial oxidative phosphorylation. *Biochim Biophys Acta*. 2005 Jan 7;1706(1-2):1-11.
35. Sánchez-Caballero L, Guerrero-Castillo S, Nijtmans L. Unraveling the complexity of mitochondrial complex I assembly: A dynamic process. *Biochim Biophys Acta*. 2016 Jul;1857(7):980-90. doi: 10.1016/j.bbabi.2016.03.031.
36. Emmanuele V, López LC, Berardo A, Naini A, Tadesse S, Wen B, D'Agostino E, Solomon M, DiMauro S, Quinzii C, Hirano M. Heterogeneity of coenzyme Q10 deficiency: patient study and literature review. *Arch Neurol*. 2012 Aug;69(8):978-83. doi: 10.1001/archneurol.2012.206. Review. Erratum in: *Arch Neurol*. 2012 Jul;69(7):886.
37. Lee CP, Eubel H, Millar AH. Diurnal changes in mitochondrial function reveal daily optimization of light and dark respiratory metabolism in Arabidopsis. *Mol Cell Proteomics*. 2010 Oct;9(10):2125-39. doi: 10.1074/mcp.M110.001214.

38. Geisler DA, Broselid C, Hederstedt L, Rasmusson AG. Ca²⁺-binding and Ca²⁺-independent respiratory NADH and NADPH dehydrogenases of *Arabidopsis thaliana*. *J Biol Chem*. 2007;282(39):28455-64.
39. Carrie C, Murcha MW, Kuehn K, Duncan O, Barthet M, Smith PM, Eubel H, Meyer E, Day DA, Millar AH, Whelan J. Type II NAD(P)H dehydrogenases are targeted to mitochondria and chloroplasts or peroxisomes in *Arabidopsis thaliana*. *FEBS Lett*. 2008 Sep 3;582(20):3073-9. doi: 10.1016/j.febslet.2008.07.061.
40. Soole KL, Dry IB, James AT, Wiskich JT. The kinetics of NADH Oxidation by complex I of plant mitochondria. 1990. *Physiol. Plant*. 80:75-82.
41. Rasmusson AG, Møller IM. NAD(P)H dehydrogenases on the inner surface of the inner mitochondrial membrane studied using inside-out particles. *Physiol. Plant*. 1991; 83:357-65
42. Hatefi Y, Stiggal DL, The enzymes, ed PD Boyer, 1976 pp. 175-297. New York: Academic. 3rd ed.
43. Vinogradov AD. Kinetics, control, and mechanism of ubiquinone reduction by the mammalian respiratory chain-linked NADH-ubiquinone reductase. *J Bioenerg Biomembr*. 1993 Aug;25(4):367-75. Review.
44. Majander A, Huoponen K, Savontaus ML, Nikoskelainen E, Wikström M. Electron transfer properties of NADH:ubiquinone reductase in the ND1/3460 and the ND4/11778 mutations of the Leber hereditary optic neuroretinopathy (LHON). *FEBS Lett*. 1991 Nov 4;292(1-2):289-92.
45. Barrientos A, Kenyon L, Moraes CT. Human xenomitochondrial cybrids. Cellular models of mitochondrial complex I deficiency. *J Biol Chem*. 1998 Jun 5;273(23):14210-7.

46. de Wit LE, Scholte HR, Sluiter W. Correct assay of complex I activity in human skin fibroblasts by timely addition of rotenone. *Clin Chem*. 2008 Nov;54(11):1921-2; author reply 1922-4. doi: 10.1373/clinchem.2008.104802.
47. Bénit P, Goncalves S, Philippe Dassa E, Brière JJ, Martin G, Rustin P. Three spectrophotometric assays for the measurement of the five respiratory chain complexes in minuscule biological samples. *Clin Chim Acta*. 2006 Dec;374(1-2):81-6. Epub 2006 Jun 2.
48. Yano T. The energy-transducing NADH: quinone oxidoreductase, complex I. *Mol Aspects Med*. 2002 Oct;23(5):345-68. Review.

Figures and Tables:

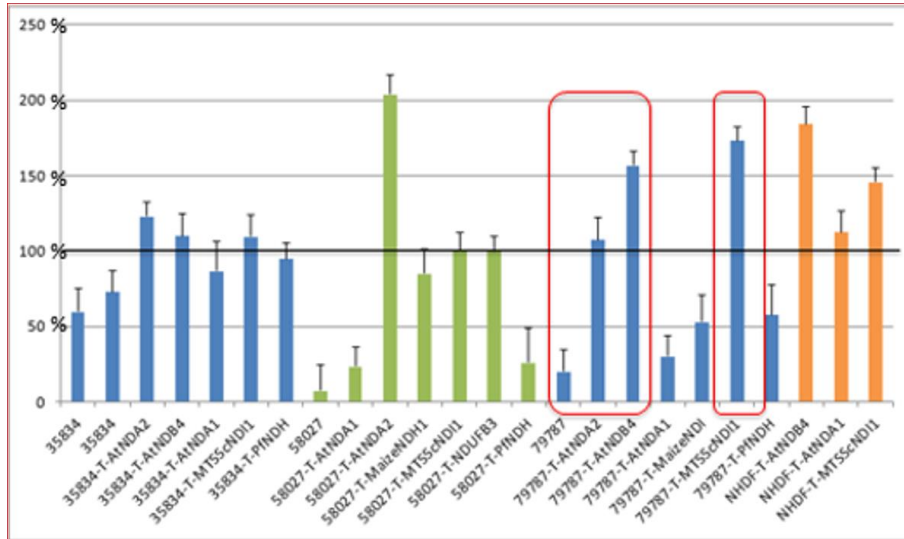
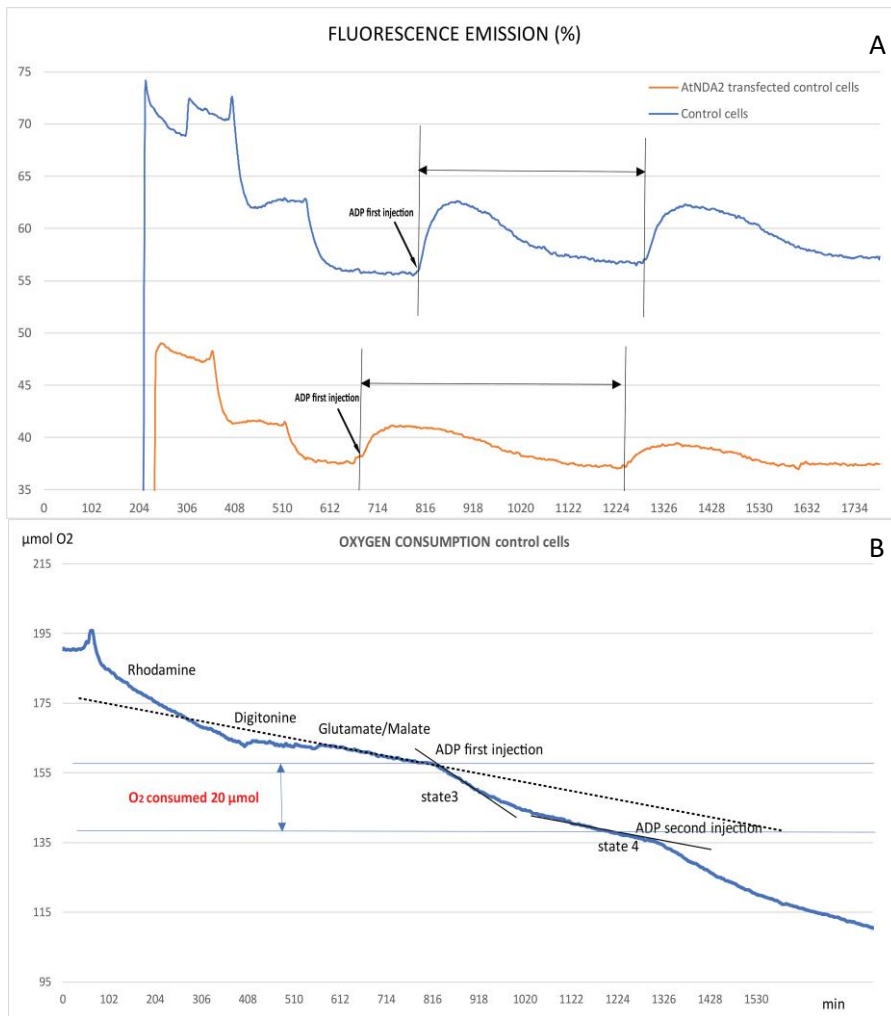


Figure 1. Seahorse analysis (provided by the group of H. Prokisch-Helmholtz Zentrum, Munich): oxygen consumption (OCR) expressed in % vs control cells. Three fibroblast cell lines with a CI defect (35834, 58027 and 79787) have been transfected with several NDH-2. A control cell line (NHDF) has been also transfected with the same constructs. 79787 cell line shows a reduced basal respiratory activity which is significantly restored after ScNDI1-, AtNDB4- and AtNDA2-transfection.

Cell line	NADH:quinone oxidoreductase specific activity w/o rotenone (nmol/min/mg Prot)	NADH:quinone oxidoreductase specific activity with rotenone (nmol/min/mg Prot)	Inhibition (%)
NHDF	7,7 (±0,5)	1,7 (±0,2)	78,3%
79787	2,5 (±0,2)	1,4 (±0,1)	42,6%
79787-T-ScNDI1	24,0 (±8,7)	20,7 (±8,3)	13,7%
79787-T-AtNDB4	11,8 (±2,4)	10,6 (±1,9)	10,0%
79787-T-ATNDA2	5,3 (±0,9)	5,3 (±0,9)	2,7%

Table 1: Spectrophotometric assessment of NADH:quinone oxidoreductase specific activity in control cells (NHDF) and *NDUFS4* cell line untransfected (79787) and transfected with alternative NADH oxidases (ScNDI1, AtNDA2 and AtNDB4). Values are expressed as mean ± SD



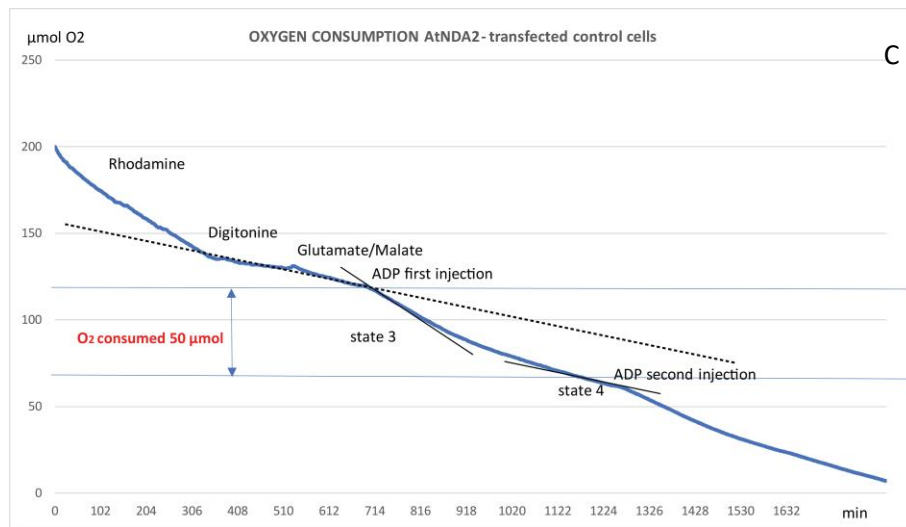


Figure 2. Mitochondrial membrane potential variations assessed by rhodamine fluorescence (A) and oxygen uptake measured with optode device in non-transfected control cells (B) and AtNDA2 transfected control cells (C). The reaction was started by the addition of glutamate/malate, followed by two sequential injections of ADP (see text). Note that AtNDA2 transfected cells take more time to go back to state 4 baseline after ADP injection (A) and that oxygen consumption during state 3 to state 4 transition is higher in AtNDA2 transfected cells (C) comparing to control (B).

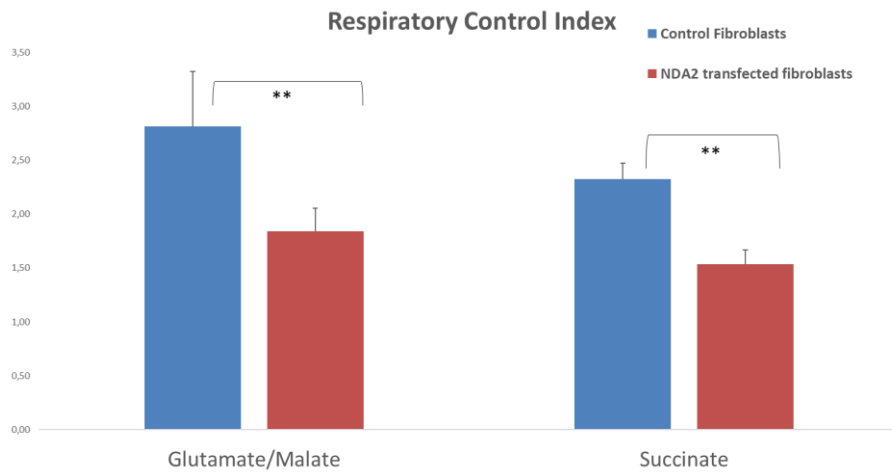


Figure 3. Comparison of Respiratory Control Index with Glutamate/Malate and Succinate in non-transfected control and AtNDA2 transfected control cells.

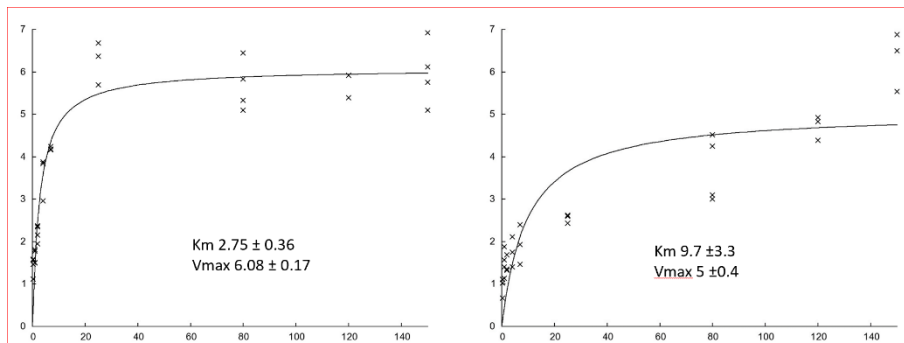


Figure 4. Preliminary plots of NADH:quinone oxidoreductase activity (y) as a function of NADH concentration (μM) (x): (A) rotenone-sensitive NADH:quinone oxidoreductase activity in control cells; (B) rotenone-resistant NADH:quinone oxidoreductase activity in AtNDA2 transfected control cells.

Chapter 7

SUMMARY

My work as a PhD student in DIMET course has been at the crossway between basic science and clinical activity.

Having always been passionate about basic neurobiology, I spent most of my time in the laboratory of the Molecular Neurogenetics Unit of the Besta Neurological Institute. In parallel, as a medical doctor board certified in Neurology, during the firsts months of my PhD I attended the outpatient service for Alzheimer and related dementia evaluation of Hospital San Gerardo in Monza, and from then on, the outpatient service for mitochondrial diseases evaluation in Carlo Besta Neurological Institute.

Since mitochondrial diseases are very heterogeneous and often multi-systemic, clinical management and molecular diagnosis are frequently a challenge for clinicians and researchers. Working in a third level service specifically dedicated to such diseases, I was able to phenotypically characterize patients and I actively participated to targeted clinical studies. Hence, taking advantage of the tight link between the laboratory and the clinic, I was directly involved in all the subsequent steps leading to the identification of genetic variants possibly responsible for the phenotype, interpretation of results and, eventually, biological and functional characterization of the affected protein.

With the indispensable contribution of molecular geneticists and bioinformaticians, I was trained in performing genetic tests used for diagnostic purposes (mainly NGS and Sanger sequencing) and in the analysis of results. Proceeding to the following steps, I finally carried out experiments to characterize biological effects of the identified variants at cellular or molecular level when needed.

The most important results within this collaborative network, have been the identification and characterization of novel variants responsible for early onset neurological phenotypes in diverse genes (*NDUFAF6*, *TFG1*, *OTX2*, *LETM1*, *DNMT1*). As a consequence, some of them have been included in our panel for mitochondrial diseases in order to increase its diagnostic yield. Already published or submitted results have been summarized in my thesis. Preliminary results which have not been submitted yet are just hint in my thesis and have been briefly presented.

Being the Molecular Neurogenetics Unit partner of an international network for mitochondrial disorders, I was also involved in the GENOMIT project; within this frame I contributed to the establishment and the enlargement of the Italian National network (Mitocon) and the International clinical Network for mitochondrial diseases. These networks are specifically designed to overcome fragmentation due to identification of suspected genetic variants in isolated families and to give deeper insight on mitochondrial disease natural history. Furthermore, the creation of national and international tissue biobanks to collect biological specimens (DNA, RNA, fibroblast, myoblast, serum, plasma) from patients affected by extremely rare pathological

entities, allows to perform more reliable translational studies in order to better understand the pathophysiological mechanism of diseases and set the ground for the development and the validation of personalized therapies and new treatment strategies.

Within the above-mentioned framework objective, I spent a period in France to study the biological implication of a new therapeutic option designed to bypass complex I deficiencies. Preliminary results of this side project are summarized in this thesis.

CONCLUSIONS AND FUTURE PERSPECTIVES

Opportunities and drawbacks of next generation sequencing (NGS) technologies

In the last decade, the development of new next generation sequencing (NGS) technologies such as whole genome/exome sequencing, has rapidly offered a growing opportunity to provide large-scale and high sensitivity genomic screening allowing the identification of new pathogenic variants associated with rare inherited diseases, rapidly increasing the yield of diagnostic tests for rare neurological diseases and overcoming most of the limitations of a candidate-gene based approach to diagnostics. Nevertheless, clinicians and researchers dealing with neurogenetics have to take into consideration that, besides the advantages, the application of these new techniques also holds limitations and drawbacks.

Low coverage of some genomic regions, missing of large-scale deletions/insertions and copy-number variations are some of the most critical technical ones.

Moreover, NGS often leads to the identification of novel disease genes encoding for proteins whose functions are not completely defined, or to the recognition of novel variants with uncertain pathogenicity (VUS-variants of unknown significance). All these factors contribute to puzzle the likelihood of genotype-phenotype relationship. Application of available standard guidelines¹ can improve the accuracy of sequence variants interpretation. In some cases, a fruitful collaboration between clinicians and geneticists integrated with functional studies are particularly helpful to clarify the biological consequences of the variants and hopefully establish their direct causative role in disease.

Nevertheless, in other cases, the causative role of variants in a specific phenotype still remains unclear: this is commonly true when dealing with variants falling in genes which encode for proteins that are expressed only during ontogenesis or in barely accessible tissues such as the central nervous system and the retina (see Chapter 4). Complex congenital phenotypes without a clear Mendelian inheritance pattern still represent one of the main pitfalls of these techniques and a diagnostic challenge for researchers involved in the field of rare disorders.

However, remarkable advantages deriving from the application of NGS technologies to rare neurodegenerative diseases workup are already indisputable². Frequently overlapping biological pathways are emerging as responsible of their pathogenesis: in light of this

knowledge more reliable experimental models are already being established as an essential starting point for the future development of effective disease-targeted therapies.

References

1. Richards S, Aziz N, Bale S, Bick D, Das S, Gastier-Foster J, Grody WW, Hegde M, Lyon E, Spector E, Voelkerding K, Rehm HL; ACMG Laboratory Quality Assurance Committee. Standards and guidelines for the interpretation of sequence variants: a joint consensus recommendation of the American College of Medical Genetics and Genomics and the Association for Molecular Pathology. *Genet Med.* 2015 May;17(5):405-24. doi: 10.1038/gim.2015.30.
2. Klein CJ, Foroud TM. Neurology Individualized Medicine: When to Use Next-Generation Sequencing Panels. *Mayo Clin Proc.* 2017 Feb;92(2):292-305. doi: 10.1016/j.mayocp.2016.09.008.

Publications

Catania A, Battini R, Pippucci T, Pasquariello R, Chiapparini ML, Seri M, Garavaglia B, Zorzi G, Nardocci N, Ghezzi D, Tiranti V. R106C TFG variant causes infantile neuroaxonal dystrophy "plus" syndrome. *Neurogenetics*. 2018 Jul 3. doi: 10.1007/s10048-018-0552-x.

Catania A, Ardisson A, Verrigni D, Legati A, Reyes A, Lamantea E, Diodato D, Tonduti D, Imperatore V, Pinto AM, Moroni I, Bertini E, Robinson A, Carozzo R, Zeviani M, Ghezzi D. Compound heterozygous missense and deep intronic variants in NDUFAF6 unraveled by exome sequencing and mRNA analysis. *J Hum Genet*. 2018 May;63(5):563-568. doi: 10.1038/s10038-018-0423-1.

Acknowledgments

Not even a word of my thesis could have been written without the trusty collaboration and the essential support of the ones who were besides me all along this unforgettable journey.

The following lines will be dedicated to them, being mindful that the footprints they left in my life go far beyond my professional experience.

Thanks to Valeria Tiranti, my PhD tutor, who carefully guided me throughout the course of my transition from a newbie of basic science to a passionate researcher eager to consistently integrate the laboratory experience within her future translational work.

Thanks to Daniele Ghezzi, my PhD cotutor, who supervised with dedication my neurology residency thesis and gave me my start into the both enchanting and intricate world of NGS technologies.

Thanks to Barbara Garavaglia, the director of the Neurogenetics lab, who was consistently encouraging me to pursue my inclinations and gave me a number of opportunities to integrate all my professional interests in my daily work.

Thanks to Costanza Lamperti, who made me involved and passionate on a brand-new side of neurology, and thanks to Lorenzo Peverelli as well, a neurologist already trained in mitochondrial diseases, who was by my side within this experience.

Thanks to the Neurogenetics lab team, with a special mention to Alessia, Silvia, Sabrina and Roberto, always helpful and kind.

Thanks to my patients and their families, who taught me that letting love guide us and not giving up on dreams, will give us strength to endure and a reason to smile even in times of intense suffering.

Words will never be enough to express my deep gratitude to Pierre Rustin, to whom this thesis is dedicated. His brilliance, positive attitude, persistence and generosity patently overcome human limitations. He is the teacher, the boss, the friend I've been always dreaming of.

Thanks to Malgorzata Rak, my friend Gosia, who was beside me all along my experience abroad, sharing with me her knowledge and great intuitions, participating to my joy, fears and scientific growth.

Thanks to Manuel Schiff, an extraordinarily perceptive person and a strikingly skilful doctor I will always feel blessed to have met.

Thanks to Paule Benit, the qualified but always humble and devoted researcher I met in Paris.

Thanks to Holger Prokisch, Arcangela and Juliette, who sowed the seeds for my contribution to the GENOMIT project.

Thanks to Manuela, Julien, Arielle, Giulia, Marta and Poojia, researchers of the INSERM unit: life in Paris has been amazing with you, guys!

Least but obviously not last at all, thank you Andrea, my beloved bro: you're so much more than my informatics wizard, you're definitely a genius! Actually, you should be awarded an honorary PhD degree.

